Distribution of Excitation Energy in Photosynthesis: A Study of Heat Loss, Photochemical Activity and Fluorescence Emission in Intact Cells of Cyanobacterium *Synechococcus sp.* PCC 6301

by
Omid Salehian

A thesis
submitted to the Department of Biological Sciences
in partial fulfillment of the requirements
for the degree of
Master of Science

Brock University
St. Catharines, Ontario

Table of Contents

Materials and Methods

Results

Discussion

LIST OF FIGURES

LIST OF TABLES

ABSTRACT

Photosynthetic state transitions were investigated in the cyanobacterium *Synechococcus sp.* PCC 6301 by studying fluorescence emission, heat loss, and PS I activity in intact cells brought to state 1 and state 2. 77K fluorescence emission spectra were modelled with a sum of 6 components corresponding to PBS, PS II, and PS I emissions. The modelled data showed a large decrease in PS II fluorescence accompanied with a small increase in the PS I fluorescence upon transition to state 2 for excitation wavelengths absorbed by both PBS and Chl a. The fluorescence changes seen with Chl a excitations do not support the predictions of the mobile PBS model of state transition in PBS-containing organisms. Measurements of heat loss from intact cells in the two states were similar for both Chl a and PBS excitations over three orders of magnitude of laser flash intensity. This suggests that the PBS does not become decoupled from PS II in state 2 as proposed by the PBS detachment model of state transition in PBS-containing organisms. PS I activity measurements done on intact cells showed no difference in the two states, in contrast with the predictions of all of the existing models of state transitions.

Based on these results a model for state transition in PBS-containing organisms is proposed, with a PS II photoprotectory function.

ACKNOWLEDGEMENTS

First and foremost I would like to thank my supervisor Doug Bruce who put up with me for the last few years. He provided guidance and encouragement through the hard times.

I would like to also thank the people in the lab, Jill Lazenby-Homer-Dixon (how is the married life?), Scott (how about some lab baseball?), Cindy, Jody, Cynthia and Li. These people (especially Jill) provided many hours of fun-filled scientific discussions (ya sure !!).

I also would like to thank the people down the hall. Mike (are you eh.... M. Crinson?), the other Mike, Mitzi, Rob, Lesley C., Gary and Nezar. These guys were a lot of fun! Also I would like to thank the new comers, Kirsty (Bulls are No. 1), Dave, the other Lesley, Bruce, Alex and Mabrouk.

I would also like to thank the guys in the electronics shop and the machine shop without whom this project would not be finished. Thanks to Dr. Peter Nichols for the use of DW2 spectrometer and the BBA journals I borrowed over the years, and also the glassblower John Vandenhoff. I would also like to thank Lisa.

I also would like to thank my parents who encouraged and supported me through the years. Finally, I would like to thank one person who has been an inspiration to me and many others, Michael Jordan (keep on jammin'). **GO BULLS!!!**

INTRODUCTION

Photosynthetic organisms having antenna complexes containing Chl a/b light harvesting complexes (LHC) or phycobilisomes (PBS) are capable of regulating the distribution of excitation energy between the two photosystems by a process known as the state transition (Bonaventura and Myers, 1969; Murata, 1969). The excitation energy is regulated between photosystems in response to preferential excitation of either one. In Chl a/b LHC containing organisms such as green algae and higher plants almost all of Chl b is associated with PS II (photosystem II) and most of Chl a is associated with PS I (photosystem I). In cyanobacteria and red algae, phycobilisomes are associated with PS II and most of Chl a is associated with PS I. Hence, with selection of the appropriate wavelength of light one can excite PS II and PS I preferentially. Overexcitation of PS I yields what is known as state 1 while preferential excitation of PS II causes a transition to state 2. The mechanism of the state transition in Chl a/b LHC containing organisms is thought to be understood (Williams and Allen, 1987) while the mechanism for the PBS-containing organisms remains controversial (Mullineaux and Allen, 1988; Biggins and Bruce, 1989; Bruce *et al.*, 1989a). The original model proposed by Murata (1969) for the mechanism of the state transition in PBS-containing organisms involved a spillover of excitation energy from PS II Chl a to PS I Chl a, with the rate of spillover being high in state 2 and low in state 1 (for a review see Biggins and Bruce, 1989; Bruce *et al.*, 1989a).

Two other models have been suggested for the mechanism of the state transition in these organisms (See section on state transitions). The Mobile PBS model is identical to the model of state transition in LHC II Chl a/b-containing organisms. In this model phosphorylation of PBS causes it to dissociate from PS II and associate with PS I in state 2 (Allen *et al.*, 1985). The PBS detachment model is a modification of the mobile PBS model (Mullineaux and Allen, 1988). In state 2, the PBS after phosphorylation detaches from PS II and does not associate with either photosystem. There is also an increase in spillover from PS II Chl a to PS I Chl a. The question that arises from this model is what happens to the energy absorbed by the PBS? There have been no recorded cases of increase in the fluorescence emission of PBS in state 2 (Mullineaux and Allen, 1988; Salehian and Bruce, 1991). There has been suggestions that the energy could be dissipated by non-radiative processes. Measurements of prompt heat loss could give an answer to this question.

The objective of this study was to characterize the mechanism of the state transition in the cyanobacterium *Synechococcus sp.* PCC 6301 by studying fluorescence emission and excitation spectra, heat loss measurements and monitoring the photochemical activity of PS I. The results show that the organism undergoes a typical state transition, however the apparent decrease in PS II activity as observed by fluorescence spectroscopy does not result in an increase in the PS I activity for both PBS and Chl a absorbed wavelengths. There was also no significant difference in heat loss as measured by laser induced optoacoustic spectroscopy (LIOAS) in the two states for

both PBS and Chl a excitations. Modelled fluorescence emission spectra do not show a complementary change in the PS II and PS I as predicted by the models. These results do not support any of the existing models for state transitions in PBS-containing organisms. A photoprotective function for the state transition is suggested based on these findings.

LITERATURE REVIEW

Photosynthetic electron transport

Conversion of solar energy into stored chemical energy in the form of ATP and NADPH is the main function of oxygenic photosynthesis. This is achieved by a series of electron transfer steps initiating with water and ending with the terminal electron acceptor $NADP^+$. This transfer of electrons represents a potential difference of about 1.1 V and requires the cooperation of two photoreactions. The transfer of electrons also results in movement of protons into the lumen of the thylakoid membrane creating a proton electrochemical gradient, driving the synthesis of ATP. The currently accepted sequence of electron transfer steps is shown in figure 1. Each of the redox components are stabilized by specific polypeptides which are housed by specialized complexes known as PS II, the cytochrome b6/f complex, and PS I. Each of these are discussed in detail below.

Photosystem II (PS II)

PS II is functionally defined as the chlorophyll-protein complex which catalyses the light-driven transfer of electrons from water to plastoquinone (PQ), evolving oxygen in process. Two protons are generated for every molecule of water oxidized while two additional protons are pumped across the thylakoid membrane in full reduction of PQ (Ort, 1986).

If we compare the components of the PS II reaction center (RC) to those of the purple bacteria RC, a remarkable similarity is seen

Figure 1. The Z-scheme of photosynthesis in oxygen-evolving organisms.

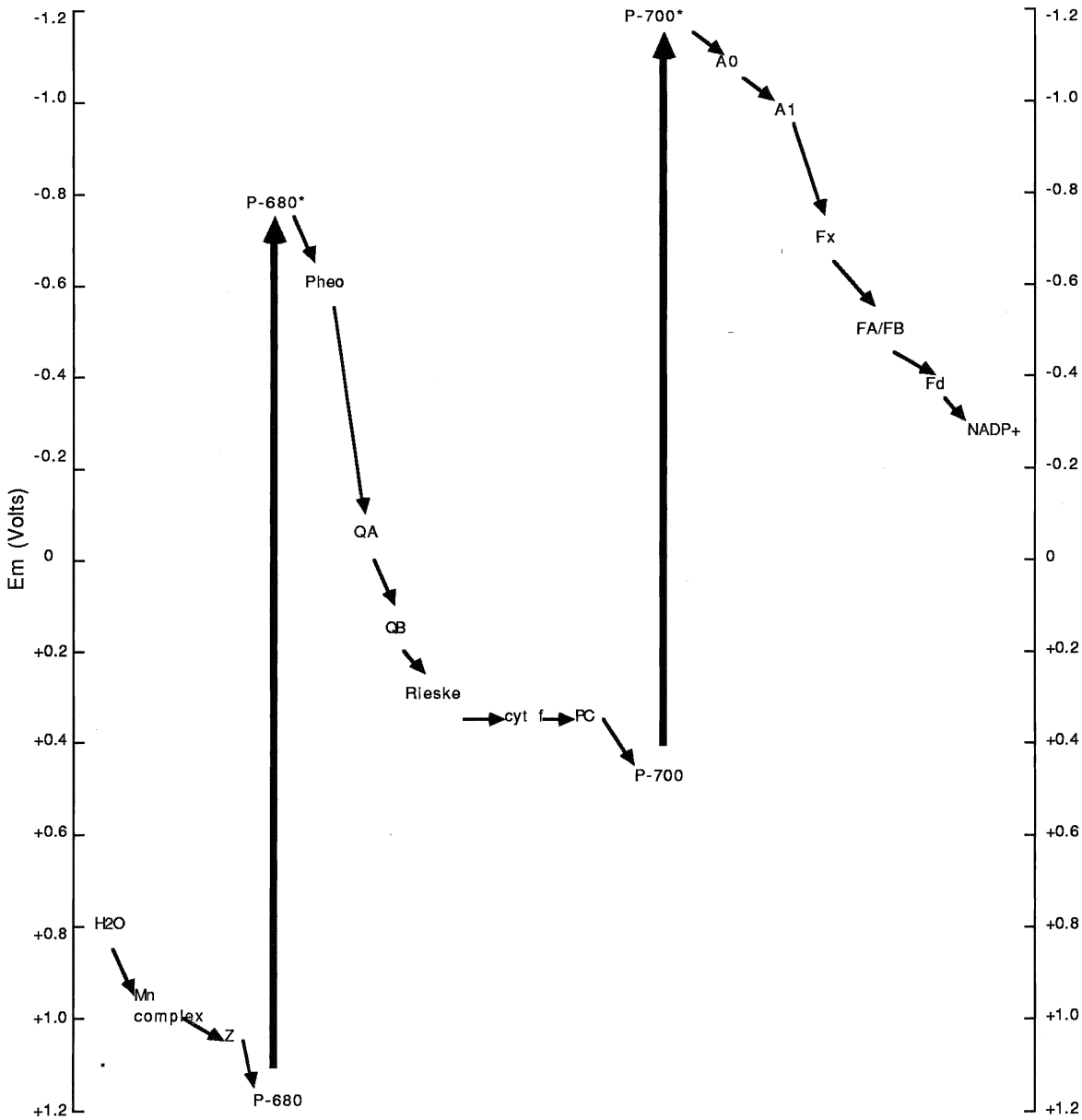
Em (Volts)
-1.2
-1.0
-0.8
-0.6
-0.4
-0.2
0
+0.2
+0.4
+0.6
+0.8
+1.0
+1.2
H2O
Mn
complex
Z
P-680
P-680*
Pheo
QA
QB
Rieske
cyt f
PC
P-700
P-700*
A0
A1
Fx
FA/FB
Fd
NADP+

between the electron carriers. The chemical nature of these electron carriers are very similar, there are complex of two quinones, an iron atom and a pheophytin (bacteriopheophytin in purple bacteria). The donor side of PS II however is not comparable to that in bacteria. P-680 appears to be structurally similar to P-870 in bacteria, in that it is made up of chlorophyll (bacteriochlorophyll in bacteria) and that it acts as the primary donor; however the P-680/P-680$^+$ redox couple is about 600-800 mV more positive than the equivalent bacterial redox couple. In addition PS II has an array of high-potential components which make up the oxygen-evolving complex and are unique to that system (Mathis and Rutherford, 1987).

P-680

The primary electron donor to PS II was detected as a flash-induced absorption change attributable to chlorophyll a (Chl a) oxidation (Doring *et al.*, 1967). Its bleaching maximum is at near 680 nm and hence the name P-680. The monomeric or dimeric nature of P-680 is still controversial. Time resolved EPR (electron paramagnetic resonance) spectra of P-680$^+$ have been reported (Ke *et al.*, 1982; Malkin and Bearden, 1975) with g value (2.0027) and linewidth (8G) compatible with the oxidation of single Chl a molecule. An EPR signal of spin-polarized triplet state of P-680 formed by recombination of P-680$^+$ and Pheo$^-$ was detected by illuminating PS II preparations at liquid helium temperatures (Rutherford *et al.*, 1981). The zero-field splitting parameters are identical to those of triplets of monomeric Chl *in vitro*. The triplet minus singlet spectrum of P-680 measured by absorption-detected magnetic resonance (den

Blanken, 1983) indicated a monomeric triplet but a dimeric ground state. According to the above results it is likely that the hole of P-680$^+$ and the triplet state of P-680 reside on a monomeric species. It could be that P-680 is a pair of Chl a molecules which interact strongly in the singlet excited state and weakly in the triplet and cationic states.

Studies on the triplet state of P-680 (Rutherford, 1985a) indicate that the chlorophyll is oriented differently to what is found in the purple bacteria (Thiede and Dutton, 1981). It is possible that the triplet state of P-680 migrates to an accessory monomeric chlorophyll with a different orientation (Rutherford, 1985b).

In the PS II preparations where an antenna is present, the rate of primary charge separation will be determined by the migration and trapping of excitation energy, a process that takes place on the ps timescale (Hodges and Moya, 1988; Kischkoweit *et al.*, 1988). However, for the recently developed D1/D2/cyt b_{559} preparations the time constant for the primary charge separation has been measured to be 3.09 ± 0.6 ps (Wasielewski *et al.*, 1989). In a photochemical hole-burning study of D1/D2/cyt b_{559} preparations at 4.2 K the value for charge separation was 1.9 ± 0.2 ps (Jankowiak *et al.*, 1989). A model calculation of the excitation energy trapping gave a similar value of 3 ps (Schatz *et al.*, 1988). These rates are close to those reported for the rate of primary charge separation in purple bacteria (Kirmaier and Holten, 1987).

Pheophytin

It was first reported that pheophytin might play a role as an intermediate acceptor analogous to bacteriopheophytin in purple bacteria, when Klimov *et al.* (1977) reported the photoaccumulation of reduced pheophytin in PS II under reducing conditions. The photoreduction potential of pheophytin is -610 mV, this is low enough to reduce Q_A (Klimov and Kranovskii, 1981). The optical, EPR (Klimov and Kranovskii, 1981) and ENDOR (electron-nuclear double resonance) (Fajer *et al.*, 1980) spectra of the reduced species are all consistent with the monomeric anion of reduced pheophytin a.

It has been reported that there are two pheophytin molecules per RC in PS II particles (Omata *et al.*, 1984), though as in photosynthetic bacteria only one of these appears to be photoactive (Klimov *et al.*, 1980). There have also been reports of an acceptor acting prior to pheophytin based on formation of a radical following illumination at 200 K in PS II particles (Rutherford, 1981).

Q_A (The first quinone acceptor)

The identity of this acceptor was first established when an absorption spectrum was obtained by Van Gorkom (1974). This spectrum of Q_A showed similarities to the *in vitro* spectrum of plastosemiquinone anion. After extraction of iron, PS II particles give rise to EPR signals for Q_A^- with characteristic features typical of semiquinone (Klimov *et al*, 1980). In centers where the iron was still present the resulting EPR signal was similar to a signal attributed to

the semiquinone anion interacting with the iron in purple bacteria (Pierson and Olson, 1987).

The Q_A molecule is firmly bound to PS II reaction center protein. As a result of this binding and the influence of the protein, the chemistry of Q_A is very different from that of other free plastoquinones. Q_A can not be doubly reduced and it does not, at least on the time scale relevant to electron transfer, bind a proton when reduced (Ort, 1986). Electron transfer from pheophytin to Q_A is thought to occur in about 100 ps (Glazer and Melis, 1987).

Q_A donates an electron to the next acceptor, Q_B, with kinetics that depend on the redox state of Q_B. This transfer is inhibited by a number of herbicides, of which DCMU is the most commonly used (Mathis and Rutherford, 1987).

Q_B (the second quinone acceptor)

After the first turnover of the reaction center, the electron is stabilized on the primary quinone acceptor Q_A and then within about 10 μs it is transferred to the secondary quinone acceptor Q_B (Crofts and Wraight, 1983). Following the second turnover of the reaction center, there is a repetition of events, producing a doubly reduced Q_B. At some point two protons are taken up from the external aqueous phase, producing a fully reduced and protonated plastoquinol. This quinol is loosely associated with the quinone-binding site and its dissociation from the PS II center is how the plastoquinone pool is reduced. The vacated quinone-binding site on the 32 kDa protein is then available to bind another PQ from the pool. Hence PQ acts as the

interface between one electron events of the reaction center and two electron events of the PQ pool (Ort, 1986).

The full optical Q_B^- minus Q_B spectrum is similar to that of Q_A^- minus Q_A. The spectra show differences in the blue and green regions, indicating Q_B^- is different from Q_A^- in terms of its proximity to pheophytin (Schatz and Van Gorkom, 1985). E_m values for the $Q_B/Q_B(H^+)$ redox couple close to 0 mV have been reported (Robinson and Crofts, 1983).

PS II heterogeneity

About 25% of PS II centers designated ß centers have antenna different from the majority of centers designated α centers (Melis, 1991). This difference in the antenna results in slower kinetics for Q reduction when measured by fluorescence induction. The E_m for Q_A/Q_A^- in ß centers is much higher (120 mV) than in the PS II_α centers (Horton, 1981; Thielen and Van Gorkom, 1981). The PS $II_ß$ centers do not show energy transfer between centers and appear to have a far red spectrum more like PS I (Diner, 1986). These centers have been reported not to be involved in transmembrane electron transfer (Thielen and Van Gorkom, 1981). All the evidence for the existence of PS $II_ß$ centers comes from fluorescence measurements in the presence of DCMU with PS $II_ß$ phenomena arising from centers that are less sensitive to DCMU (Hodges and Barber, 1986). It has been proposed that these centers are one of the intermediates in a PS II repair cycle responsible for replacements of the damaged 32 kDa quinone binding protein (Guenther and Melis, 1990).

Electron Donor side of PS II

Z

The time-resolved absorption spectrum of Z^+ minus Z in tris-washed (Dekker *et al.*, 1984) and native (Lavergne, 1984) membranes are similar. These spectra are also compatible with that of oxidation of a hydroquinone to a semiquinone cation. The results from EPR spectroscopy led to the proposal that Z^+ could be a plastosemiquinone cation (O'Malley and Babcock, 1984). The problem with this assignment was that extraction experiments do not account for quinones other than Q_A and Q_B (DeVitry *et al.*, 1986). This conflict led to re-evaluation and the current assignment of Z^+ as oxidized tyrosine (Barry and Babcock, 1987). Subsequent site-directed mutagenesis studies (Debus *et al.*, 1988a; Vermaas *et al.*, 1988) have established firmly that the EPR signal called signal II_{slow} arises from the oxidized form of tyrosine 160 in D2 subunit.

It has been shown that the kinetics of Z oxidation exactly follow the reduction kinetics of P-680$^+$ (Greken *et al.*, 1988). EPR data also support this finding (Hogansson and Babcock, 1988). Therefore it is generally agreed that Z is the immediate donor to P-680$^+$.

D

The EPR signal arising from Z^+ (signal II_{slow}) is almost identical to that of another component D^+ (signal $II_{very\ fast}$) (Babcock and Sauer, 1973), but unlike Z^+, D^+ is extremely stable. Optical (Greken *et al.*, 1988) and EPR (Hogansson and Babcock, 1988; 1989) evidence have shown that signal $II_{very\ fast}$ also arises from an oxidized form of

tyrosine. More recent site-directed mutagenesis experiments have indicated that it is tyrosine 161 in D1 subunit (Debus *et al.*, 1988b).

Although the chemical identity of D is known its function is still obscure. The kinetics of formation and disappearance of D^+ are too slow to have a direct role in main electron transport sequence (Hansson and Wydrzynski, 1990). It has been shown that D can donate electrons to manganese (Mn) complex in S_2 and S_3 states after 1 and 2 flashes (Vermaas *et al.*, 1984). However D^+ can accept electrons from the Mn complex in the S_0 state in the dark (Nugent *et al.*, 1987). The specific modification of tyrosine 161 of D2 subunit reduces the photoautotrophic growth of the cyanobacterium (Debus *et al.*, 1988b). This suggests that D may play a role in PS II oxygen evolution.

The oxygen-evolving complex (OEC)

Joliot and co-workers (Joliot *et al.*, 1969) were the first to show the quarternary gating function on the oxidizing side of PS II by oxygen flash yield measurements. Later on Kok *et al.* (1970) described the oxygen flash yield pattern in terms of a S-state cycle which is driven by successive photoactivation of PS II. The S_1 state has accumulated one oxidizing equivalent, S_2 two and so on. Each photon absorbed by P-680 advances the S-state upto S_4, which returns to S_0 upon release of oxygen in a light-independent reaction (Kok *et al.*, 1970).

Upon removal of manganese from PS II, the S-state dependence in Z^+ reduction as well as all other four-step phenomena is lost. Therefore the functionally bound manganese in PS II has been

associated with the redox reactions involved in the OEC (Babcock, 1987; Amesz, 1983). Quantitation of Mn release after destruction of OEC reveals that 4 Mn are released (Yocum, 1986).

Besides manganese other ions are also needed for oxygen evolution. Chloride (Cl^-) depleted OEC has been shown to be more sensitive to hydroxyl amine (NH_2OH) inhibition (Kelly and Izwa, 1978) and to alkaline inactivation (Theg and Homann, 1982). After Cl^- depletion the transition beyond S_2 state is blocked (Itoh *et al.*, 1984). It was also shown that inhibitory amines compete with Cl^- for a binding site on the Mn complex (Sandusky and Yocum, 1984). It has been proposed that Cl^- acts as bridging ligand between Mn atoms in OEC (Yocum, 1986).

Another ion that interacts with the OEC is calcium. The site of Ca^{2+} binding has been identified as a complex of water-soluble polypeptides involved in oxygen evolution activity (Ghanotakis *et al.*, 1984). It has been suggested that calcium plays a functional role in photoactivation of the Mn cluster (Ono and Inoue, 1989).

Ono and Inoue (1991) based on luminescence studies have proposed that there is a photooxidizable histidine residue on the donor side of PS II that provides a redox-active ligand for Mn complex. Sequence homology and computer modelling have shown that the histidine 92 on the D1 subunit is the putative Mn ligand (Svensson *et al.*, 1990).

Other donors to PS II

The PS II reaction center contains at least one heme, cyt b_{559} (for a review see Cramer *et al.*, 1986). It has long been known that this

cytochrome can be photooxidized at 77 K, but the kinetics of this oxidation do not correlate with the kinetics of the main reaction sequence in PS II. Detailed studies of EPR and Raman spectra of cyt b_{559} have been interpreted to indicate that the heme is ligated by histidines from 4.5 and 10 kDa polypeptides of PS II (Babcock *et al.*, 1985).

It has been suggested that this cytochrome may have a photoprotective role (Thompson and Brudvig, 1988) or that it could be involved in the proton pump (Arnon and Tang, 1988) in connection to a cyclic electron flow around PS II (Falkowski *et al.*, 1986; 1988). This cyclic electron flow may provide a means for dissipating excess excitation energy, limiting photodamage to PS II reaction centers.

Using EPR spectroscopy it has been shown that the photooxidation of cyt b_{559} proceeds via a photooxidation of chlorophyll (Thompson and Brudvig, 1988) which is the first step in photoinhibition of PS II. There have also been suggestions that carotenoid share a common electron transfer pathway with cyt b_{559} (Diner, 1986).

Cytochrome b_6/f complex

Cyt b_6/f complex isolated from spinach chloroplasts consist of four major polypeptides, cyt f corresponding to 34 and 31 kDa polypeptides, cyt b_6 a 23 kDa protein, the Rieske Fe-S protein at 20 and 22 kDa, and a 17 kDa subunit (Hauska, 1986). Clark *et al.* (1984) reported that the ferredoxin-$NADP^+$ oxidoreductase (FNR) a 37 kDa protein, was isolated along with the b_6/f complex. The presence of FNR does not affect the plastoquinone-plastocyanin oxidoreductase

activity since active b_6/f complexes lacking FNR can be obtained from higher plant plastids (Hauska, 1985). Therefore FNR is not a subunit of the cyt b_6/f complex but plays a part in the ferredoxin-mediated cyclic electron flow around PSI.

Two forms of cyt b_6 with different redox potentials are present in the complex (Hurt and Hauska, 1983; Clark and Hind, 1983), these two forms are associated with the same peptide and have E_m values of -50 and -150 mV. The other iron-protein is the 20 kDa Fe-S "Rieske" protein. Its midpoint potential in chloroplast is 280 mV (Hauska, 1986). The next acceptor in the chain is cyt f. This cytochrome has an E_m of 340 mV. The redox center of this cytochrome is on the luminal side of the thylakoid membrane which provides easy access for the mobile electron carriers plastocyanin (PC) or cyt c_{553}.

Recently Chain and Malkin (1991) isolated cyt b_6/f complexes from spinach chloroplasts which were resolved into two forms, a monomeric and a dimeric form. The functional form of the mitochondrial cyt bc_1 complex is a dimer, and the role of the dimeric cyt b_6/f is being studied on similarity with the bc_1 complex.

Plastocyanin (PC) and cytochrome c_{553}

PC is a mobile copper-containing protein which mediates the transfer of electrons from cytochrome f to P-700$^+$ in plants and some cyanobacterial membranes (Haehnel, 1982). Cytochrome c_{553} acts in the same manner in certain algae grown under copper limiting conditions and in most cyanobacteria (Bohner and Bogner, 1978). The

kinetics of electron transfer from PC and cyt c_{553} to P-700$^+$ depends on the net charge on the membrane surface and the charge of the mobile electron carrier. This evidence comes from the fact that divalent cations have been shown to stimulate the transfer of electrons to P-700$^+$ (Tamura *et al.*, 1980). This is probably due to the increase in Km for PC by these cations. It was also found that the rate of these reactions increases with a decrease in pH (Takabe *et al.*, 1980). Kinetic experiments have shown that P-700$^+$ is reduced with a half time of 12 μs after one flash, but after a second flash (less than 50 μs apart from the first), P-700$^+$ is reduced with a half time of 110 μs. These findings are interpreted in terms of two PC molecules bound to the reaction center, the farther one replacing or reducing the close one after it has been oxidized (Bottin and Mathis, 1985; 1987). It has been found that the primary site of interaction of PC may be the charged region of the 17 kDa protein and the PS I core protein which extends into the inner thylakoid space (Haehnel *et al.*, 1980).

Photosystem I (PS I)

The PS I reaction center consists of a membrane-bound light-driven plastocyanin-ferredoxin oxidoreductase. The similarity of plant and cyanobacterial PS II to the reaction center of the purple photosynthetic bacteria was discussed in the earlier section. There is also a similarity between the reaction center of green sulfur bacteria and PS I. This similarity is documented by the fact that green sulfur bacteria such as *Chlorobium sp.* can photoreduce NAD$^+$ via ferredoxin without additional energy requirement (Buchanan and Evans, 1969),

that iron-sulfur centers function as early electron acceptors (Knaff and Malkin, 1976; Jennings and Evans, 1977), and that the earliest electron acceptor in the green sulfur bacteria is a lipophilic form of bacteriopheophytin c much like the PS I complex where the primary acceptor is a Chl a molecule (Braumann *et al.*, 1986).

In the case of *Chlorobium* the primary electron donor P-840 is a bacteriochlorophyll a dimer (Wasielewski *et al.*, 1982). The secondary acceptor in the *Chlorobium* , which is an Fe-S center is capable of reducing ferredoxin (Fd) directly (Knaff *et al.*, 1979). It is believed that NAD^+ can receive electrons directly from Fd. The electron from Fd can also go to cyt bc_1 complex, menaquinone pool and cyt c_{553} which is the immediate electron donor to $P\text{-}840^+$ (Pierson and Olson, 1987). This sheds some light on the cyclic electron transfer across PS I.

P-700

This is a pigment present in photosynthetic organisms responsible for absorption decrease at 700 nm. P-700 is a one electron redox agent with a midpoint potential of +430 mV (Golbeck, 1988). P-700 accepts excitation energy from all the surrounding antennae chlorophyll molecules and undergoes a photooxidation, decreasing its midpoint potential to -1300 mV. Although P-700 has long been considered a molecule of chlorophyll a its exact structure is still uncertain. The narrowing of the EPR linewidth of the $P\text{-}700^+$ over monomeric Chl a *in vitro* provided the earliest evidence for the dimeric nature of P-700 (Norris *et al.*, 1971). However the EPR signal from the triplet state of P-700 is similar to that of monomeric Chl a

triplet *in vitro* (Rutherford and Mullet, 1981), suggesting that P-700 may be a Chl a monomer. The analysis of circular dichroism (CD) and absorption spectra of P-700-enriched particles, containing about 10 Chl a per P-700, agrees with the dimeric nature of P-700 (Ikegami and Itoh, 1986; 1988). Their data showed that P-700 is a dimer absorbing maximally at 694 nm and its oxidized state, $P\text{-}700^{+}$, has twice weaker absorption at 687 nm. The optical absorption spectrum of $P\text{-}700^{+}$ can be identified as one of a weakly coupled dimer. Therefore the above data suggest that the ground state of P-700 is a Chl a dimer, but the reduced and the triplet states are localized on only one of the two chlorophylls. Recent resonance Raman spectroscopy of P-700 enriched particles (Moenne-Loccoz, *et al.*, 1990) show that P-700 is constituted of a pair of Chl a molecules which are involved in an inequivalent bonding interactions through their keto carbonyl groups. The authors suggest that these interactions do not involve Chl-Chl bridging through water molecules or other small bifunctional molecules as suggested in earlier studies (Katz, *et al.*, 1978), but most likely consist of a hydrogen binding with proteins. The magnesium atoms of these two Chl a molecules bind single axial ligands, possibly the histidines *psa* A 535 and *psa* B 521. These two histidines are homologous to the ones of the bacterial reaction center (Fish, *et al.*, 1985).

A_0 (the primary electron acceptor)

Optical absorption measurements of P700 after a laser flash in Triton PS I particles provided first evidence of an electron acceptor functioning prior to F_X. Sauer *et al.* (1978, 1979) found that when F_X

was reduced by continuous background illumination in presence of dithionite, a 3 μs rereduction of $P700^+$ occured at room temperature after a laser pulse. This transient was interpreted as the backreaction of a more primary electron acceptor A_1^- with $P700^+$. It was soon recognized with EPR spectroscopy that two electron acceptors, not just one, function in PS I before F_X (Bonnerjea and Evans, 1982). The EPR signal from A_0 has a g= 2.0026 and has a spectrum characteristic of a chlorophyll a (Chl a) monomer (Bonnerjea and Evans, 1982). These findings are supported by the difference spectrum of A_0 which consisted of bleaching at 670, 430 and 405 nm with absorbance increases at 450 nm and in the broad range at around 690 nm (Mansfield and Evans, 1985). The optical difference spectrum of A_0 closely resembles the Chl a^-/ Chl a difference spectrum generated electrolytically by Fujita *et al.* (1978). Mansfield and Evans (1985) also calculated the amount of A_0 present and found the ratio to be 0.94 A_0:1 P700, hence A_0 is present in stoichiometric amounts with P700.

A_1

The secondary acceptor is denoted A_1. The nature of this electron acceptor was the subject of much debate until recently. A_1 has an asymmetric line-shaped EPR signal similar to that of reduced quinone (Thurnauer and Gast, 1985). Broadhurst *et al.* (1986) assigned a semiquinone nature to A_1 based on the polarized EPR results. These show magnetic parameters similar to the ones for semiquinone anion *in vitro*. More direct information on A_1 can be obtained by flash absorption at low temperature, under conditions

where an electron reaches A_1 and then recombines with $P700^+$ with a half-time of about 150 μs. Flash induced absorption changes from 240 to 525 nm when F_B and F_A are prereduced results in a difference spectrum similar to that of Vitamine-K1 (Phylloquinone) (Brettel *et al.*, 1986).

Phylloquinone exists in plant and cyanobacterial reaction centers in a stoichiometry of 2 Vit. K1:1 P700 (Malkin, 1986; Ziegler *et al.*, 1987). Removal of one of these by hydrocarbon solvent hardly changes light induced electron transfer (Malkin, 1986; Biggins and Mathis, 1988). Extraction of both phylloquinones by wet ether or hexane-methanol, however, blocks forward electron transport at physiological temperatures, as if A_1 was missing (Ikegami *et al.*, 1987; Biggins and Mathis, 1988). In cyanobacterial preparations forward electron transfer can be largely reconstituted by readdition of pure phylloquinone (Biggins and Mathis, 1988). Therefore it may be considered that A_1 is one of the two phylloquinones of PS I.

F_X

When both F_A and F_B are reduced chemically prior to illumination, the low temperature photooxidation of P-700 becomes reversible and couples to the photoreduction of a new EPR component with g-values characteristic of iron-sulfur proteins (McIntosh and Bolton, 1976), however the linewidths are broader than the ones for normal Fe-S clusters. The midpoint potential of this species was measured to be -705 mV (Golbeck, 1988). The identity of this Fe-S cluster is still uncertain. The main uncertainty is that whether F_X is a 2[2Fe-2S] or a 4Fe-4S cluster. Iron extended X-ray

absorption fine structure (EXAFS) of PS I core preparations containing F_X (this preparations lacked both F_A and F_B), show that F_X may be a 4Fe-4S cluster and not a 2[2Fe-2S] clusters (McDermott *et al.*, 1989). The amplitude of Fe-Fe backscattering is compared to the one of an artificial 4Fe-4S preparation and shows a great similarity. The assignment of F_X as a tetranuclear structure rather than as a pair of binuclear clusters is more consistent with the number of available cysteins in the PS I core complex. The *psa* A and *psa* B polypeptides have less than four cystein residues each (Fish *et al.*, 1985), which implies that the F_X cluster must be ligated by cysteins by at least two polypeptides. It has been shown that there is only one copy each of *psa* A and *psa* B polypeptides per PS I complex (Bruce and Malkin, 1988; Scheller *et al.*, 1989). One copy each of the two poly peptides would contain enough cystein residues to ligate one [4Fe-4S] cluster, but not two [2Fe-2S] clusters. Therefore it is proposed that F_X is coordinated by the two conserved cystein residues from one copy of the *psa* B gene product and two conserved from a single copy of the *psa* A gene product.

F_A/F_B

In 1971, Malkin and Bearden using EPR spectroscopy described a low temperature photoreduction of a membrane-bound Fe-S protein with g values of 2.05, 1.94 and 1.86. This new electron transfer component could be photoreduced at 25 K both in far-red and red lights. Dark reduction with dithionite led to appearance of a second component (Evans *et al.*, 1972). It was suggested that these acceptors named centers A (g=2.05, 1.94 and 1.86) and B (g=2.07, 1.92 and

1.89), existed as independent, but magnetically interacting clusters on a single protein (Evans *et al.*, 1984). The redox potentials of centers A and B have been measured to be about -530 and -580 mV respectively.

Oh-oka and coworkers in 1988, isolated a 9 kDa polypeptide with an Fe-S cluster from PS I complex by *n*-butanol extraction (Oh-oka *et al.*, 1988). This polypeptide is the *psa* C gene product, and has an arrangement of cysteines similar to that found in bacterial ferredoxins which contain 2[4Fe-4S] clusters (Hoj *et al.*, 1987). EPR studies done on this protein shows the characteristic Fe-S EPR signal associated with F_A and F_B (Oh-oka *et al.*, 1988), hence it was proposed that the two clusters of cysteins in this protein bind F_A and F_B. Further evidence for the above hypothesis comes from the reconstitution experiments done with the polypeptide. It was found that electron transport was reconstituted in PS I complexes devoid of 9 kDa protein, by addition of *psa* C gene product (Zhao *et al.*, 1990). All sequences of the F_A/F_B protein so far analyzed are highly conserved, with a duplicated sequence of 4 cysteins in a typical arrangement; these two cysteins are always located between residues 10-20 and 47-57 (Lagoutte and Mathis, 1989), these are proposed to be the possible binding sites for the F_A and F_B clusters.

Ferredoxin (Fd) and ferredoxin-$NADP^+$ oxidoreductase (FNR)

The transfer of electrons from PS I to $NADP^+$ is mediated by the iron-sulfur protein, ferredoxin and flavin-containing protein FNR.

Ferredoxin(Fd)

Fd is a stable, soluble Fe-S protein with a molecular weight of 10 kDa. The protein is encoded in the nucleus and is initially synthesized with a presequence of 44 amino acids responsible for targetting it to the chloroplast stroma (Grey *et al.*, 1987). There is a conservation of spacing between the four cysteines that serve as cluster ligands to the cluster irons in more than forty ferredoxins sequenced in higher plants. The four cysteines that serve as cluster ligands are located at residues 39, 44, 47 and 77 in spinach ferredoxin sequence (Knaff and Hirasawa, 1991).

The reduction of ferredoxin by PS I probably requires this protein to dock with at least one reaction center subunit. Recent cross-linking experiments have shown that the 22kDa, *psa* D gene product plays an important role in binding ferredoxin to the PS I reaction center (Zanetti and Merati, 1987). A comparison of the amino acid sequences of four *psa* D proteins shows striking conservation of positively charged amino acids, particularly of lysine residues (Wynn *et al.*, 1989). As ferredoxin is a highly acidic protein, it is possible that several of these conserved *psa* D lysines are involved in the electrostatically-stabilized binding of ferredoxin to the PS I reaction center under physiological conditions (Knaff and Hirasawa, 1991).

FNR

The sequence of electron flow on this end of the electron transport chain includes : (1) the dark transfer of electrons from the

terminal iron-sulfur clusters to soluble ferredoxin, (2) the dark transfer of electrons from ferredoxin to FNR probably via an obligatory complex (Foust *et al.*, 1969), and (3) the dark transfer of electrons from reduced FNR to $NADP^+$.

FNR is a 35 kDa monomeric protein, its function as stated above is to catalyze the flow of electrons from reduced Fd to $NADP^+$. FNR appears attached to the thylakoid membrane by a specific, intrinsic binding protein of molecular mass of 17.5 kDa (Vallejos *et al.*, 1984). It has been shown that FNR can produce a 1:1 electrostatically stabilized complex with Fd. The stability of this complex is dependent on the pH and the ionic strength of the medium (Batie and Kamin, 1981).

Respiratory electron transport

Cyanobacteria lack both mitochondria and chloroplast. Instead they have thylakoid membranes which contain the intermediates for both photosynthetic and respiratory electron transports (Pescheck, 1987). It has been shown that these two pathways share some common electron transport components (Aoki and Katoh, 1982; 1983; Pescheck and Schmettere, 1982).

Most workers have shown that PQ function in both respiratory and photosynthetic pathways (Aoki and Katoh, 1982; 1983, Scherer *et al.* 1988). However inhibitor studies and spectroscopic evidence have shown cyt b_6/f to be active in respiration as well. It was also found that both cyt c_{553} and PC are able to reduce PS I and the terminal oxidase. In *Anabaena* the Km of PS I and cyt oxidase for reduced cyt c_{553} is very similar, but the turnover of PS I is one order

Figure 2. Interaction of respiratory and photosynthetic electron transport chains in cyanobacteria. The common redox proteins are outlined.

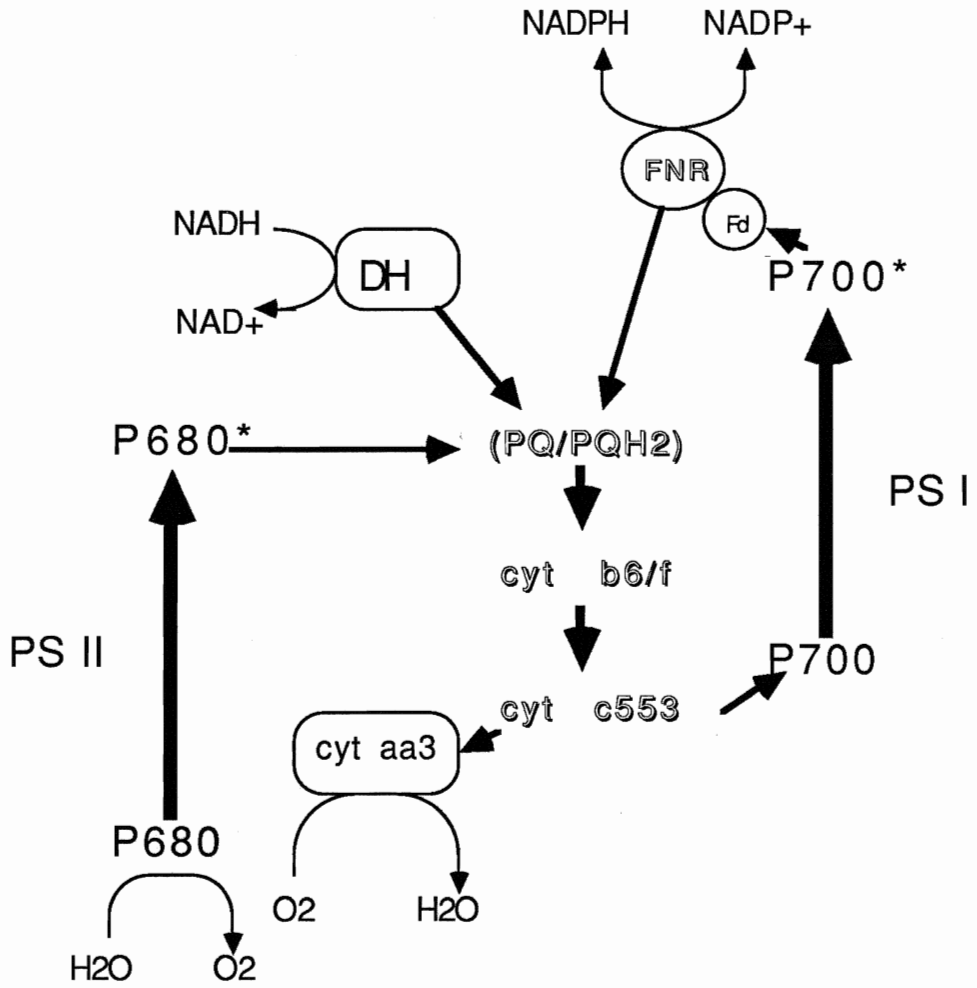
NADPH
NADP+
FNR
Fd
NADH
DH
NAD+
P700*
P680*
(PQ/PQH2)
PS I
cyt b6/f
PS II
P700
cyt c553
cyt aa3
P680
O2
H2O
H2O
O2

of magnitude higher (Scherer, 1990). This is the third common link between the two pathways. Figure 2 illustrates the accepted scheme of the interaction.

The scheme shows that both NADH and NADPH can donate electrons to the PQ pool. Inhibitor studies have concluded that the sites of oxidation are different. Reduction of PQ by NADH was blocked by antimycin A while the NADPH pathway remained open (Matthijis *et al.*, 1984). The interaction of the two electron pathways has allowed researchers to change the redox state of the PQ without altering the light quality. This has given evidence to support the hypothesis that state transitions are controlled by the redox state of PQ pool (Mullineaux and Allen, 1986; Dominy and Williams, 1987).

Excitation energy transfer

The energy transfer is a physical process between donor and acceptor. This process is regarded as one of the relaxation processes of the excited molecules, competing with chemical reactions, fluorescence, radiationless relaxation and inter-system crossings (Mimuro, 1990).

There are three types of photosynthetic pigments capable of energy transfer, these are chlorophyll, phycobilins and carotenoids. A type of Chl is always present for constructing the primary electron donor in reaction center (see section on photosynthetic electron transport). Phycobilin is found in cyanobacteria, red algae and cryptomonads. They are usually constructed into supramolecular complexes of phycobiliproteins called phycobilisomes (PBS). These PBS are attached to the stromal side of the thylakoid membrane and

act as an antenna for the photosystems (Gantt, 1986). Many types of carotenoids are found in photosynthetic organisms. Their main function is thought to be protection from photodamage produced by light in presence of oxygen.

The energy transfer properties of phycobiliproteins in photosynthesis was clearly shown by Engelmann (1884). Later on Emerson and Lewis (1942) and Haxo and Blinks (1950) showed that the contribution of phycobilins was essential for maximal photosynthetic activity.

The polypeptide composition of PBS is 85% low-molecular weight chromophore-containing polypeptides and 15% uncoloured linker polypeptides (Gantt, 1986). Three types of phycobiliproteins are associated with PBS. Phycoerythrobilin (PE), phycocyanobilin (PC) and allophycocyanobilin (APC). Gantt *et al.* (1976) after comparing immunological, biochemical, spectroscopic and electron microscopic data proposed a model for PBS that showed a core of APC surrounded by PE and PC suggesting the energy transfer sequence of PE→PC→APC. Time resolved fluorescence spectroscopic studies (Porter *et al.*, 1978; Bruce *et al.*, 1985; Yamazaki *et al.*, 1984) directly confirmed the energy transfer pathway of PE→PC→APC→Chl a. A specialized form of APC has been determined to be the bridge for energy transfer from PBS to Chl a in thylakoid membranes (Glazer and Bryant, 1975; Zilinskas, 1982), this APC is called the terminal emitter.

After a number of studies on the physical and energetic distribution of phycobilins and Chl a between PS II and PS I (Mimuro and Fujita, 1977; Wang *et al.*, 1977; Ried *et al.*, 1977) it was shown

that most of the phycobilins are associated with PS II and most of Chl a is associated with PS I. However there have been reports of PC associated with PS I in spheroplasts (Tel-Or and Malkin, 1977), and also presence of APC in PS I preparations (Pullin *et al.*, 1979).

State transitions

A large number of photosynthetic organisms containing either LHC Chl a/b or PBS as antenna complexes have the ability to regulate the excitation energy distribution between the two photosystems. This process is known as the light state transition (Bonaventura and Myers, 1969; Murata, 1969). This process balances the relative activities of the two photosystems by adjusting the distribution of excitation energy between them in response to the preferential excitation of either PS I or PS II.

Ever since the discovery of the state transitions investigators have been wondering what is the significance of state transitions?

Allen *et al.* (1981), Owens and Ohad (1983) and Staehelin and Arntzen (1983) suggest that the role of state transition is to poise the electron transport chain between the two photosystems in order to maximize the rates of linear electron flow, this is done by diverting energy away from PS II and making it available to PS I.

It is also suggested that (Fernyhough *et al.*, 1989; Turpin and Bruce, 1990; Allen and Horton, 1981) state transitions regulate the relative rates of cyclic and linear electron transport to optimize the relative rates of ATP and NADPH production in response to metabolic demand. Turpin and Bruce (1990) showed that NH_4^+ assimilation of N-starved *Selenastrum minutum* cells increased the fluorescence

yield of PS I, characteristic of transition to state 2. NH_4^+ assimilation greatly increases the demand for ATP relative to NADPH. The transition to state 2 increases the cyclic electron transport around PS I increasing the production of ATP relative to NADPH. Bulte *et al.* (1990) have shown that the intracellular demand for ATP controls state transitions *in vivo* in *Chlamydomonas reinhardtii*. They found that under low ATP level conditions, such as anaerobiosis or prolonged starvation, cells were in state 2 which favors immediate operation of cyclic electron transfer around PS I coupled to ATP synthesis. Recently Delsome (1991) has shown that fast oxidation state of cytochrome f relates to a low ATP content and state 2 while a slow oxidation state of cytochrome f relates to a high ATP content and state 1.

The idea that the state transition is a photoprotectory mechanism has won some support in recent years (Allen and Melis, 1988; Wendler and Holzwarth, 1987; Rehm *et al.*, 1989; 1990; Salehian and Bruce, 1991). It is thought that the state transitions control the rate of excitation energy transfer to PS II. This state transition prevents over excitation of PS II and does not result in a transfer of excitation energy to PS I.

State transitions in LHC Chl a/b containing organisms

The distribution of excitation energy between PS I and PS II was first observed for LHC Chl a/b containing organisms by Bonaventura and Myers (1969). By studying slow fluorescence changes they saw that a greater proportion of light 2 (light absorbed predominantly by

PS II) is delivered to PS I at the expense of PS II. This condition is known as state 2. They also reported the corresponding changes in oxygen evolution indicating an adjustment of electron transport reactions. The response to over excitation of PS II is termed state 2 while over excitation of PS I leads to state 1.

The suggested mechanism for the state transition in LHC containing organisms is as follows. Excess light 2 results in reduction of electron transport component (PQ and/or cyt b_6/f) which activates a protein kinase. This kinase then phosphorylates LHC II and PS II components. Increased negative charge on the phosphorylated LHC II results in electrostatic repulsion, causing it to migrate from the stacked regions of thylakoid membrane where it is associated with PS II to unstacked regions where it would associate with PS I. Similarly excess light 1 would oxidize the electron transport intermediate and inhibit the kinase activity resulting in dephosphorylation of LHC II by background phosphatase activity. This dephosphorylated LHC II then migrates back to the stacked regions of thylakoid membrane and associates with PS II (Fork and Satoh, 1986; Williams and Allen, 1987).

It has been shown that the molecular mechanism of transition to state 2 involves phosphorylation of thylakoid membrane polypeptides in particular LHC II (Bennett, 1977). Bennett (1977) showed that incubation of intact chloroplast with [^{32}P]-orthophosphate results in phosphorylation of thylakoid proteins evident by autoradiography. He found that among these there were 24 and 26 kDa polypeptides of LHC II as well as 10, 33, 35, and 45

kDa proteins associated with PS II. Bennett and co-workers (Bennett *et al.*, 1979; Allen *et al.*, 1981) have shown that phosphorylation of LHC II is brought about by a membrane-bound kinase that is normally inactive in the dark but can be activated by light. Recent evidences suggest that different kinases phosphorylate the LHC II and PS II proteins. Bennett *et al.* (1988) have shown that unlike the PS II protein, LHC II proteins are phosphorylated only when the cyt b_6/f complex is active. This was shown by use of mutants lacking b_6/f complexes. These mutants showed phosphorylation of PS II proteins but no phosphorylation of LHC II. Other experiments using inhibitors have led to the same conclusions (Gal *et al.*, 1988; Bennett, *et al.*, 1988).

Since the discovery of phosphorylation of LHC II and its link to the state transition it has been questioned whether the dephosphorylation of LHC II takes place by a kinase acting in reverse or by a phosphatase. It was found that inhibitors of electron transport do not inhibit the dephosphorylation but classical inhibitors of phosphatase such as fluoride and molybdate block dephosphorylation by more that 90% (Bennett, 1991).

In the mechanism of state transition in LHC-containing organisms discussed above it is suggested that phospho-LHC II migrates from stacked to unstacked regions of thylakoid membrane and associates with PS I increasing the absorption cross-section of PS I and decreasing the absorption cross-section of PS II (Williams and Allen, 1987). Much controversy exists at present as to whether the excitation energy from LHC II is transfered to P-700 and if this

transfer increases the absorption cross-section of PS I under physiological conditions.

77K fluorescence emission results (Krause and Behrend, 1983; Saito *et al.*, 1983) show a complementary increase in the emission yield at 735 nm (attributed to PS I) with a decrease in 685 and 695 nm emission (from PS II) as a result of phosphorylation. There is also evidence for increase in the rate of P-700 photooxidation by phosphorylation (Telfer *et al.*, 1984; Bassi *et al.*, 1988). However Howarth and Melis (1983) and Allen and Melis (1989) report no change in the rate of P-700 photooxidation upon phosphorylation. Also low temperature fluorescence data (Kramer *et al.*, 1985) failed to show any excitation energy transfer from Chl b to PS I upon phosphorylation of LHC II. There is also evidence from time-resolved fluorescence spectroscopy against transfer of energy from LHC II to PS I (Holzwarth 1986; Berens *et al.*, 1985; Wendler and Holzwarth, 1987).

An alternative possibility for energy dissipation by phosphorylated chloroplasts might be that the light absorbed by the phospho-LHC II is converted ultimately to heat in an energy dissipating pathway (Allen and Melis, 1988). One possible mechanism would be the transfer of excitation energy into an energy dissipating cyclic pathway around PS II (Horton and Lee, 1985). Falkowski *et al.* (1986) showed that at light saturation, about 15% of the maximum electron flow through Q_A enters a cyclic path around PS II. They proposed a model for this cyclic flow of $Q_A \rightarrow Q_B \rightarrow$ PQ pool $\rightarrow$ Cyt $b_{559} \rightarrow$ Z. They suggested that this cyclic flow around PS II provides a means of dissipating excess energy and limiting

photodamage to PS II reaction centers (Falkowski, 1988; Falkowski *et al.*, 1986).

It has also been suggested that state 2 to state 1 transition causes no change in PS I absorbance but a 35% decrease in PS II_β and a 25% increase in PS II_α centers (Mauzerall and Greenbaum, 1989). Such an observation would be supportive of the heat dissipation model discussed above (see section on PS II heterogeneity).

State transitions in PBS-containing organisms

History

For PBS-containing organisms the state transition was first observed by Murata (1969). By studying room temperature and 77K fluorescence emission of Chl a in red alga, he observed that preillumination by PBS-absorbed light resulted in change of the proportion of excitation energy transferred to PS II and PS I. He proposed a conformational change in the thylakoid membranes to modify the orientation of, or distance between the pigments allowing the regulation of the distribution of excitation energy.

Unlike the LHC Chl a/b-containing organisms which undergo typical state transitions in 7 to 8 min., red algae go to state 1, in 1 to 5 s and state 2, in 10 to 20 s (Ried and Reinhardt, 1980; Biggins and Bruce, 1985). In cyanobacteria it takes about 20 s for a typical state transition.

Fluorescence emission changes from Chl a of PS I and PS II has been widely used to study state transitions in PBS-containing organisms. Because of its ease of use, fluorescence emission

spectroscopy has been used as an assay for visualization of state transitions (Ley and Butler, 1976; 1980). Ley and Butler (1976; 1980) observed that the yield of energy transfer from PS II to PS I calculated at the F_m level (fluorescence yield when all PS II reaction centers are closed) was 0.97 in state 1 and 0.94 in state 2, while if the values were calculated at the F_0 level (minimal fluorescence yield with open PS II reaction centers) different values were obtained. These values were 0.48 in state 1 and 0.61 in state 2.

State transition models

Biggins and Bruce (1989) suggest that any model should address the following three points in order to elucidate the mechanism of state transition. (1) The mechanism responsible for sensing the imbalance of activities of PS II and PS I to trigger the state transitions, (2) the changes in the pathway of excitation energy transfer from PBS to the two photosystems, and (3) the physical changes in the photosynthetic apparatus responsible for controlling the pathway of excitation energy transfer.

All three models shown in figure 3 agree on the antenna and photosystem configuration in state 1. There is a transfer of energy from PBS to PS II directly and there is a minimum spillover of excitation energy from PS II Chl a to PS I Chl a.

Spillover

This model was originally proposed by Murata (1969) and has been supported more recently (Ley and Butler, 1977; 1980; Bruce *et*

Figure 3. This figure shows the three proposed models for mechanism of state transition in PBS-containing organisms. They share the common state 1 configuration. However their state 2 configurations differ. Spillover model proposes a conformational change in the membrane bringing the two photosystems closer to each other, mobile PBS model proposes association of PBS with PS I in this state, and the PBS detachment model proposes a detachment of PBS from PS II and conformational change in the membrane bringing the two photosystems closer to each other.

STATE 1

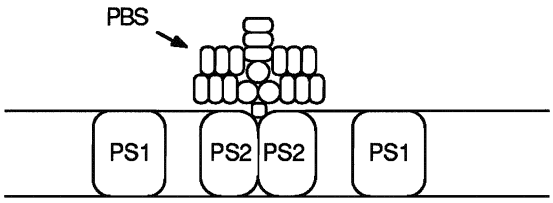

STATE 2

Spillover

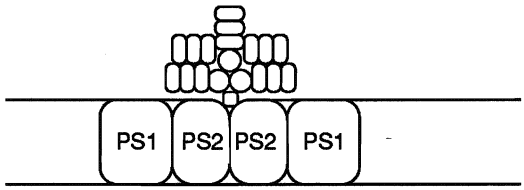

Mobile PBS

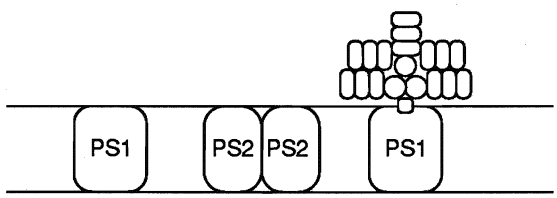

PBS
Detachment

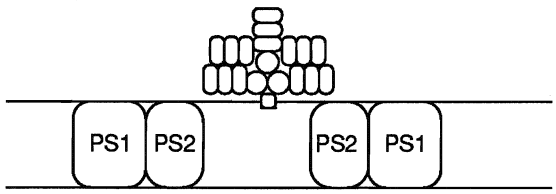

al., 1989 a; b; Brimble and Bruce, 1989). During the transition to state 2, there is an increase in the amount of excitation energy spillover from PS II Chl a to PS I Chl a as a result of a change in distance and/or orientation between PS I and PS II, since excitation energy transfer between two pigments is proportional to the reciprocal of the distance between them raised to the sixth power. Hence small changes in distance can produce large changes in excitation energy distribution. In this model the PBS remains associated with PS II and the energy transfer from PBS to PS II remains the same in the two states. Therefore according to this model in state 2 when PBS and Chl a absorption contributions to PS II decrease, there should be a complementary increase in the contributions to PS I.

Evidence for conformational change comes from several sources. Biggins (1983), Bruce *et al.* (1985) and Bruce and Biggins (1985) chemically cross-linked *Porphyridium cruentum* and *Anacystis nidulans* cells in state 1 and state 2 using glutaraldehyde. Fork and Satoh (1983) have shown that state transitions will not occur below the lipid phase transition temperature in cyanobacterium *Synechococcus lividus*. The above suggests a requirement for fluidity of membrane, which is required for the mobility of components in the lipid bilayer. Electron microscopic studies (Olive *et al.*, 1986; Vernotte *et al.*, 1990) have shown randomization of EF particles (PS II centers) during transition to state 2. The EF particles were arranged in rows in state 1. This randomization is suggested to increase the energy transfer from PS II to PS I (Olive *et al.*, 1986).

Polarized spectroscopic studies (Bruce and Biggins, 1985) have shown that allophycocyanin (APC) core of PBS changes its orientation

during the state transition. However similar studies done on membrane fragments of both *Synechococcus* and *P. cruentum* showed no change in the APC orientation (Brimble and Bruce, 1989). But it was concluded that the change in linear dichroism (LD) accompanying state transition are due to change in orientation of APC core with respect to the long axis of intact cells and not the plane of the thylakoid membranes.

Mobile PBS

This model is essentially the same as the model for the state transition in LHC Chl a/b-containing organisms (see section on state transition in LHC Chl a/b-containing organisms). In transition to state 2, reduction of the PQ pool activates a protein kinase, this kinase will then phosphorylate PBS and PS II components. Electrostatic repulsion causes detachment of PBS from PS II, PBS then relocates on the thylakoid membrane and directly associates with PS I (Allen *et al.*, 1985). Dephosphorylation by background phosphatase activity causes the PBS to reassociate with PS II in state 1. The energy initially absorbed by PBS will now be transferred directly to PS I. Protein phosphorylation plays an important part in this model, evidences for and against differential protein phosphorylation in the two states have been mounting in recent years. Biggins *et al.* (1984b) have reported phosphorylation of at least 12 polypeptides in *P. cruentum* and *A. nidulans*. However the phosphorylation was light as well as wavelength independent. There have also been reports that phosphorylation of polypeptides in light and dark in *P. cruentum* have similar kinetics (Kirschrer and Senger, 1986).

Allen *et al.* (1985) and Sanders *et al.* (1986) presented evidence for light dependent phosphorylation of two polypeptides in *Synechococcus* 6301 following long term labeling with ^{32}P *in vivo.* These polypeptides were of molecular weights 15 kDa and 18.5 kDa and identified as PS II and PBS components respectively (Sanders and Allen, 1988). Harrison *et al.* (1991) showed that phosphorylation of 18.5 kDa polypeptide is reversibly light-dependent but is not coupled to the reduction of PQ pool. However the phosphorylation of 15 kDa polypeptide occured specifically under PQ-reducing conditions giving rise to state 2. Canaani (1986; 1987) provided indirect evidence for involvement of protein phosphorylation *in vivo* state transition. Treatment of *Nostoc sp.* with NaF, a potent phosphatase inhibitor, prevented state 1 transition.

Based on the observed changes in absorption cross-section during Chl a excitation (Murata, 1969; Dominy and Williams, 1987; Salehian and Bruce, 1991) this model has been retracted (Williams and Allen, 1987) and modified as the PBS detachment model.

PBS detachment

This is a photoprotective model suggested by Mullineaux and Allen (1988). It proposes that in transition to state 2, reduced PQ activates a protein kinase which phosphorylates PBS, phospho-PBS then detaches from PS II and remains dissociated from both photosystems. There is also a proposed conformational change in the membrane bringing the two photosystems closer to each other increasing transfer of excitation energy from PS II Chl a to PS I Chl a (Mullineaux and Holzwarth, 1990). Upon transition to state 2 PBS

contributions to both PS II and PS I will decrease. However complementary changes will be expected for Chl a excitations. The authors indicate that the excitation energy absorbed by PBS does not dissipate by fluorescence as no fluorescence increase of the terminal emitter is seen at room temperature or at low temperatures. It has been suggested that the excitation energy from phycobilisomes with no attached PS II reaction center could be dissipated by non-radiative decay processes (Mullineaux and Allen, 1988). Manodori and Melis (1986) have suggested that the 75 kDa terminal exciton acceptor polypeptide of the PBS may act as a fluorescence quencher when the PS II reaction center is not attached.

Electron transport measurements

Since the discovery of state transitions fluorescence has been the common assay used by investigators. However fluorescence is not the direct measure of activity. Measuring electron transport properties of PS II and PS I should give a direct measurement of excitation energy distribution. Fork and Satoh (1983), Satoh and Fork (1983), Biggins (1983) and Biggins *et al.*, (1984) showed a 30-100% increase in PS I turnover upon transition to state 2. EPR studies (Weaver, 1984) have also shown an increase in the rate of P-700 photooxidation.

When looking at P-700 redox changes, we see the steady state redox level in P-700. PS II activity reduces P-700 whereas PS I turnover results in oxidation of P-700. The reduction of PS I has two components, electrons arriving from water and electrons arriving from the respiratory electron transport chain. While the PS II activity can be eliminated in the presence of DCMU the respiratory

electron transport will still reduce P-700. This is mainly due to the intersection of the respiratory and photosynthetic electron transport chains in these organisms (discussed in the section respiratory electron transport). The solution to this problem is to use single reaction center turnover flashes. This will turnover the centers once and oxidize P-700 on a much faster time scale than the subsequent reduction via the respiratory chain.

Changes in PS II electron transport have also been reported by Ley (1984) showing differences in O_2 flash yields and Canaani (1986, 1987) using photoacoustic spectroscopy to monitor oxygen evolution. These studies showed that the rate of oxygen evolution decreased in transition to state 2 indicative of less excitation energy reaching PS II.

The models for state transition in PBS-containing organisms discussed earlier make specific predictions about the extent of P-700 oxidations in the two states. The mobile PBS model predicts an increase in extent of P-700 photooxidation for wavelengths of light absorbed by PBS only. For the PBS-detachment model the extent is expected to be higher for Chl a absorbed light, but a decrease is predicted for PBS absorbed wavelengths. The spillover model predicts an increase in the extent of P-700 oxidation for wavelengths of light absorbed by both Chl a and PBS.

Fluorescence measurements

If the purpose of photosynthesis is to convert excited state energy into chemical free energy with the maximum efficiency, it might seem strange that any light energy at all is wasted as fluorescence from photosynthetic apparatus. However, Bolton *et al.* (1981) have argued from the second law of thermodynamics that for maximal energy storage a certain small loss by fluorescence is unavoidable, and that part of fluorescence from plants is believed to result from back electron transfer at reaction centers.

Absorption of a photon raises a pigment molecule to its lowest singlet excited state or to one of its many higher energy excited states. Usually, energy in excess of its lowest excited state is dissipated quickly as heat. There are always at least three options for the decay of the lowest singlet excited state. These are fluorescence, in which the molecule returns to the ground state by emission of a quantum of light, internal conversions, in which the energy of the molecule is converted into vibrational energy of the ground state, and intersystem crossing to the triplet with descent to the lowest triplet excited state.

The photosynthetic pigments except carotenoids, when extracted from the photosynthetic membrane with polar organic solvents, emit fluorescence with high quantum yields. In intact chloroplasts, isolated thylakoid membranes and intact cells the room temperature fluorescence is attributed mainly to PS II; since the fluorescence from PS I is very weak. In PBS-containing organisms, fluorescence from PBS is observed due to a less efficient energy transfer to PS II.

The fluorescence yields of the reaction center complexes are affected by changes in energy trapping, excitation energy transfer between pigment protein complexes and the absorption cross section. The changes seen in fluorescence are regarded as indicators of the rates of transfer of excitation energy within the photosynthetic pigment system (Papageorgiou, 1975).

Duysens and Sweers (1963), studying room temperature fluorescence of Chl a, correlated the fluorescence changes seen with the redox state of an electron acceptor of PS II. This acceptor has since been recognized as Q_A, the first quinone acceptor immediately after pheophytin.

During illumination with continuous excitation light, the F_{685} (fluorescence at 685 nm) of whole cells or chloroplasts poisoned with DCMU rises to a minimal level F_0. At F_0 all PS II reaction centers are open and hence Q_A is maximally oxidized. The fluorescence yield, ϕF_0 at F_0 is given by,

$$\phi F_0 = K_f/(K_f + K_h + K_{t(II-I)} + K_p) \qquad (1)$$

where K_f is the rate constant for fluorescence, K_h is the rate constant for radiationless decay to heat, $K_{t(II-I)}$, is the rate constant for energy transfer from PS II to PS I and K_p is the rate constant for PS II photochemistry (Hipkins and Baker, 1986).

After this initial rise to F_0, a slower rise of fluorescence to a final maximum level known as F_m is observed. At F_m all of PS II reaction centers are closed and Q_A is maximally reduced. The fluorescence yield at F_m is given by,

$$\phi F_m = K_f/(K_f + K_h + K_{t(II-I)}) \quad (2)$$

The variable part of the fluorescence is termed F_v and is given by

$$F_v = F_m - F_0 \quad (3)$$

The origin of variable fluorescence (F_v) has been attributed to the back reaction from pheo to P-680 producing singlet excited state of P-680 and not the triplet states (Klimov *et al.*, 1977). This back reaction increases with reduction of Q_A. Time-resolved fluorescence studies (Haehnel *et al.*, 1983) supports an alternative hypothesis that the fluorescence arises directly from the pigments rather the forementioned charge recombination (for a review see Holzwarth, 1986).

The fluorescence studies done at room temperature show contributions mainly by PS II Chl. To be able to see Chl fluorescence from PS I at room temperature spectrometers with fast time resolutions are required. Freezing the sample in liquid nitrogen (77K) resolves the PS II fluorescence into three bands at approximately 685, 695 and 750 nm and a broad PS I band seen at 715-720 nm. Studies done on isolated PS I particles (Satoh, 1982) shows a PS I band at 720 nm with a half-band width of about 25-30 nm. In isolated PS II particles there are distinct 77K fluorescence emissions at 685 nm and 695 nm with half-band widths of about 10 nm and 15 nm respectively (Satoh, 1979a; Satoh, 1979b). In PS II particles completely devoid of PS I contamination no fluorescence is seen at

720 nm however a wide emission band with a half-band width of about 35-40 nm is seen in the region near 750 nm (Murata and Satoh, 1986).

A fluorescence emission band is seen at about 650 nm. This band has been attributed to emission by the phycobillins. Second derivative analysis by Rijgersberg and Amesz (1980) showed that this band is comprised of three bands, one at 650 nm (phycocyanin), another at 658 nm (allophycocyanin) and a smaller band at 679 nm attributed to the terminal emitter of the phycobilisome (Zilinskas, 1982). This band has a half-band width of 13-16 nm.

Heat Loss measurements

The term photoacoustics (PA) or optoacoustics (OA) usually refers to generation of acoustic waves by modulated optical radiation. The PA effect was discovered by A.G. Bell (1880) who observed that audible sound is produced when chopped sunlight is incident on optically absorbing materials. Electronically excited molecules are deactivated by radiative (e.g. fluorescence) and radiationless decay processes. The later can be of chemical or physical nature and normally involves heat release to the surrounding medium.

Two modes can be used for the excitation of the sample. One utilizes an intensity-modulated continuous wave source, and phase sensitive detection. The other mode uses a pulse of light (normally a laser) to excite the sample, the heat released is then detected by a fast detector attached to an amplifier.

Modulated excitation

When a solid or liquid sample is irradiated by a modulated beam of radiation absorbed by the sample, the fraction converted to heat diffuses through thermal conduction to the sample surface. In every cycle, at the gas-sample boundary a thin layer of gas is expanded through heat, thus creating a pressure wave. This wave is detected by a microphone attached to a closed gas compartment. The heat emited by the sample is at the same frequency as the excitation light but phase-shifted. The magnitude of the phase shift will depend on the lifetime of the species (Moore, 1983). Thus if this species decays with a time constant larger than the modulation frequency of excitation it will act as energy storing species, and the heat emitted will be less than that from a standard releasing all of the absorbed energy. However if the time constant of decay of the species is smaller than the modulation frequency, the action spectrum of heat emission will be identical to the absorption spectrum of the sample (Braslavsky, 1986).

The photoacoustic spectroscopy (PAS) technique has been used extensively to quantitatively evaluate the photosynthetic energy storage and oxygen evolution *in vivo* in various organisms (Canaani and Malkin, 1984; Canaani, 1986; 1990; Carpentier *et al.*, 1985a and 1985b). Carpentier *et al.* (1984) observed that *Anacystis nidulans* releases 45% of the absorbed energy as heat with a lifetime of less than 740 μs, using a lower frequency the authors estimated that 25% of the absorbed energy is used to form products with lifetimes longer than 74 ms, most likely ATP and NADPH. Carpentier *et al.* (1985b)

subsequently reported that a photochemical loss was observed at modulation frequency of 35 Hz in PS II particles isolated from spinach. Thus reduced forms of electron acceptors in the electron transport chain decay with lifetimes longer than 30 ms. The PQ pool and the autooxidation products of the electron transport chain were postulated as possible candidates for this function. Polarized PAS studies on oriented chloroplasts (Frackowiak *et al.*, 1985) along with fluorescence and absorption spectroscopy were used to gain quantitative information on the influence of orientation in the excitation energy transfer of pigments within chloroplasts and thylakoids. Energy transfer *in vitro* between excited Chl a molecules and various quenchers was analyzed using PAS (Upadhyaya *et al.*, 1985). PAS has also been used to investigate the energy storage in the primary photochemistry of rhodopsin (Boucher and Leblanc, 1981).

Canaani (1986) used PAS to measure the modulated oxygen evolution in cyanobacteria during the state 1 to state 2 transition. She saw a 10 to 15% decrease in the oxygen evolution concomitant with an equal increase in the cross-section of PS I during the transition. Upon addition of NaF which blocks dephosphorylation of proteins, state 1 was abolished and only state 2 could be observed. Based on these results she suggested that in organisms containing phycobiliproteins, the level of protein phosphorylation controls the distribution of excitation energy between the two photosystems.

Malkin *et al.* (1990) used the photoacoustic method to monitor energy storage in the red algae *Porphyra perforata* in state 1 and state 2. They found that maximum energy storage was obtained with

modulated light absorbed by the PBS (light 2). Modulated light absorbed by the Chl a (light 1) gave much smaller energy storage (about 1/3 of the maximum). They suggest that light 2 is divided between the two photosystems by a different mechanism in each state. In state 1 there is strong dependence on the closure of PS II reaction centers, implying competitive energy transfer from PS II to PS I by spillover. In state 2 there is excitation balance already with open PS II reaction centers either by energy transfer from open reaction centers or by direct interaction of PS I with PBS. However it should be noted that all of these measurements are done on a long time scale of tens of milliseconds.

Pulsed excitation

For pulsed excitation the heat produced by the radiationless processes generates a pressure pulse which can be detected as an acoustic wave and a change in temperature resulting in change in the refractive index and formation of a thermal lens. The time-profile of heat released after absorption of a laser pulse is determined by the lifetime of the excited species. It can be studied by analyzing the acoustic wave (laser-induced optoacoustic spectroscopy, LIOAS) and the temporal changes in the refractive index (time-resolved thermal lensing, TRTL). Only LIOAS and its applications will be discussed here.

LIOAS allows the measurement of heat dissipation following the absorption of pulsed-laser events with the time-resolution of ns to μs (Tam, 1984; 1985) and even ps range when it is combined with other optical procedures (Rothberg *et al.*, 1983). For a weakly absorbing

solution of calorimetric standard the amplitude of the acoustic wave is determined by the time-width of the laser beam, τ_1 and by the acoustic transit time, τ_a which is given by,

$$\tau_a = R/v_a \qquad (4)$$

τ_a is the time required by the acoustic wave to travel across the laser beam of radius R with the velocity of sound v_a in the medium. For a general case the amplitude of the acoustic wave is proportional to

$$(\tau_a^2 + \tau_1^2)^{-3/4} \qquad (5)$$

using ns laser pulses $\tau_1 << \tau_a$ and τ_a is the limiting factor in determining the amplitude of the acoustic pulse (Tam, 1986).

With molecular species undergoing relaxation via non-radiative processes with lifetime τ_{nr}, for a particular τ_a the heat delivered to the medium by all processes with $\tau_{nr} < 2\tau_a$, is integrated in the first amplitude of the pressure signal (Heihoff *et al.*, 1987). The shortest time resolution for the pulsed techniques is determined by τ_1. For a particular τ_1, τ_a can be decreased by decreasing R to a limit compatible with the limit of the technique. Therefore τ_1 determines the prompt heat integration time. All processes delivering heat with a time constant shorter than τ_1 will be detected as fast, while those slower than τ_1 will act as energy storing steps (Braslavsky and Heihoff, 1989).

The amplitude of the signal is dependent on the thermoelastic properties of the medium. For example the generation of an acoustic

wave by thermal expansion is determined by the expansion ΔV of the heated volume V_0,

$$\Delta V=\beta H/(c_p.\rho) \qquad (6)$$

where β is the volume expansion coefficient, H is the heat deposited in volume V_0, c_p is the specific heat at a constant pressure per unit mass and ρ is the density. Thus the acoustic efficiency is characterized by,

$$M_{PA}=\beta/(c_p.\rho) \qquad (7)$$

where M_{PA} is the photoacoustic figure of merit (Tam, 1986). Therefore increasing the above ratio increases the optoacoustic signal amplitude.

Signal handling in LIOAS

The amplitude of the pressure detected by the piezoelectric element is as follows,

$$P(r,t\ \pm) = F(v_a/R,\ \beta/c_p)\ E_0(1-10^{-A})\ (\tau_a^2+\tau_1^2+\tau_{nr}^2)^{-3/4}\ f(\xi) \qquad (8)$$

where $F(v_a/R,\ \beta/c_p)$ is function of thermoelastic parameters in the medium, τ_{nr} is the lifetime of the species decaying in non-radiative process, $f(\xi)$ is the spatial and temporal distribution of the pressure profile, E_0 is the incident excitation energy and A is the absorbance of the sample (Braslavsky and Heihoff, 1989). Hence the amplitude

and the form of the pulse is determined by the absorbed energy, the thermoelastic parameters of the medium and the time-width of the excitation beam. The amplitude of the LIOAS signal H obtained with piezoelectric element is related through an apparative constant to the pressure from the above equation and can be written as,

$$H = \text{constant}.P(r,t \pm) \qquad (9)$$

for constant excitation beam conditions, H has the following form,

$$H = K\alpha E_0(1-10^{-A}) \qquad (10)$$

with K containing the thermoelastic parameters and the apparent constant, and α is the fraction of the absorbed energy that is dissipated as heat. In order to eliminate K, a calorimetric reference is needed. Using this reference with $\alpha=1$, the value of α for the sample will be the ratio between H/E_0 for the sample and reference. This ratio can be calculated from the slopes of linear plots of H Vs. E_0 for the sample and reference. Hence, with external heat calibration α is equal to the ratio of the normalized signals from the sample with open reaction centers, H_{op} and from the reference, H_{ref}

$$\alpha = H_{op}/H_{ref} \qquad (11)$$

However, for the case of internal heat calibration increased fluorescence should be taken into account. Then α is given by

$$\alpha = (1- \phi_f^{cl} \upsilon_f/\upsilon_e) \; H_{op}/H_{cl} \qquad (12)$$

Where ϕ_f^{cl} is the fluorescence yield of closed reaction centers, υ_f and υ_e are the frequencies of the weighted average of fluorescence and excitation respectively, and H_{op} and H_{cl} are the energy-normalized optoacoustic signal amplitudes of samples with open and closed reaction centers respectively.

Reference systems

In order to obtain quantitative information from the data we need the use of a calorimetric standard. This is a substance with an absorption spectrum overlapping that of the sample and losing all absorbed energy as heat with lifetime shorter than the time-resolution of the method and showing no fluorescence and no photochemistry. The signal produced by the standard should be measured under identical conditions of geometry, temperature and solvent composition since the signal is dependent on these factors. Copper (II) and Cobalt (II) salts (chloride and sulfate) are ideal for this use. This method of calibration is known as external calibration. Another possibility to obtain a reference signal is to use the system studied under conditions such that the photochemical reaction is inhibited. This principle has been used for study of heat release in photosynthetic units. The same sample under background illumination to close the reaction centers was used as reference (Nitsch *et al.*, 1988; 1989; Bults *et al.*, 1982). This form of calibrating the setup is known as the internal calibration.

LIOAS applications

A highly corrosion-resistant cell design for LIOAS with PZT ceramic (Tam and Patel, 1980) has been modified and used for different substances (Braslavsky, 1985). Radiationless processes of biliverdin dimethyl ester in ethanol was studied by LIOAS (Braslavsky, 1983). Jabben *et al.* (1984) used LIOAS to study the phytochrome photoconversion processes. The first report on the application of LIOAS *in vivo* (Jabben and Schaffner, 1985) showed that the technique could be used as probe to study the time-course in the ns to μs range of heat dissipation during the early steps in photosynthetic electron transfer. Nitsch *et al.* (1988) studied the heat loss properties of isolated PS I and PS II particles form cyanobacterium *Synechococcus sp.* in early stages of electron transfer (1.4μs). From these midpoint potentials for A_1^-/A_1 and Q_A^-/Q_A was calculated. The same technique was applied to whole cells of *Rhodospirillum rubrum* and midpoint potentials for the Q_A^-/Q_A couple was calculated (Nitsch *et al.*, 1989).

Limits of detection of parts per billion levels or below were reported for a series of porphyrins, vitamines and drugs using LIOAS (Voigtman *et al.*, 1981), these results indicate the power of LIOAS to detect non-luminescent substances in an easy fashion.

MATERIALS AND METHODS

Growth and harvesting of cells

The cells of *Synechococcus sp.* PCC 6301 (formerly *Anacystis nidulans* were grown photoautotrophically at 30°C on BG-11 medium (Appendix B). The cells were grown on a gyratory shaker providing aeration with air mixed with 4% CO_2 and illuminated at a white light intensity of 25 $\mu E\ m^{-2}\ s^{-1}$. The cells were harvested during the exponential growth phase by centrifugation (5000 rpm), washed and resuspended in growth medium (BG-11) to desired optical density of 0.6 at 680 nm.

Induction of state transitions for 77K fluorescence studies

State transitions were induced in the presence of 1μM DCMU (dichlorophenyl dimethyl urea). 75μl aliquots were placed in sealed pasteur pipettes (Kimble) and brought to state 1 by 1 min. illumination with red light (>670 nm) of 200 Wm^{-2} and after a 5 s dark adaptation were quickly frozen in liquid nitrogen. To bring cells to state 2, 75 μl aliquots were kept in the dark for a period of 2 min and quickly frozen in liquid nitrogen. When NMR tubes were used (Wilmad glass Co. PP-504-9) the procedure was same as above except that 200 μl of the sample was used.

Measurement of 77K fluorescence emission

77K fluorescence emission spectra were obtained with a lab built spectrofluorimeter based on a Jarrel Ash 1/4 m spectrograph and EG&G detector (1420 R) controlled by an EG&G detector interface (1461) accessed by IBM-386 compatible computer. Excitation light

was supplied by a 100 W tungsten halogen lamp dispersed by a Jobin Yvon H 20 spectrometer. The fluorimeter was calibrated using a standard Neon lamp (Instrumentation Laboratory Inc.).

A spinning NMR sample tube holder driven by compressed extra-dry nitrogen (Varian A60-A high resolution NMR spinning assembly) held sample tubes in the optical path of the spectrofluorimeter. These NMR tubes (Wilmad Glass Co. PP-504-9) were spun at about 1000 rpm using the above assembly during the 25 second exposure time of the diode array used to obtain the emission spectra, resulting in a signal averaging of the fluorescence emission over the NMR tube surface. This technique corrects for the random scattering and sample inhomogeneities that interfere with fluorescence yield determinations from frozen samples (Bruce *et al.*, 1989a). Using this technique repeated fluorescence yield determinations were always within 4% (Salehian and Bruce, 1991; Bruce *et al.*, 1989a). Fluorescence was detected at 90 degrees to the excitation axis. Spectra were corrected for diode array sensitivity.

Fluorescence excitation spectra

Emission spectra were collected for cells in state 1 and state 2 using the spinning NMR tubes for excitation at four wavelengths in the Chl a absorption region (425, 430, 435 and 440 nm) and four wavelengths in the PBS absorption region (590, 595, 600 and 605 nm). Excitation spectra for PS I and PS II were constructed from PS I and PS II components' amplitudes used to model the emission spectra collected at the excitation wavelengths in the Chl a and phycobilin absorption region. These spectra were corrected for the

monochrometer output by measuring the intensity of light at the specific wavelength (LI-COR photometer).

Spectral Fitting

Emission spectra of relative fluorescence intensity versus wavelength were converted to frequency units (wavenumbers) and modelled with a commercial curvefittng progam, Spectra Calc (Galactic Industries). Log-normal or gaussian/lorentzian mixtures distributions were used to fit the components of the emission spectra. A minimum of 6 components were used to model the fluorescence emission spectra, they are PBS at 655 and 682 nm, PS II at 685, 695 and 750 nm and PS I at 717 nm. Each component has four parameters, these are amplitude, half-band width, position and shape. Table 1 lists the fixed parameters for all of the components. Each set of curves (PBS or Chl a excitation) were modelled with the same set of parameters. The amplitude of the component was the only parameter that was allowed to change during the fitting procedure.

Heat loss measurements

50 mls of cell suspension were constantly circulated at a rate of 10 ml/min from a 35 ml reservoir thermostated at 30°C, to a 1 cm^2 glass cuvette and back with a peristaltic pump (Masterflex) to replace the irradiated sample volume after every 3 laser pulses and to prevent sedimentation of cells. State 2 was achieved by keeping the reservoir in the dark and state 1 by illuminating the reservoir with >670 nm light (200 Wm^{-2}). There was a 4 second dark interval between the reservoir and the measuring cuvette to allow the

Table 1. Fixed parameters for the 6 components used to model the 77K fluorescence emission spectra of intact cells in state 1 and state 2. The amplitude of the component was the only parameter allowed to change during the fitting procedure. Half-band width refers to the width of the distribution in nm, at half the maximum height. A mixture of gaussian and lorentzian distributions were used as component shape for all the components except the PBS and PS I components which were set as log-normal distributions.

Wavelength (nm)	Half-band width (nm)	Component shape
657 PBS	18	log-normal
679 PBS	13	mixture
685 PS II	9.6	mixture
695 PS II	12	mixture
713 PS I	25	log-normal
747 PS II	53	mixture

reaction centers (RC) to open before measurement in state 1. A 75 µl sample for 77K fluorescence emission spectroscopy was removed from the cuvette prior to the laser flash. The laser induced optoacoustic detector and amplifier were home-built following the design of Patel and Tam (1981). A PZT cylinder of 4 mm diameter and 3 mm height is pressed against a stainless steel diaphragm that is polished on both sides. The PZT element is enclosed in the stainless steel shell to minimize electromagnetic pickup, corrosion and absorption of stray light. A 250 ns pulse from a flash-lamp pumped dye laser (Phase-R, DL-32) at a repetition rate of 0.2 Hz was used. For excitations between 600 nm and 690 nm, DCM was used as laser dye (Exciton), and for 590 nm, Rhodamine G (Phase-R) was used as the laser dye. Intensity of the exciting laser flash was attenuated with neutral density filters and a variable neutral density wedge. The energy of each laser pulse was determined directly with a laser pulse pyrometer (Molectron). Figure 4 shows the schematics of the setup for laser induced optoacoustic spectroscopy (LIOAS).

The laser beam diameter was varied by using pinholes of 2 and 3 mm corresponding to an effective acoustic transit time (τ_a) of 1.35 µs and 2 µs respectively, since

$$\tau_a = 2R/ v_a$$

where τ_a is the transit time, v_a is the speed of sound, (for an EG / water mixture it is 1465 $m.s^{-1}$) (Heihoff *et al.*, 1987) and 2R is the diameter of the laser beam.

Figure 4. Schematic of laser-induced optoacoustic spectroscopy (LIOAS) setup. Excitation light is supplied by a tunable flashlamp dye laser. Using a beam splitter 50% of the laser beam is reflected into a pyrometer for measurement of the intensity. Simultaneous measurements of LIOAS signals and laser flash intensity are made using this setup.

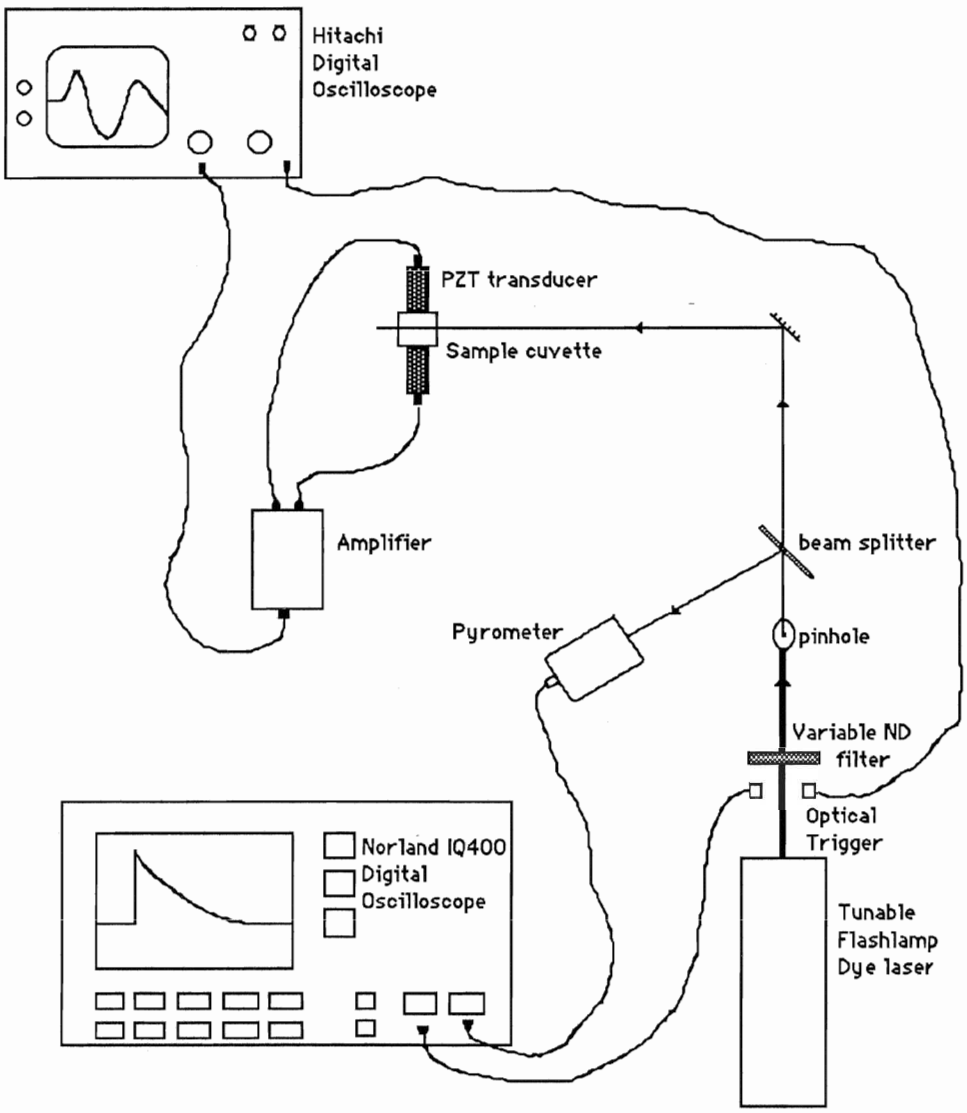
Hitachi
Digital
Oscilloscope
PZT transducer
Sample cuvette
Amplifier
beam splitter
Pyrometer
pinhole
Variable ND
filter
Optical
Trigger
Norland IQ400
Digital
Oscilloscope
Tunable
Flashlamp
Dye laser

In order to increase the signal-to-noise ratio a combination of two PZT transducers attached to the opposite walls of the cuvette was used (Figure 5). If the laser beam passes exactly through the middle of the cuvette the signals from the two detectors will be in phase and can be superimposed (Nitsch *et al.*, 1988).

An additional signal contribution due to scattered light absorption by the detectors was observed as a small shoulder to the first peak. This was specially a problem at lower laser intensities. In order to minimize the effect of this signal on our measurements I used a different measurement than used by others (Nitsch *et al.*, 1988, 1989). Instead of measuring from baseline to the first peak, measurements were done from height of the first peak to the trough of the second peak (Figure 6). This mode of measuring the optoacoustic signal also minimized the distortion of measurment by the radiofrequency (RF) pick up by the amplifier and detectors.

In order to obtain larger optoacoustic signals the suspension of cells was diluted with ethylene glycol (EG) to a final concentration of 10% v/v. It has been shown that addition of EG has no visible effect on the electron transport in PS II and PS I particles (Nitsch *et al.*, 1988) and the presence of EG did not affect the 77K fluorescence emission spectra of the cells. The amplitude of the pressure pulse is directly proportional to the ratio β/c_p of the medium (Patel and Tam, 1981), where β is the coefficient of cubic expansion and c_p is the specific heat capacity. This ratio for EG is five times larger than the ratio for water (Nitsch *et al.*, 1988) and is used to increase the signal-to-noise ratio.

Figure 5. Closeup of piezoelectric transducer. In order to increase signal to noise ratio two transducers are placed on opposite walls of the cuvette. If the laser beam is passed through the middle, signals from the two transducers are in phase and can be superimposed. The PZT ceramic is enclosed in a stainless steel cover to reduce electromagnetic pickup. The outputs from the PZT transducers are then amplified and digitized (see materials and methods).

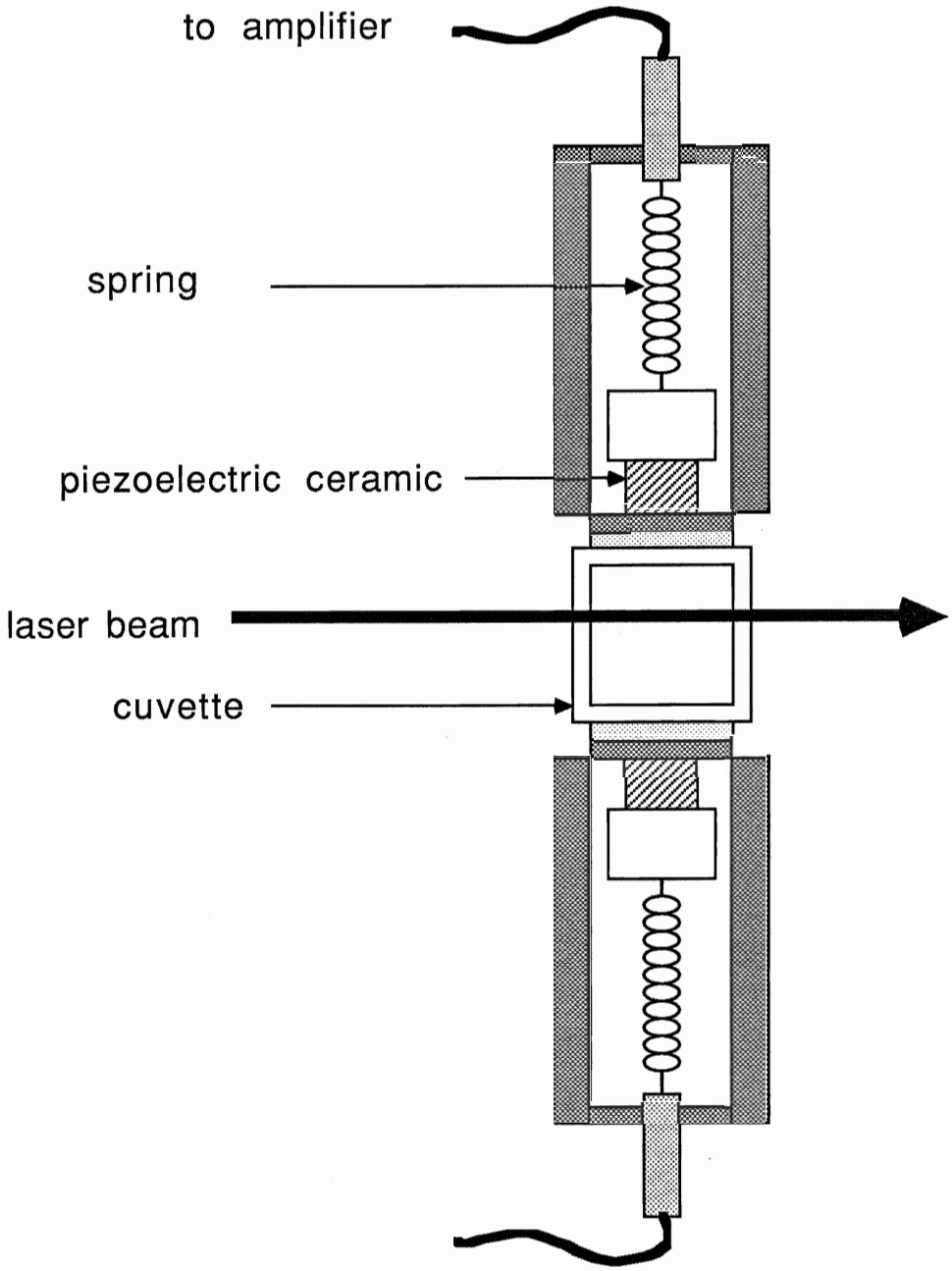
to amplifier
spring
piezoelectric ceramic
laser beam
cuvette

Figure 6. This figure shows the LIOAS signal trace for 590 nm (E= 0.15 mJ) excitation and a beam diameter of 3 mm obtained from intact cells of *Synechococcus sp.* PCC 6301. The laser was fired at time 0. Distance H is the size of optoacoustic signal (see materials and methods).

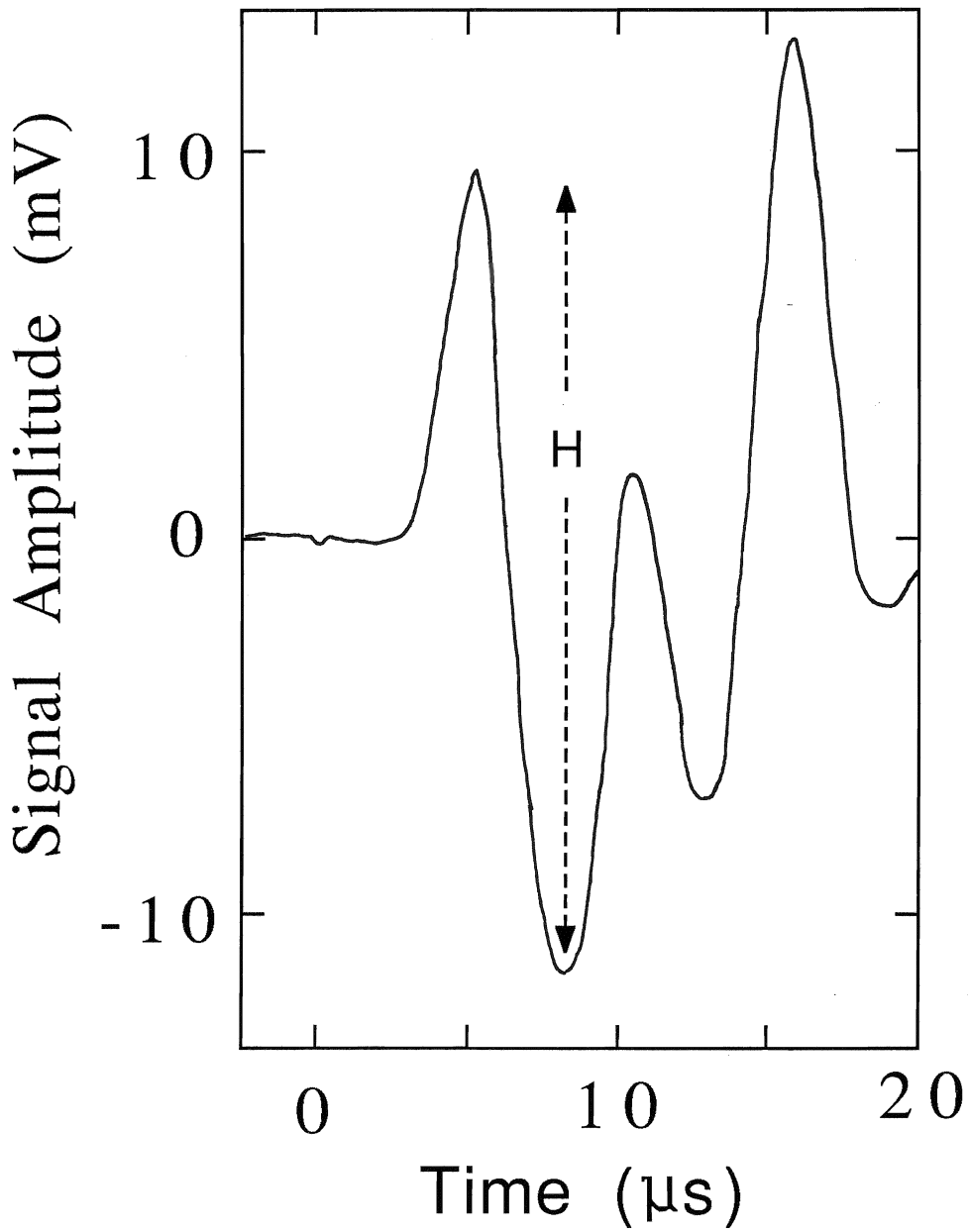
Signal Amplitude (mV)
10
0
-10
H
0
10
20
Time (µs)

Temperature dependence of the LIOAS signal was studied as follows. A hollow copper coil was attached between the reservoir and the cuvette and placed in a refrigerating circulator (Lauda RMS-6). A 6 X 10^{-4} M solution $CuCl_2$ (calorimetric standard) made in doubly distilled water was then pumped through this setup. The temperature inside the cuvette was measured using a Digi-Sense thermocouple simultaneously with the LIOAS measurements. Measurements of the optoacoustic signals were then made between 4 and 20°C using the procedure described above. A suspension of cells was brought to the same optical density at 665 nm as the $CuCl_2$ solution using the DW2 spectrophotometer. Measurements of the optoacoustic signal were then made between 4 and 20°C in the same manner. NaCl was added to the $CuCl_2$ solution to a final concentration of 0.5 M. Optoacoustic signals were then measured at different temperatures on this sample as described above.

For LIOAS action spectra of cells, the wavelength of exciting laser flashes was varied from 605 nm to 690 nm (DCM laser dye) and LIOAS signals were measured from cells with closed reaction centers (background illumination). Simultaneous measurements of laser flash intensity was done as described previously. This action spectrum is then compared to the absorption spectrum of the same cell suspension collected using the DW2 spectrophotometer. As a control 100 µl of domestic bleach (Javex) was added to the circulating sample of cells and action spectra were collected for the bleached cells as described above.

The error in the measurements of LIOAS signals was calculated to be between 0.2% for high intensity laser flashes and 55% for very low intensity laser flashes (see appendix A).

Heat calibration

For a dilute sample the voltage amplitude H of the optoacoustic signal is given by the following equation (Braslavsky, 1987)

$$H = K \alpha E_0 (1-10^{-A}) \qquad (10)$$

where K is the proportionality constant containing geometrical and thermoelastic parameters, E_0 is the incident excitation energy, A is the sample absorbance and α is the fraction of of absorbed energy that is dissipated as heat within the effective acoustic time (τ_a). For a calorimetric standard such as $CuCl_2$ and $CoCl_2$ which release all energy absorbed by prompt thermal deactivation proceses within a few nanoseconds, α is equal to 1 (Braslavsky *et al.*, 1983) and can be used for external heat calibration. For a sample whose energy is stored by products longer than τ_a or lost as fluorescence, α is less than 1. Internal heat calibration in photosynthetic systems can be achieved by measurements on closed reaction centers for the same sample. External heat calibration was done by using a solution of $CuCl_2$ with the same optical density at 590 nm as the cell suspension. Internal heat calibration was done by illuminating the measurement cuvette with white light (2000 Wm^{-2}) to close the reaction centers.

Calculations for energy storage

Heat emission measured by LIOAS can be calibrated externally by using $CuCl_2$ or internally by closing all the reaction centers in a photosynthetically active system. For $CuCl_2$ the fraction of the absorbed energy lost as heat, α, is equal to one and a $CuCl_2$ solution adjusted to the same absorbance as the sample acts as an external reference for the maximum heat emission. For photosynthetically active samples internal heat calibration is possible by determination of heat loss when all the reaction centers are closed. Under these conditions all the energy absorbed by the antenna pigments is released either as heat or fluorescence. Hence the fraction of absorbed energy released as heat, α, should be corrected for fluorescence loss of the closed reaction centers by equation 12,

$$\alpha = (1- \phi_f^{cl} \upsilon_f/\upsilon_e) H_{op}/H_{cl} \qquad (12)$$

The first approximation of the amount of photosynthetic energy storage (ΔE) is $1-\alpha$ if we assume a quantum yield of 1 for both reaction centers and the losses due to entropic changes and fluorescence from open reaction centers are insignificant. This energy can be corrected for the internal conversion losses from antenna pigment absorbing the excitation flash to the reaction center by the factor λ_{rc}/λ_e. where λ_{rc} is the wavelength of maximal absorption of the reaction center and λ_e is the excitation wavelength, then

$$\Delta E_{rel} = (1-\alpha) \lambda_{rc}/\lambda_e. \qquad (13)$$

As PS II and PS I are both contributing to the energy storage in intact cells I chose 690 nm as the approximate value for λ_{rc}.

PS I activity measurements

To measure P-700 redox kinetics a single beam spectrometer was designed and constructed. Light from a 40 mW 820 nm diode laser (Spindler and Hoyer DC 25F) was directed through a variable beam splitter into a PIN diode (United Detector Technology PIN diode 10D) placed behind the sample cuvette. The reflected fraction of the beam was directed off a gold mirrror into a reference photodiode (UDT 10D). 800 nm cut on filters (Corion LL-800) were placed in front of both the photodiodes. A concave mirror was used to collect the fluorescence at 90° from the sample and direct it into the reference PIN diode. The signals from the photodiodes were differentially amplified using a conventional high gain lab-built amplifier (Brock Electronics Shop). Hence the fluorescence and diode laser noise were subtracted from our measuring beam. Excitation flashes of 250 ns durations were generated by a Phase-R DL-32 flash lamp pumped dye laser. This laser beam was directed through a pinhole of 3 mm diameter and attenuated using a variable neutral density wedge. 50% of this beam was reflected into a Molectron laser pulse pyrometer for monitoring intensity of each laser flash.

Figure 7. Schematic for PS I activity measurement at 820 nm. The measuring beam was supplied by an 820 nm diode laser and excitation light supplied by a tunable flashlamp dye laser (see materials and methods). Correction for fluorescence was made by using a reference photodiode detecting fluorescence collected by a concave mirror. The excitation flash was directed through the bottom of the cuvette. Simultaneous measurements of P-700 transmittance change at 820 nm and laser flash intensity was done using this setup.

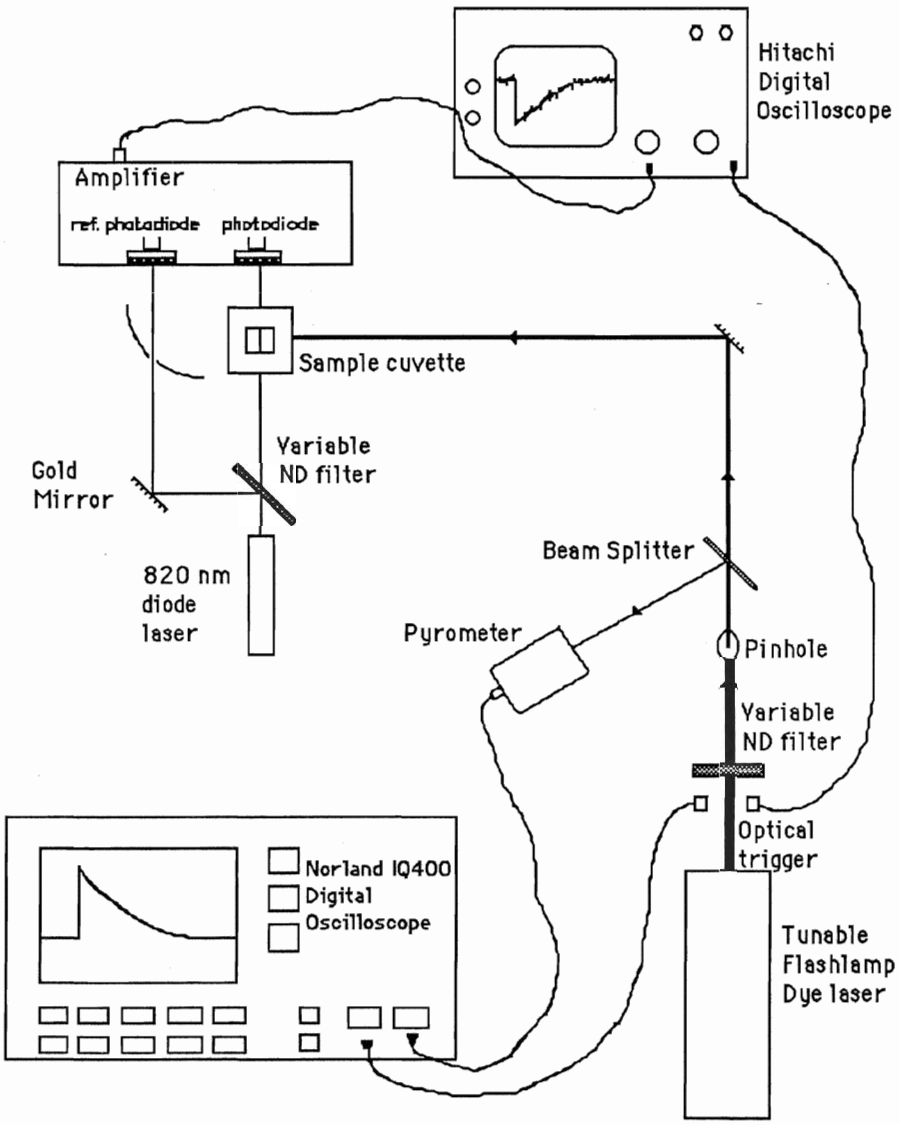
Hitachi
Digital
Oscilloscope
Amplifier
ref. photodiode
photodiode
Sample cuvette
Gold
Mirror
Variable
ND filter
820 nm
diode
laser
Beam Splitter
Pyrometer
Pinhole
Variable
ND filter
Optical
trigger
Norland IQ400
Digital
Oscilloscope
Tunable
Flashlamp
Dye laser

The other 50% was passed through a biconcave lens and reflected through the bottom of our sample cuvette. DCM was used as a laser dye for experiments between 605 and 690 nm. Signals from the pyrometer were digitized using a Norland IQ-400 digital oscilloscope and the signals from the photodiode amplifier were digitized using a Hitachi digital oscilloscope. Hence simultaneous measurements of P-700 at 820 nm and laser pulse intensity for every excitation were achieved. Figure 7 shows the schematic for the setup. To do measurements with cells in state 2 determinations were done in total darkness. For state 1 induction, >670 nm light (200 Wm^{-2}) was used to bring the cells into state 1. A shutter (Uniblitz SD-1000) was used to control the exposure of our sample to this light. Cells were brought to state 1 and state 2 in the presence of 1 μM DCMU. Before signal averaging began there was an initial 40 s exposure of sample to this light, and during signal averaging a 4 s exposure was followed by a 3 s dark interval before the excitation flash. This was done to ensure reopening of the reaction centers after the initial exposure. A Grass Instruments stimulator was used to trigger the actinic laser and the shutter with the appropriate delay. 75 μl samples were taken just prior to the laser flash for both cells in state 1 and state 2 for 77K fluorescence emission determinations. The error in the measurements of P700 photooxidations was calculated to be between 3% for high intensity laser flashes and about 70% for very low intensity flashes (see appendix A).

Absorption spectra

Absorption spectra of cells were obtained using a Beckman DU-50 spectrophotometer interfaced to a Comptech 286 computer by Beckman Instruments. BG-11 medium was used as a blank. An Aminco DW-2 spectrophotometer interfaced to a Compaq 286 computer by OLIS Inc. (Georgia) was used to match the absorbances of the $CuCl_2$ and the suspension of cells for the use in LIOAS measurements.

Chlorophyll determinations

1 ml. of the sample was removed and centrifuged at 13000 rpm for 2 min, the supernatent was discarded and the pellet was extracted with 90% methanol at 4°C in dim light. The solution was centrifuged at 13000 rpm for 2 min. and the supernatent was removed and its absorbance taken at 665 nm (Beckman DU-50) . The chlorophyll a content is calculated from this absorbance value using the following equation (Tandeau de Marsac and Houmard, 1988).

$$[\text{Chl.}]\ \mu g.ml^{-1} = 13.42 \times A_{665} \qquad (14)$$

PS I preparations

PS I particles were prepared following the procedure of (Williams *et al.*, 1983). Market spinach leaves were cut to small pieces and suspended in buffer solution containing 0.5 M sucrose, 0.1 M NaCl, 50 mM Tris-HCl and 20 mM sodium ascorbate (pH 8.0). The mixture was then blended and centrifuged at 3000g for 1 min to

remove the debris. The supernatent was then centrifuged at 20000g for 10 min and chloroplasts were pelleted. This pellet was then resuspended in a solution containing 0.1 M NaCl, 50 mM Tris-HCl, 20 mM sodium ascorbate and 1 mM EDTA (pH 8.0) and centrifuged at 30000g for 20 min. The pellet was resuspended in the same solution and the centrifugation step repeated. The pellet was then homogenized in 1% triton X-100, 50 mM Tris-HCl and 20 mM sodium ascorbate (pH 7.4) at a Triton:Chl ratio of 75:1 (w/w). The mixture was then stirred at 4°C for 15 min and centrifuged at 27000g for 10 min. The green supernatent was then loaded on a 60% to 40% discontinuous sucrose density gradient and centrifuged at 100000g for 30 min. The PS I particles settle at the boundary between the 40% and 60% sucrose solutions. The PS I particles removed are then diluted with the suspension buffer and centrifuged at 180000g for 10 min. The pellet containing PS I particles was then resuspended in the buffer for future use to a final Chl a concentration of 2 $\mu g.ml^{-1}$ using the following equation after extraction with 80% acetone.

$$\text{Total Chl. } (\mu g/ml) = 20.2A_{645} + 8.02A_{665}$$

RESULTS

Fluorescence

The low-temperature fluorescence emission spectra for intact cells of *Synechococcus sp.* PCC 6301 in states 1 and 2 are shown in figure 8. This figure shows the fluorescence emission spectra for 200 µl aliquots brought to state 1 and state 2 as described in materials and methods. The actinic wavelength was chosen to excite PC (590 nm). There are three PS II associated peaks at 685 nm, 695 nm and 747 nm and one PS I peak at 713 nm. There is a large change in the relative yields of PS II Chl a and PS I Chl a emission indicative of a state transition between the dark-adapted cells (state 2) and cells preilluminated in presence of DCMU (state 1).

Figure 9 shows the 77K fluorescence emission spectra of cells in state 1 and state 2 for excitation at 585 nm. The spectra have been modelled with the sum of six components. These are two PBS components at 657 nm and 679 nm, three PS II Chl a components at 685 nm, 695 nm and 747 nm, and one PS I Chl a component at 713 nm. The parameters for all these components are listed in table 1. On transition to state 2 a large decrease in amplitude of the 685 nm and 695 nm PS II components is apparent as is a smaller decrease in the amplitude of the 747 nm PS II component. These large changes are accompanied by a small increase in the 713 nm PS I component. A small increase in the

Figure 8. Shows the 77K fluorescence emission spectra for cells of *Synechococcus sp.* PCC 6301 in state 1 and state 2 for excitation in the PBS-absorbed region (585 nm). These spectra are not normalized. The 655 nm peak is associated with PBS emission, 685, 695 and 750 nm peaks associated with PS II emission and 713 nm peak is associated with PS I emission.

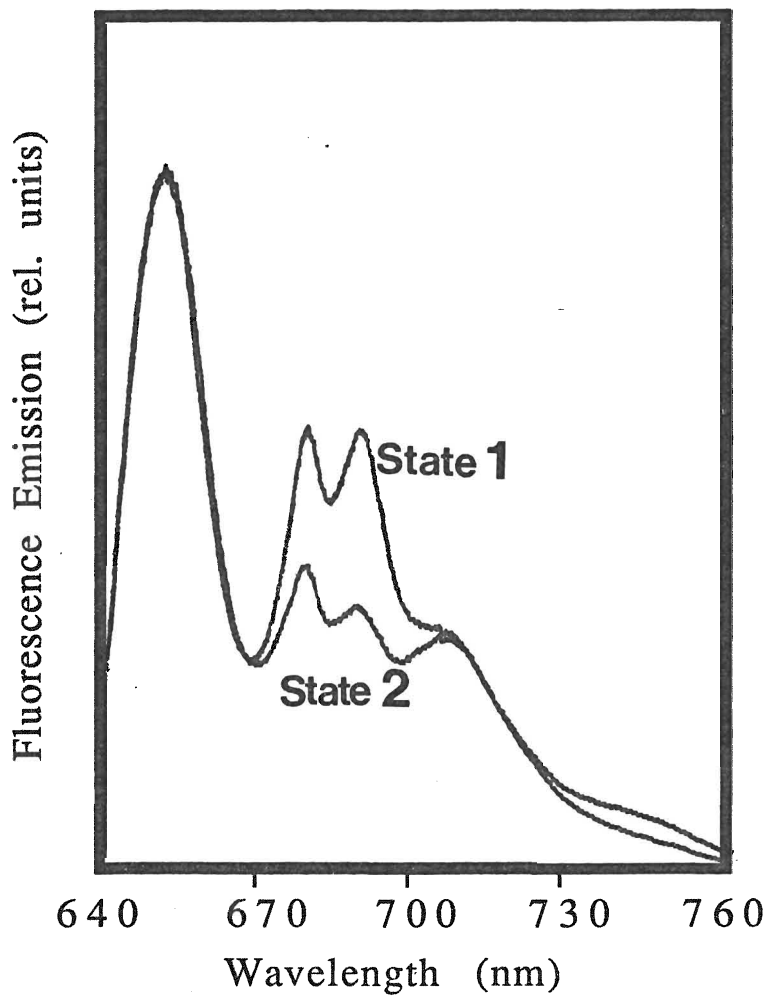
Fluorescence Emission (rel. units)
State 1
State 2
640
670
700
730
760
Wavelength (nm)

Figure 9. 77K fluorescence emission spectra for PBS excitation at 595 nm, modelled with 2 PBS components at 655 and 682 nm, 3 PS II components at 685, 695 and 750 nm, and one PS I component at 713 nm in the two states. The parameters used for each of these components are shown in table 1. Both the individual components and the sum of components are shown. The differences between the fits and the spectra are shown as residuals in the lower boxes.

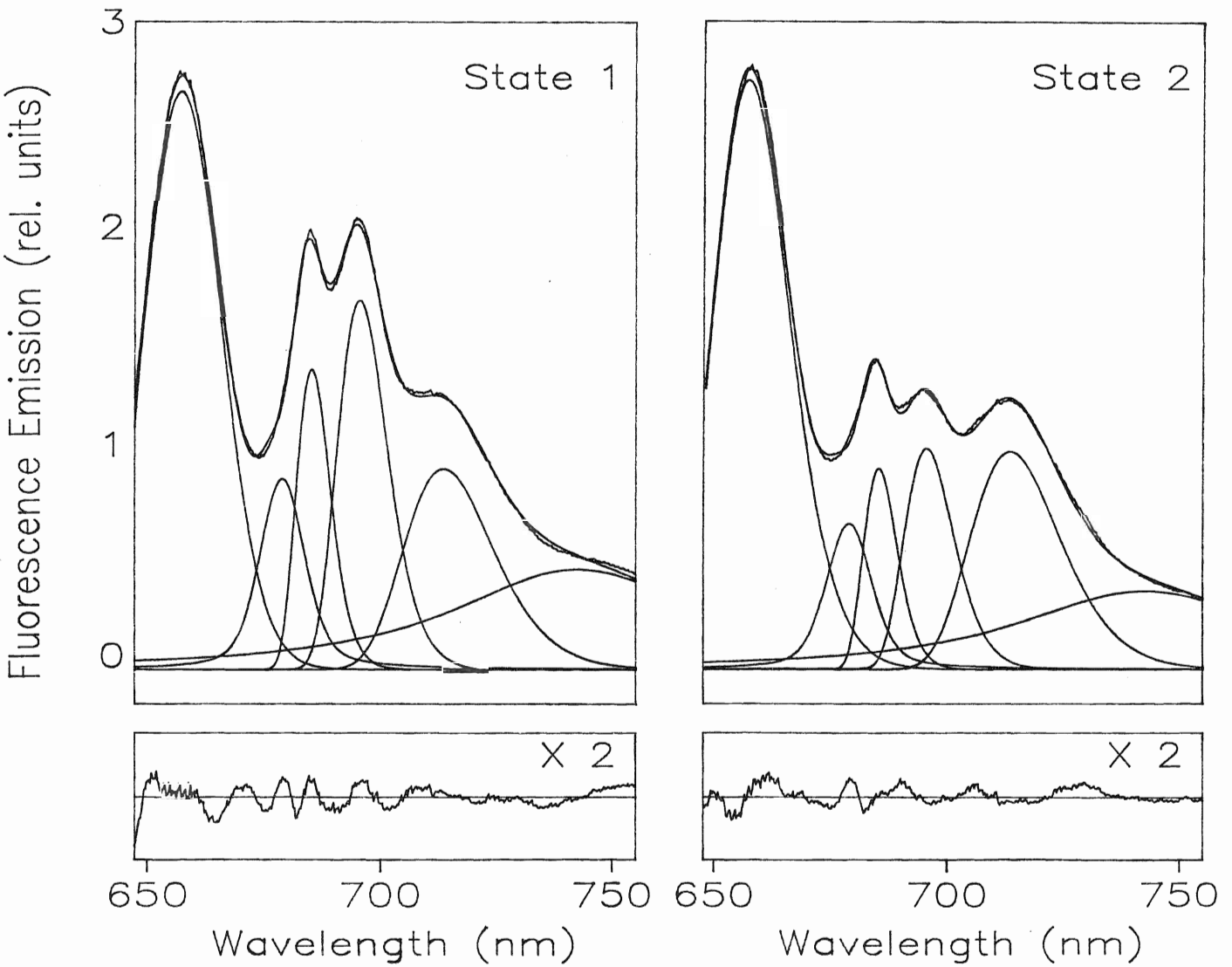
Fluorescence Emission (rel. units)
3
2
1
0
State 1
State 2
X 2
X 2
650
700
750
650
700
750
Wavelength (nm)
Wavelength (nm)

Figure 10. 77K fluorescence emission spectra of intact cells in state 1 and state 2 for Chl a excitation at 435 nm. The spectra have been modelled with a sum of 3 PS II components at 685, 695 and 750 nm and one PS I component at 715 nm. The emission from the PBS was negligible at this excitation wavelength and were set to zero amplitude. The differences between the fits and the spectra are shown as residuals in the lower boxes.

State 1
State 2
X 2
X 2
1
0.5
0
Fluorescence Emission (rel. units)
700
720
740
Wavelength (nm)

657 nm PBS component and decrease in the 679 nm PBS components are also noted.

Figure 10 compares the fluorescence emission spectra of cells in state 1 and state 2 for excitation at 435 nm. These spectra have been modelled with the same PS II Chl a and PS I Chl a components shown in figure 9. The PBS contributions at this wavelength are negligible and were set to zero amplitude. The amplitude of the 685 nm and 695 nm PS II components are observed to decrease dramatically from state 1 to state 2 with a smaller decrease in the 747 nm PS II component. The 713 nm PS I component increases on transition to state 2.

Fluorescence emission spectra similar to the ones in figure 9 and 10 were collected for three more excitation wavelengths in the Chl absorption region and three more excitation wavelengths in the PBS absorption region (see materials and methods). These spectra were then modelled with the same components. The components' parameters are listed in table 1. The fits were of very similar quality. These data were then used to create point by point excitation spectra in the PBS and Chl a absorption regions for PS II and PS I component amplitudes.

Figure 11 compares excitation spectra for the amplitudes of the 695 nm PS II component in state 1 and state 2. The large decrease in the yield of the 695 nm component on transition to state 2 is observed at both Chl a and PBS excitations. This change amounts to a 30 ± 2% decrease for the excitation in the Chl a region and a 40 ± 1% decrease for the excitation in the PBS region.

Figure 11. 77K fluorescence excitation spectra for the amplitude of the 695 nm PS II component for intact cells in state 1 (filled circles) and state 2 (triangles). These were generated from the modelled emission spectra at different excitation wavelengths absorbed by PBS and Chl a . Each point represents data from three different sets of experiments and the error bars reflect the standard deviation.

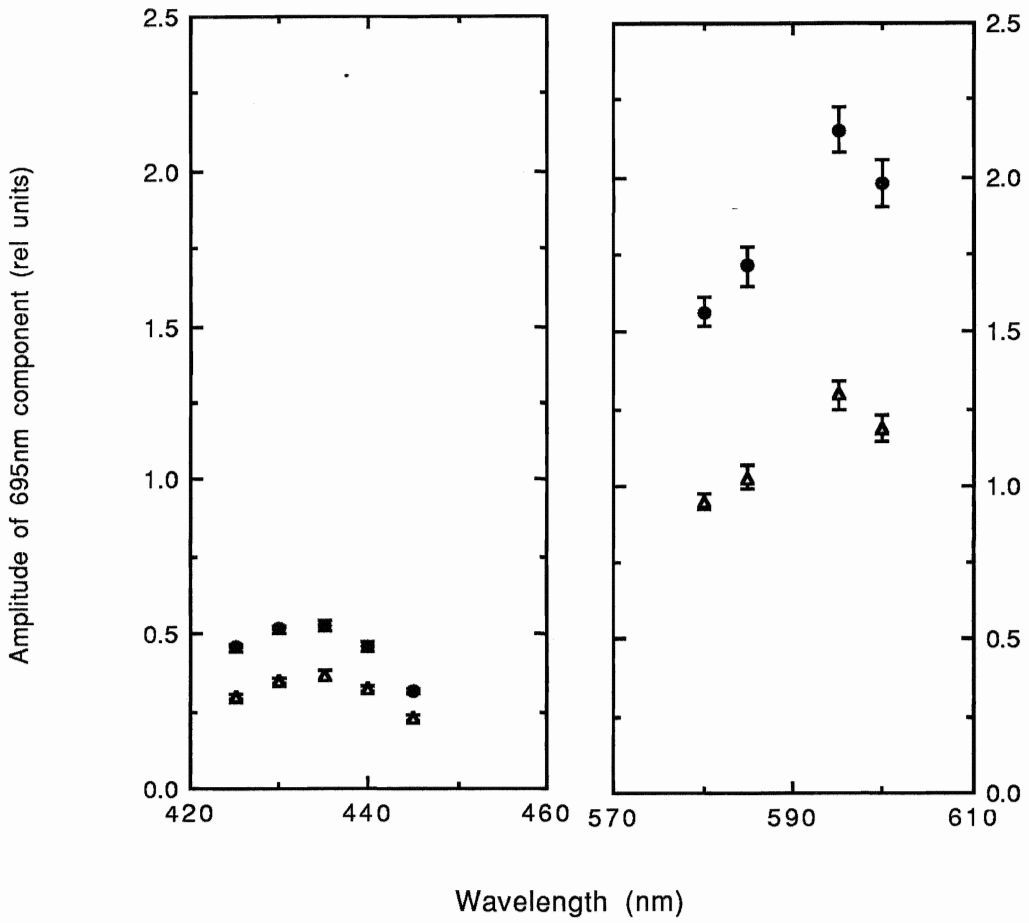
Amplitude of 695nm component (rel units)
2.5
2.0
1.5
1.0
0.5
0.0
420
440
460
570
590
610
Wavelength (nm)

Figure 12. 77K fluorescence excitation spectra for the amplitude of 713 nm PS I Chl a component for intact cells in state 1 (filled circles) and state 2 (triangles). These were generated from modelled emission spectra at different wavelengths absorbed by PBS and Chl a.

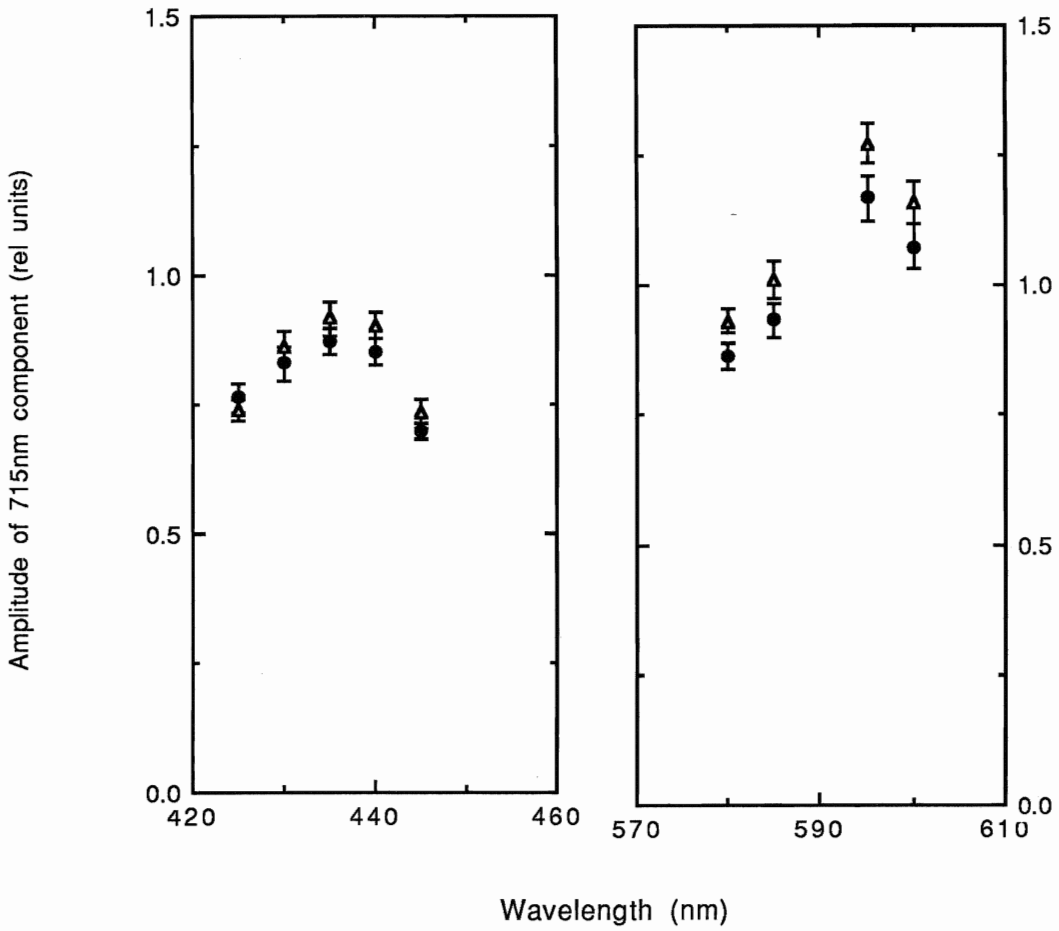
Amplitude of 715nm component (rel units)
1.5
1.0
0.5
0.0
420
440
460
570
590
610
Wavelength (nm)

Figure 12 compares the 713 nm PS I component excitation spectra in state 1 and state 2. The increases in the 713 nm PS I component on transition to state 2 are much smaller than the PS II decreases. This amounts to a 5.0 ± 1% for Chl a excitation and 8.4 ± 0.5% for the excitation of PBS.

Figure 13 compares the increased contribution to the PS I excitation spectra on transition to state 2 (the PS I state 2 minus state 1 difference spectrum) to the decreased contribution to the PS II excitation spectrum (the PS II state 1 minus state 2 difference spectrum). The PS II excitation spectrum in state 2 is also shown. These spectra were normalized to peak amplitudes to allow comparison of the relative contributions of PBS and Chl a to the spectra. The PS I difference spectrum shows the largest contribution of Chl a relative to PBS while the PS II difference spectrum shows the smallest contribution of Chl a relative to PBS. Both of these difference spectra substantially differ from the PS II excitation spectrum in state 2.

Heat loss

Figure 6 shows an example of the photoacoustic signal generated by intact cells of cyanobacterium *S. sp.* PCC 6301 after absorption of a laser pulse of 150 μJ intensity and 3 mm diameter. The amplitude of the first peak is proportional to the amount of the heat released by the suspension of cells and is given by equation 10. This first peak is followed by a series of oscillations at the resonance frequency of the piezoelectric crystal.

Figure 13. 77K fluorescence excitation spectra for 695 nm PS II component and the 713 nm PS I component amplitudes normalized to the peak emissions. The filled circles show the state 2 minus state 1 difference spectrum of the PS I component. The open squares show the state 1 minus state 2 difference spectrum of the PS II component and the crosses show the excitation spectrum for the PS II component at 695 nm.

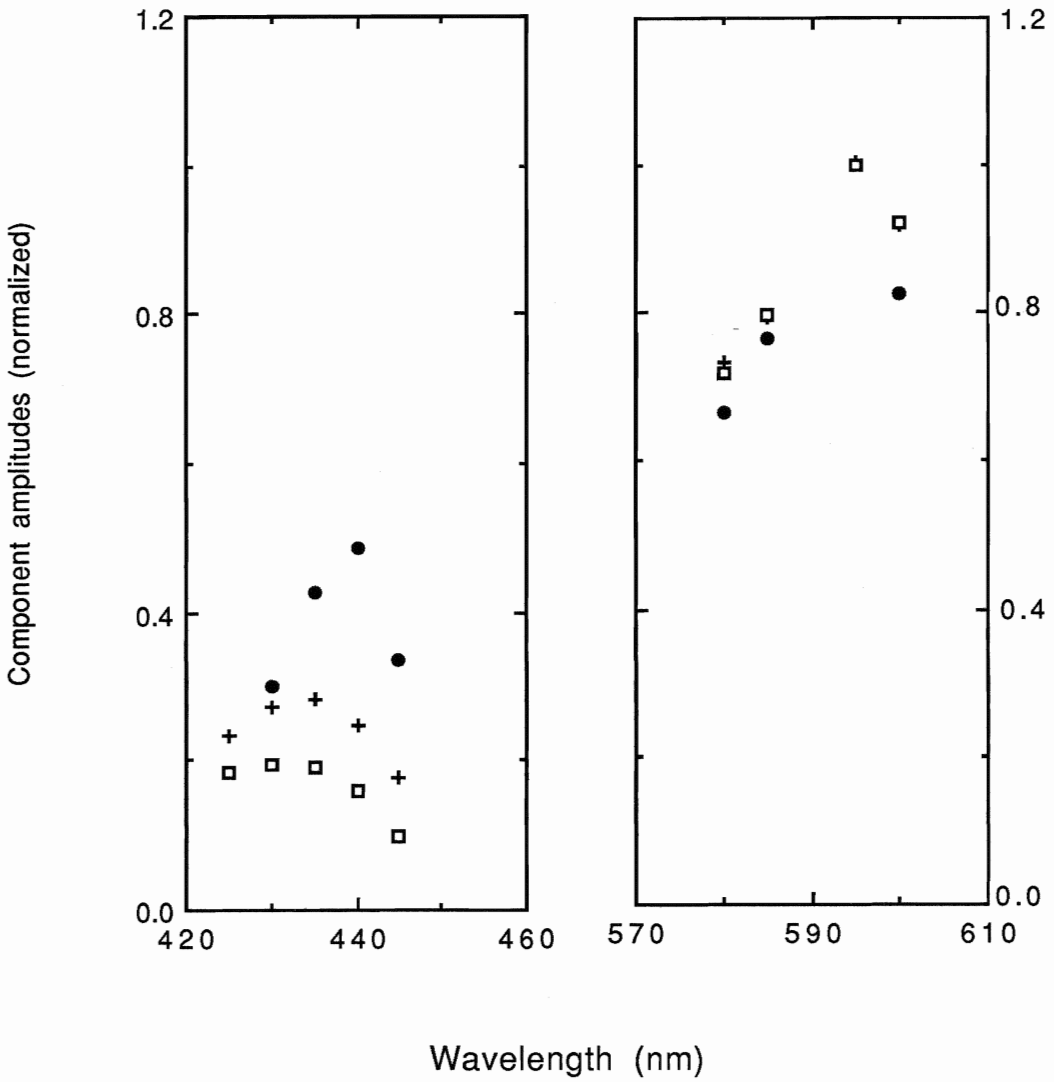
Component amplitudes (normalized)
1.2
0.8
0.4
0.0
420
440
460
570
590
610
Wavelength (nm)

Figure 14. Energy-normalized LIOAS signals of calorimetric standard $CuCl_2$ and intact cells of *Synechococcus sp.* PCC 6301 as a function of temperature. Open circles represent a signals from a solution of $CuCl_2$ in distilled water, open squares are signals from intact cells and filled circles are signals from $CuCl_2$ solution in distilled water with the addition of 0.5 M NaCl.

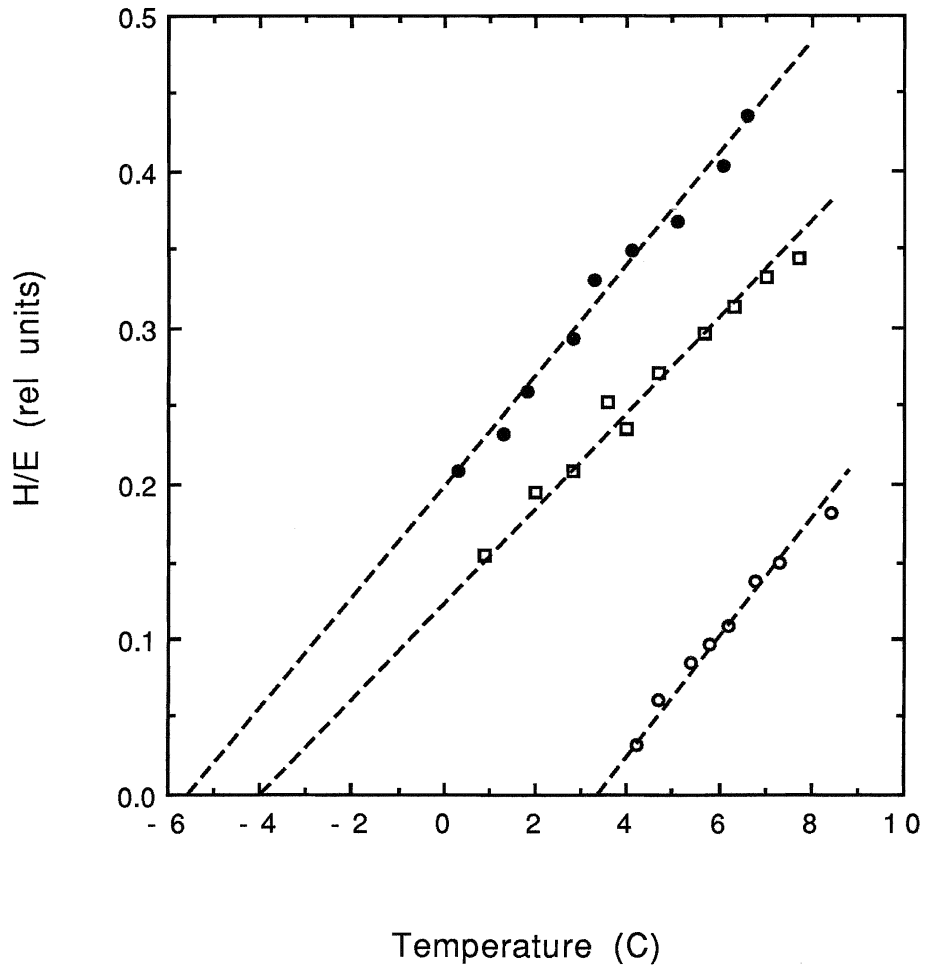
0.5
0.4
0.3
0.2
0.1
0.0
H/E (rel units)
- 6
- 4
- 2
0
2
4
6
8
10
Temperature (C)

Figure 14 shows the temperature dependence of the laser induced optoacoustic (LIOAS) signal. LIOAS of photosynthetic systems is potentially sensitive to acoustic pulses generated by both heat release and conformational changes induced by charge separation in the reaction centers. These two contributions can be theoretically separated by measuring the acoustic signal at 4°C where water reaches maximum density and its thermal expansion coefficient is zero. For $CuCl_2$ solution in distilled water the acoustic signal decreased with temperature vanishing near 4°C. The acoustic signal generated by intact cyanobacteria suspended in distilled water decreased linearly with temperature and did not vanish at 4°C. About 25% of the signal at 28°C was still present at 4°C. Extrapolation of the linear fit to the data indicates that a zero signal would have occured at approximately -4°C. We could make the $CuCl_2$ solution to mimic the cyanobacteria by the addition of NaCl. The temperature of the $CuCl_2$ solution where the optoacoustic signal amplitude reached zero was depressed to about -6°C by the addition of 0.5 M NaCl.

Action spectra for the energy-normalized (H/E) optoacoustic signals in intact cyanobacteria and bleached cyanobacterial cells are compared in figure 15. The LIOAS action spectrum of the cells closely matches its absorbance spectrum normalized at 675 nm, with a PC peak at 625 nm and a Chl a peak at 675 nm. Upon addition of bleach the waveform of the signal changed and its amplitude decreased tremendously.

Heat loss properties studied using LIOAS are plotted as a function of energy of the incident excitation. The optoacoustic

Figure 15. Action spectrum of the energy-normalized LIOAS signals for intact cells with closed reaction centers (filled circles) and bleached cells (open circles) of *Synechococcus sp.* PCC 6301 from 605 nm to 690 nm. The solid line is the absorption spectrum of the same cells normalized to the Chl absorption peak at 680 nm.

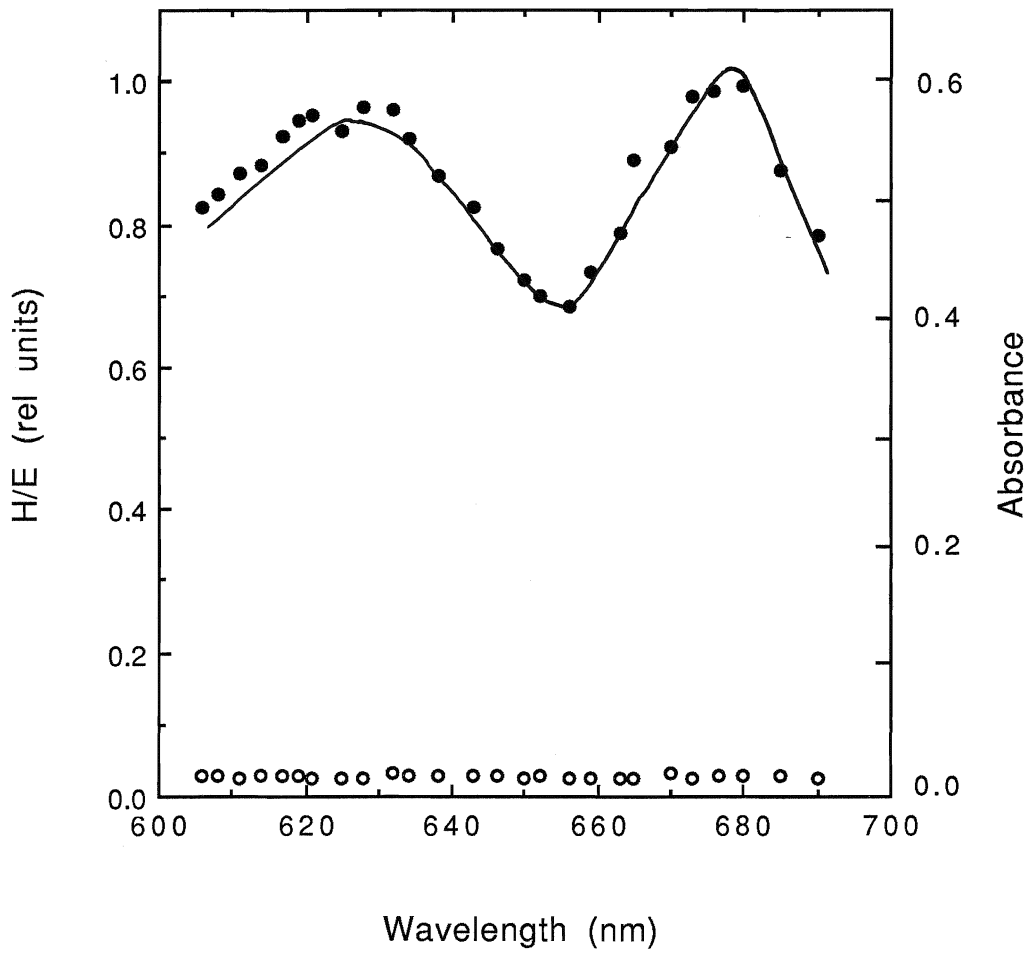
H/E (rel units)
Absorbance
Wavelength (nm)
1.0
0.8
0.6
0.4
0.2
0.0
0.6
0.4
0.2
0.0
600
620
640
660
680
700

Figure 16. Energy-normalized LIOAS signals plotted against the log of flash intensity in mJ for the calorimetric standard $CuCl_2$.

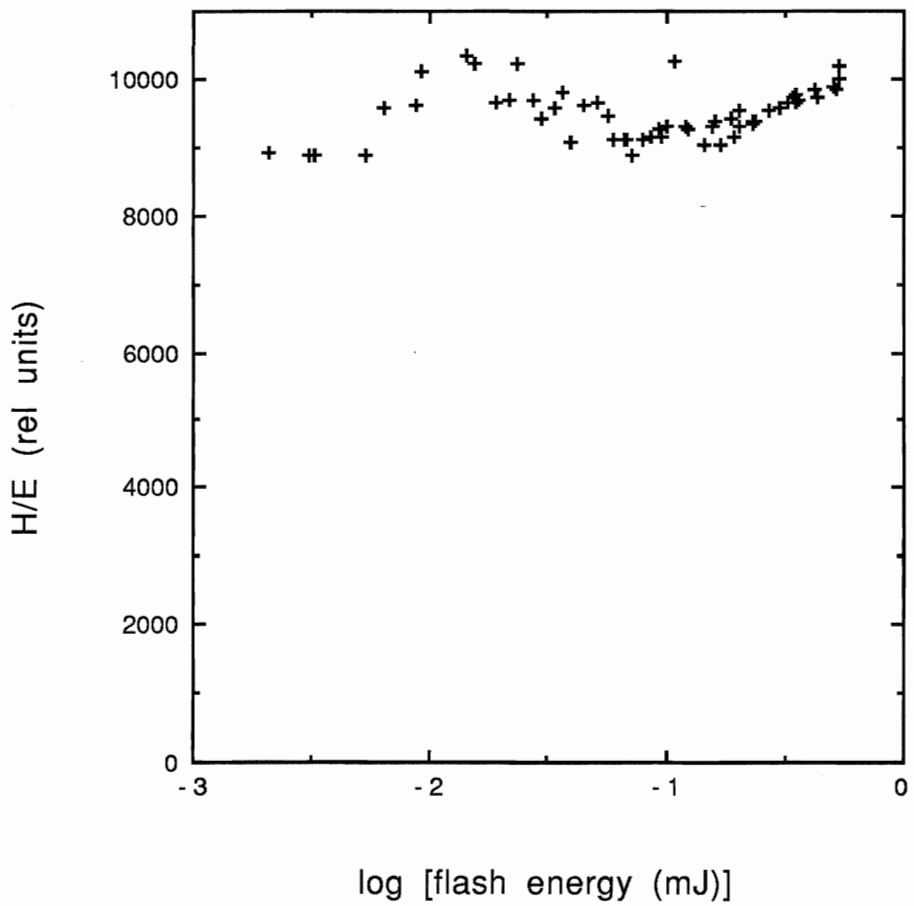
10000
8000
6000
4000
2000
0
H/E (rel units)
-3
-2
-1
0
log [flash energy (mJ)]

amplitudes are normalized for the energy of the excitation. Figure 16 shows the energy-normalized optoacoustic signals plotted as logarithmic functions of laser flash intensity for a $CuCl_2$ solution. $CuCl_2$ is a calorimetric standard and loses all of the absorbed energy as heat within a few nanoseconds (Nitsch *et al.*, 1988) and shows a constant energy-normalized signal for all excitation energies. Figure 17 shows energy-normalized optoacoustic signals for a $CuCl_2$ solution and intact cells of *S. sp.* PCC 6301 with closed reaction centers at the same optical densities. Signals from the $CuCl_2$ solution show constant normalized values at all intensities (H_{ref}). Signals from the cells with closed reaction centers also show a constant normalized values at all intensities (H_{cl}) however this value is about 12% less than the one from the $CuCl_2$ solution, some of this loss is due to loss of energy as fluorescence and scattering effects of cells. These are two types of calorimetric calibrations done in this system and discussed under reference systems in materials and methods, external heat calibration with $CuCl_2$ and internal heat calibration by closing the reaction centers with background illumination.

Energy-normalized optoacoustic signals from isolated spinach PS I particles with open and closed reaction centers are shown in figure 18. This was done to match the LIOAS setup with previously published studies on PS I particles using the same system (Nitsch *et al.* , 1988). Signals from the PS I particles with closed reaction center show a constant value at all flash energies. This maximum value of H/E from closed reaction centers serves as an internal control and is referred to as H_{cl}. Signals from PS I

Figure 17. Energy-normalized LIOAS signals plotted against the log of flash intensity in mJ for intact cells with closed reaction centers (filled circles) and the calorimetric standard $CuCl_2$ (crosses) with matched optical density at 665 nm. The intensity of the laser flash is also represented in terms of photons per cm^2.

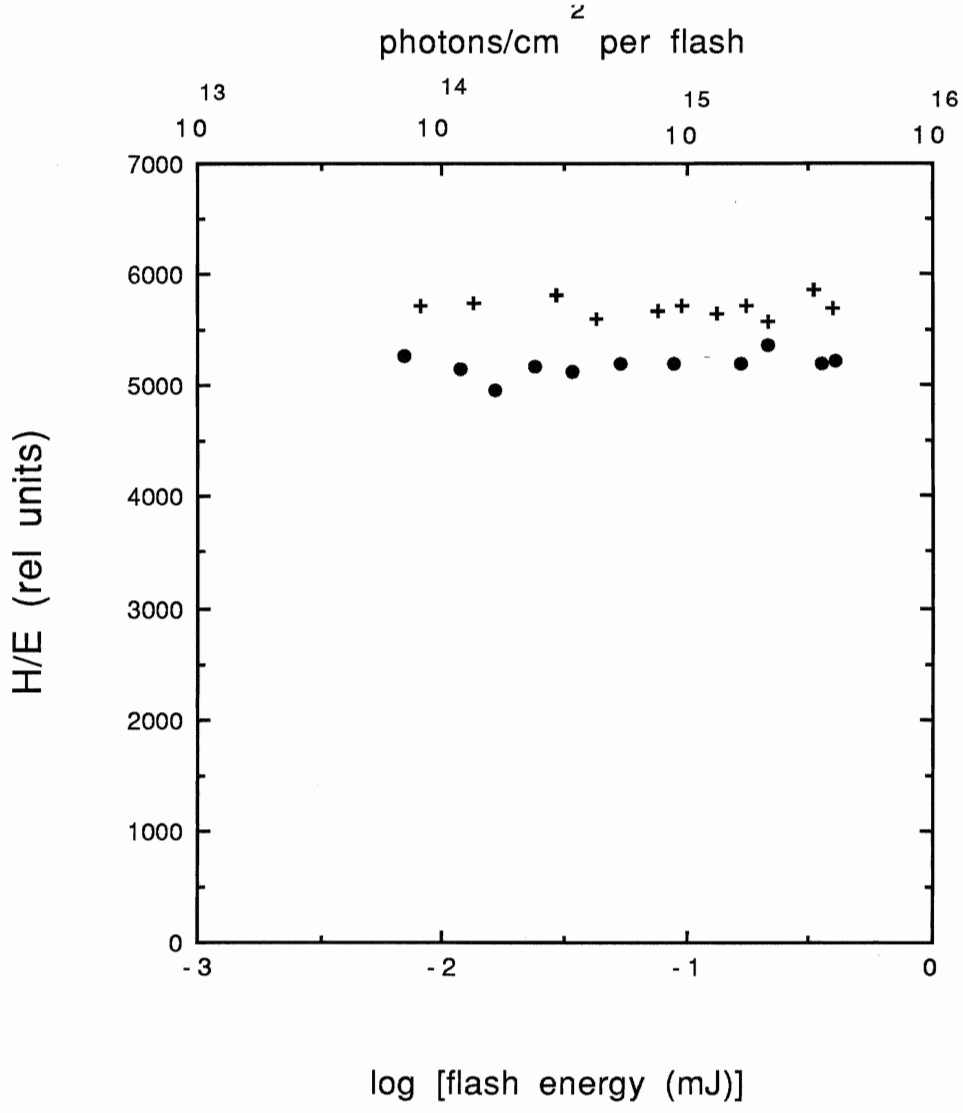
photons/cm 2 per flash
13
10
14
10
15
10
16
10
7000
6000
5000
4000
3000
2000
1000
0
H/E (rel units)
-3
-2
-1
0
log [flash energy (mJ)]

Figure 18. Energy-normalized LIOAS signals plotted against log of laser flash intensity for spinach PS I particles. The PS I reaction centers were closed with ferricyanide (filled circles) and opened by the addition of DCPIP and ascorbate (open circles).

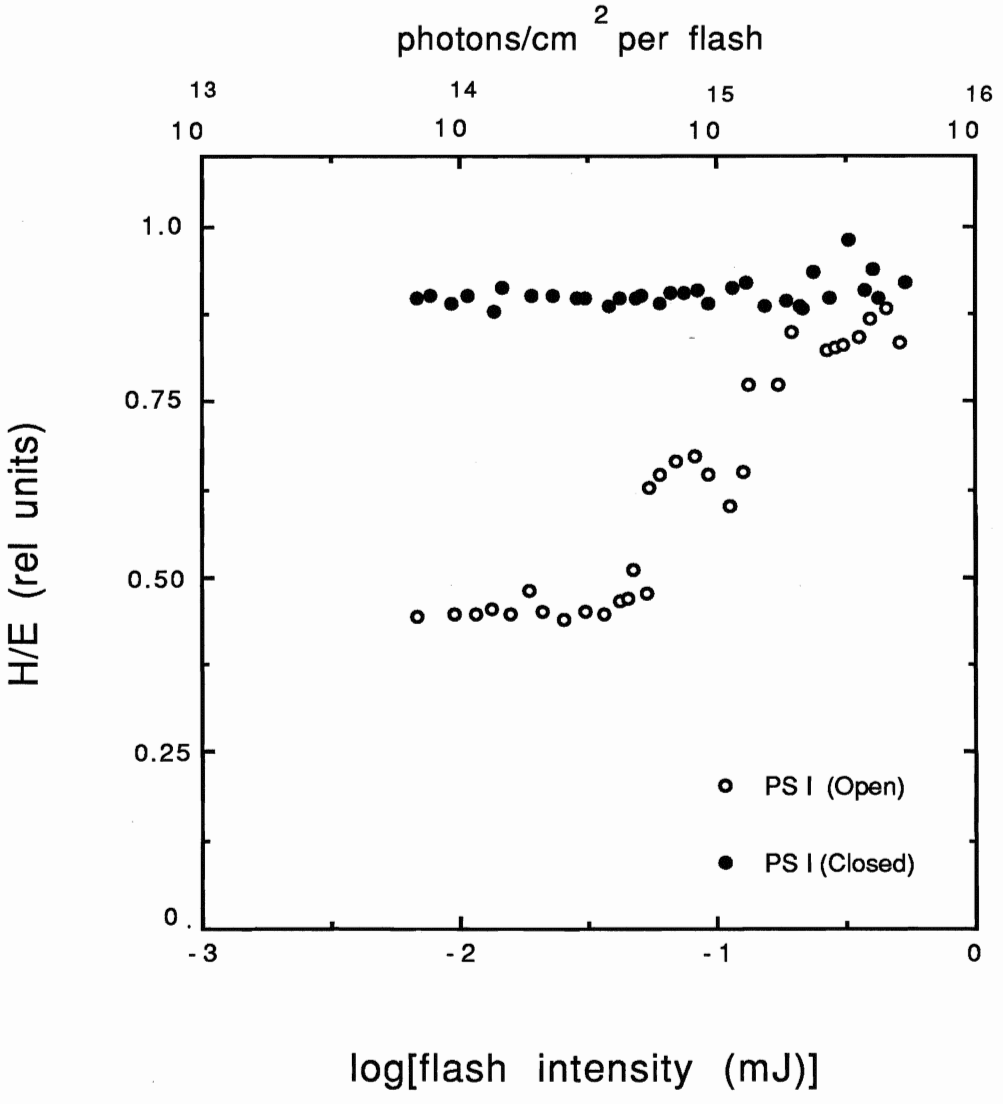
photons/cm 2 per flash
13 14 15 16
10 10 10 10
1.0
0.75
0.50
0.25
0
H/E (rel units)
PS I (Open)
PS I (Closed)
-3 -2 -1 0
log[flash intensity (mJ)]

Figure 19. Energy-normalized LIOAS signals plotted against log of flash intensity for intact cells of *Synechococcus sp.* PCC 6301 with closed reaction centers using background illumination (filled circles) and open reaction centers (open circles). The dashed line represents the minimum energy-normalized LIOAS signal achieved by the cells with open reaction centers at low laser flash energies. This value is used to calculate the energy storage by comparing it to the energy-normalized signal from cells with closed reaction centers.

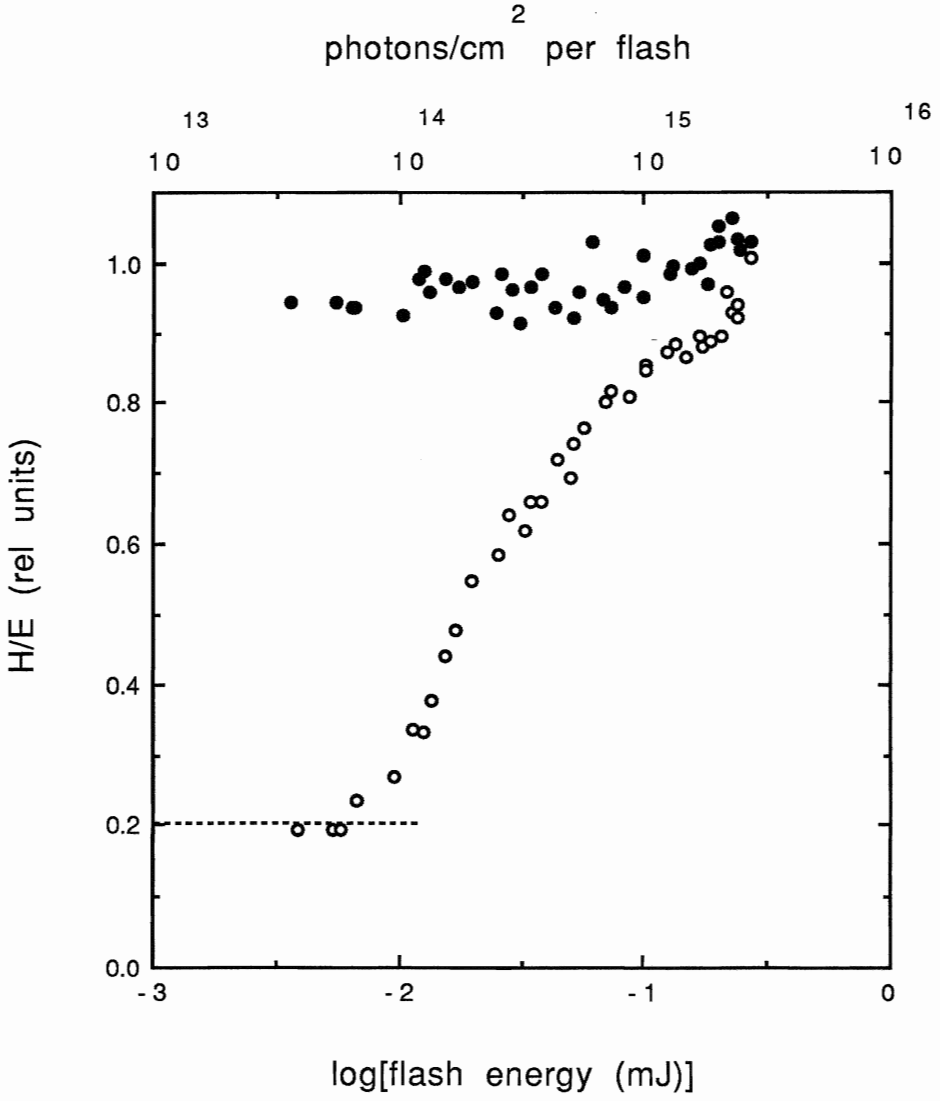
photons/cm 2 per flash
13 14 15 16
10 10 10 10
1.0
0.8
0.6
0.4
0.2
0.0
H/E (rel units)
-3 -2 -1 0
log[flash energy (mJ)]

particles with open reaction centers increase with increasing flash energy till it gets to the maximum value achieved by cells with closed reaction centers. Figure 19 shows similar signals from intact cells of *S. sp.* PCC 6301 with open and closed reaction centers. The dashed line represents the minimum constant value of the energy-normalized heat loss amplitude by the cells with open reaction centers (H_{op}).

The pulse energy-normalized amplitudes (H/E) of the acoustic signal for intact cyanobacteria with open reaction centers in state 1 and state 2 is compared to that for cells with closed reaction centers in figure 20. The excitation wavelength was at 590 nm, chosen to excite PBS on the short wavelength side. Cells with closed reaction centers showed a constant normalized amplitude over three orders of magnitude of flash energy. Cells with open reaction centers show a much lower heat loss at low energies, this amount of heat released increases with flash energy as multiple hits start to close a larger fraction of the reaction centers during the measurements. This continues until all the reaction centers are closed at high laser flash energies. There was no difference in the amplitude of the energy-normalized optoacoustic pulse at low flash energies, H_{op}, or at high flash energies, H_{cl}, or the shape of the saturation curves for cells in state 1 and state 2. 77K fluorescence emission spectra of cell samples taken during optoacoustic measurements are shown in the inset. These spectra show characteristic changes associated with the state 1-state 2 transitions discussed earlier.

Figure 20. Energy-normalized LIOAS signals plotted against log of laser flash intensity from intact cells of *Synechococcus sp.* PCC 6301 in state 1 (open squares) and state 2 (filled circles) for 590 *nm* excitation (PBS absorption) These values have been normalized to the maximum generated by cells with closed reaction centers (open triangles). Inset shows the 77K fluorescence emission spectra for the cells taken during the LIOAS measurements (see materials and methods) showing typical state transition characteristics. The laser flash energies have been also shown in terms of photons per cm^2. The dashed line represents the minimum energy-normalized signal achieved by the cells with open reaction centers at low laser flash energies.

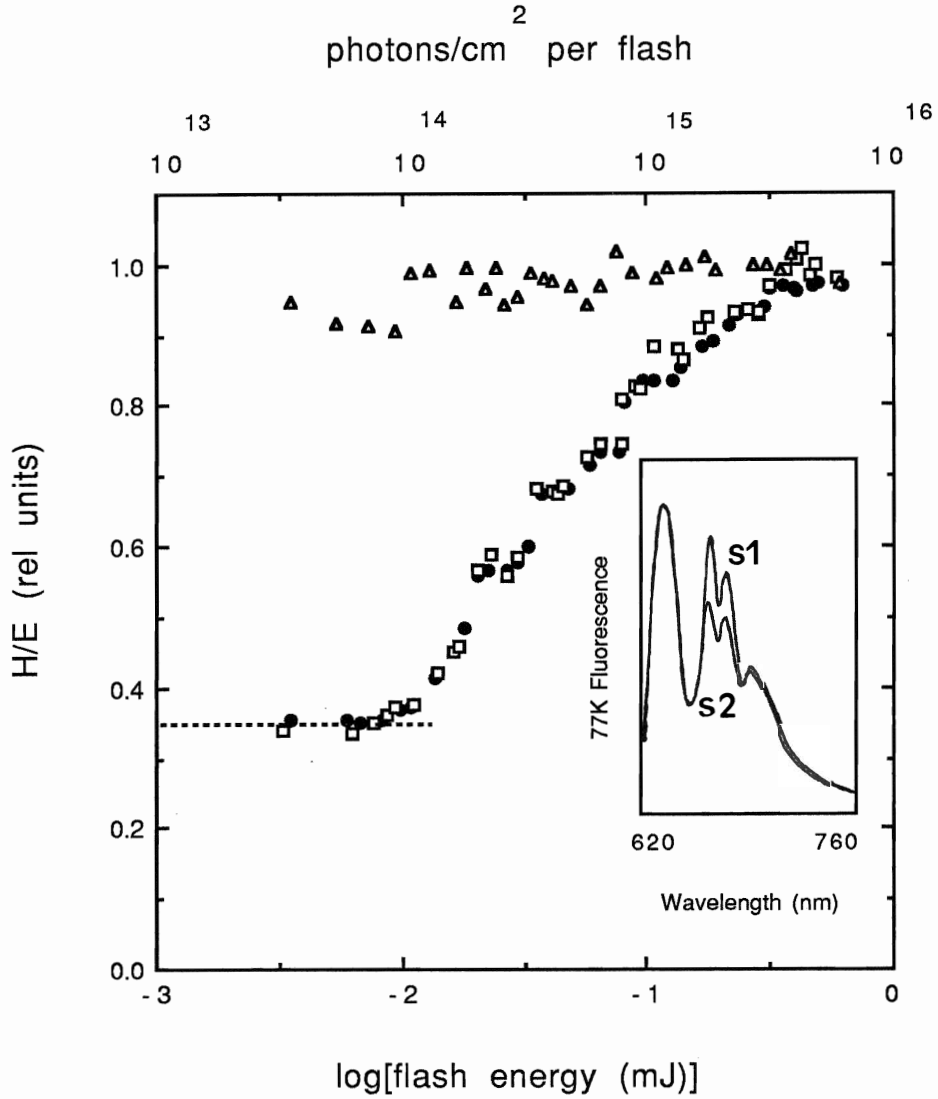
photons/cm 2 per flash
13 14 15 16
10 10 10 10
1.0
0.8
0.6
0.4
0.2
0.0
H/E (rel units)
-3 -2 -1 0
log[flash energy (mJ)]
77K Fluorescence
s1
s2
620 760
Wavelength (nm)

Figure 21. Energy-normalized LIOAS signals plotted against log of laser flash intensity from intact cells of *Synechococcus sp.* PCC 6301 in state 1 (open squares), state 2 (filled circles) and cells with closed reaction centers (open triangles) for 620 nm excitation (PBS absorption). Inset shows the 77K fluorescence emission spectra for the cells in the two states showing typical characteristics of state transition.

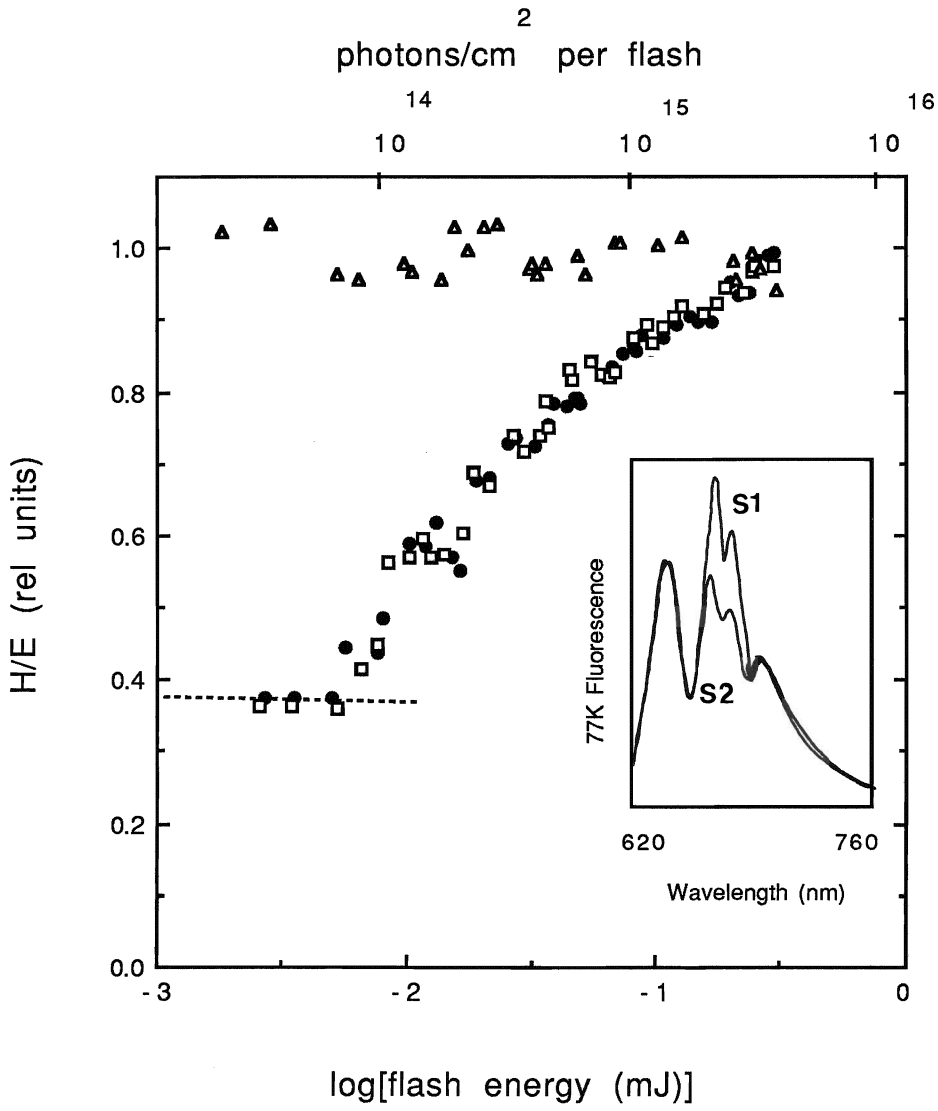
photons/cm 2 per flash
14 15 16
10 10 10
1.0
0.8
0.6
0.4
0.2
0.0
H/E (rel units)
-3 -2 -1 0
log[flash energy (mJ)]
S1
S2
77K Fluorescence
620 760
Wavelength (nm)

Figure 22. Energy-normalized LIOAS signals plotted against log of laser flash intensity from intact cells of *Synechococcus sp.* PCC 6301 in state 1 (open squares), state 2 (filled circles) and cells with closed reaction centers (open triangles) for 663 nm excitation (Chl a absorption). Inset shows 77K fluorescence state transition assay for these cells. The laser flash energies have been also shown in terms of photons per cm^2.

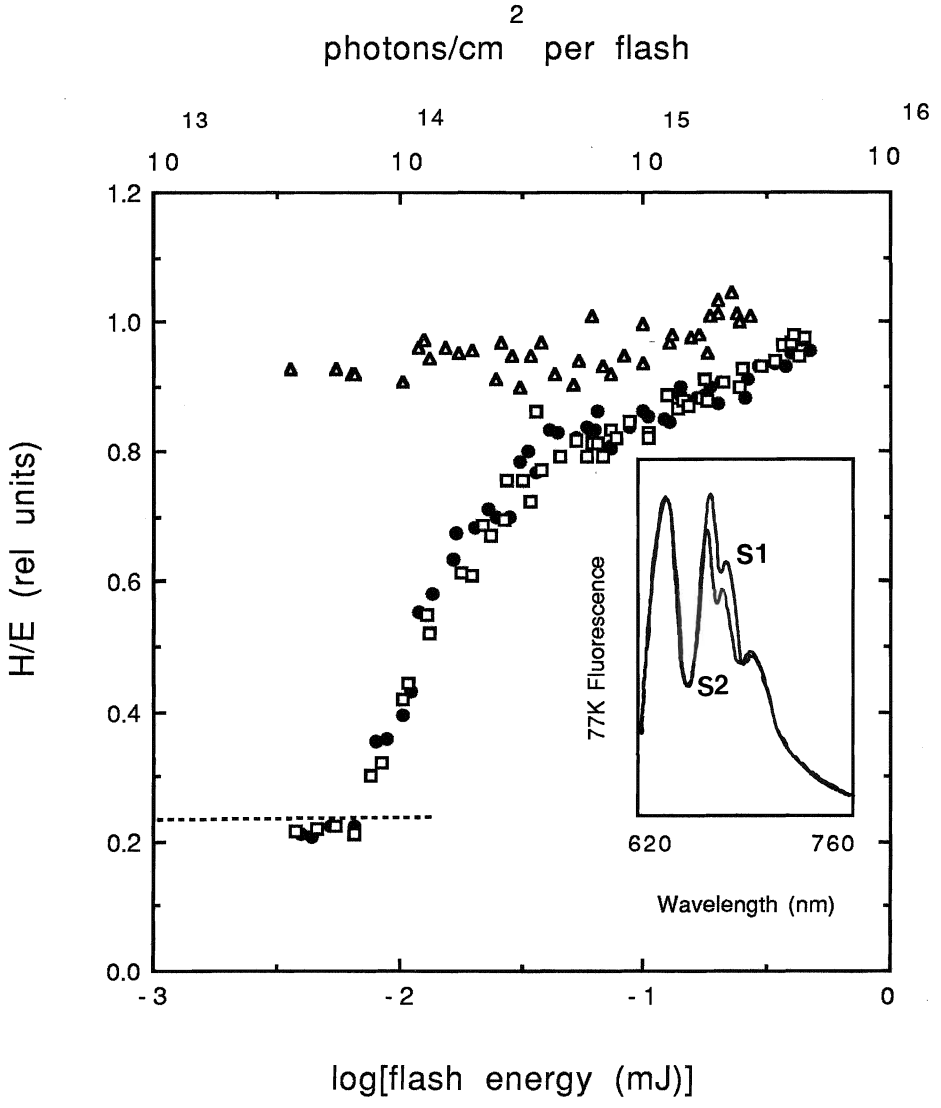
photons/cm 2 per flash
13 14 15 16
10 10 10 10
1.2
1.0
0.8
0.6
0.4
0.2
0.0
H/E (rel units)
-3 -2 -1 0
log[flash energy (mJ)]
77K Fluorescence
S1
S2
620 760
Wavelength (nm)

Figure 23. Energy-normalized LIOAS signals plotted against log of laser flash intensity from intact cells of *Synechococcus sp.* PCC 6301 in state 1 (open squares), state 2 (filled circles) and for cells with closed reaction centers (open triangles) for 670 nm excitation (Chl a absorption). Inset shows 77K fluorescence state transition assay for these cells. The laser flash energies have been also shown in terms of photons per cm^2.

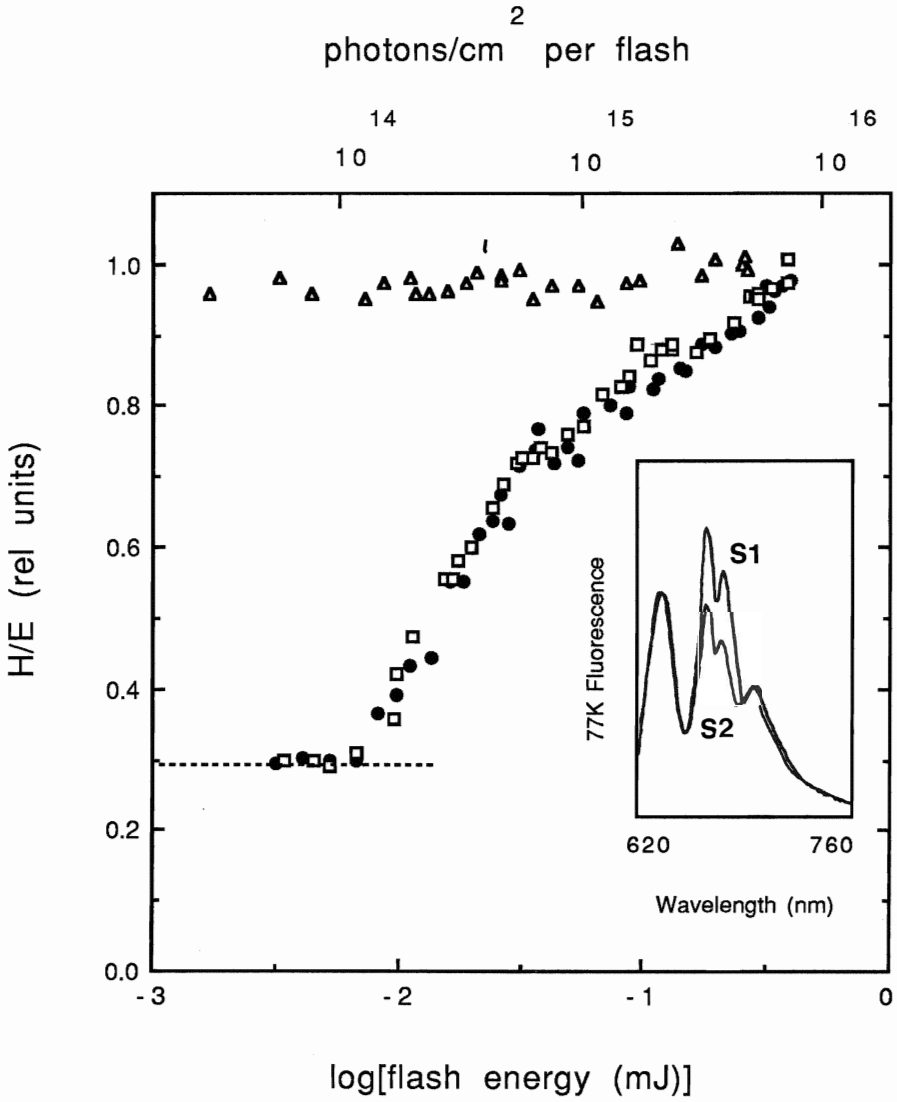
photons/cm 2 per flash
14
10
15
10
16
10
1.0
0.8
0.6
0.4
0.2
0.0
H/E (rel units)
77K Fluorescence
S1
S2
620
760
Wavelength (nm)
-3
-2
-1
0
log[flash energy (mJ)]

In figure 21 the excitation wavelength was changed to 620 nm, exciting PBS. There was no difference in H_{op}, H_{cl} or the shape of the saturation curve for cells in state 1 and state 2. The inset confirms state transitions in these cells. In figure 23 the excitation was changed to 670 nm to excite Chl a. The experiment was then repeated with the same cells as in figure 21. There was again no difference in H_{op}, H_{cl}, or in the shape of the saturation curves for cells in state 1 and state 2.

Figure 22 shows an independent experiment where the excitation of Chl a was accomplished at 663 nm. No difference in the values for H_{op}, H_{cl}, or the shape of the saturation curve for cells in state 1 and state 2 was observed.

The H_{op} and H_{cl} values from the above figures were used to calculate the fraction of absorbed energy released as heat, α, using equation 12 as follows. Most of the Chl a fluorescence in intact photosynthetic systems originates from pigments associated with PS II. The maximum yield with closed reaction centers ϕ_f^{cl}, from chloroplast and intact cells of higher plants is approximately 5% (Murty *et al.*, 1965; Beddard *et al.*, 1979). The chlorophyll fluorescence yield is relatively smaller in cyanobacteria since most of the Chl a is associated with PS I, which has a much lower fluorescence yield than PS II. It is estimated that cyanobacteria in state 2 excited in the Chl a absorption region will have a 3% fluorescence yield (ϕ_f^{cl}=0.03). Upon transition to state 1 the Chl a fluorescence yield almost doubles which would make ϕ_f^{cl}= 0.06 for cells in state 1. The phycobilin fluorescence yield is relatively unaffected by the state transition (Williams and Allen, 1987;

Table 2. Comparison of the ratio of acoustic pulse amplitudes for open and closed reaction centers (H_{op}/H_{cl}), the fraction of the absorbed energy released as heat (α), and the relative energy storage (ΔE_{rel}) for intact cells in state 1 and state 2 for excitation at 590 nm, 620 nm (PBS absorption), 663 nm, and 670 nm (Chl absorption).

Wavelength (nm)		Hop/Hcl	α	ΔErel
590	state 2	0.47 ± 0.09	0.45 ± 0.09	0.64 ± 0.09
	state 1	0.47 ± 0.09	0.44 ± 0.09	0.65 ± 0.09
620	state 2	0.43 ± 0.04	0.41 ± 0.04	0.66 ± 0.04
	state 1	0.43 ± 0.04	0.40 ± 0.04	0.67 ± 0.04
663	state 2	0.27 ± 0.04	0.26 ± 0.04	0.71 ± 0.04
	state 1	0.27 ± 0.04	0.25 ± 0.04	0.72 ± 0.04
670	state 2	0.28 ± 0.05	0.27 ± 0.05	0.75 ± 0.05
	state 1	0.28 ± 0.05	0.26 ± 0.05	0.76 ± 0.04

Biggins and Bruce, 1989; Salehian and Bruce, 1991). By addition of a constant phycobilin fluorescence yield of 0.02, it is estimated that ϕ_f^{cl}=0.05 for cells in state 2 and ϕ_f^{cl}=0.08 for cells in state 1 for excitation of PBS. The term υ_f/υ_e in equation 12 includes the additional heat losses due to internal conversion associated with fluorescence emission. For PBS excitation at 620 nm, the fluorescence emission peak is at 670 nm, therefore υ_f/υ_e=0.93, and at 590 nm it is 0.88. For Chl a excitation the weighted fluorescence emission peak is at 685 nm, so υ_f/υ_e=0.98 for excitation at 670 nm and 0.97 for excitation at 663 nm. These values along with the ratio of H_{op}/H_{cl} and relative energy storage (ΔE_{rel}) for all four excitation wavelengths are listed in table 3. These values were the averages of at least three independent experiments for each excitation wavelength. The fraction of the energy lost as heat is significantly larger for excitation of the PBS at 590 nm and 620 nm than it is for Chl a excitations at 663 nm and 670 nm. However the relative energy storage values (ΔE_{rel}) are higher for Chl a excitations (663 nm and 670 nm) than for PBS excitations (590 nm and 620 nm).

PS I Activity

Transmittance changes at 820 nm due to photooxidation of P-700 are plotted as a function of energy in figure 24 for intact cells of *S. sp.* PCC 6301 in state 1 and state 2. Excitation of 621 nm was chosen to excite PBS. The transmittance signal increases with increasing intensity till it reaches a maximum value at high laser flash energies. No difference is seen between the saturation level

Figure 24. Transmittance changes at 820 nm as a function of log laser flash intensity for 621 nm excitation (PBS absorption) for intact cells of *Synechococcus sp.* PCC 6301 in state 1 (open squares) and state 2 (filled circles). Inset shows the 77K fluorescence assay for state transition in these cells taken during the measurement of transmittance change. The laser flash energies have also been shown in terms of photons per cm^2.

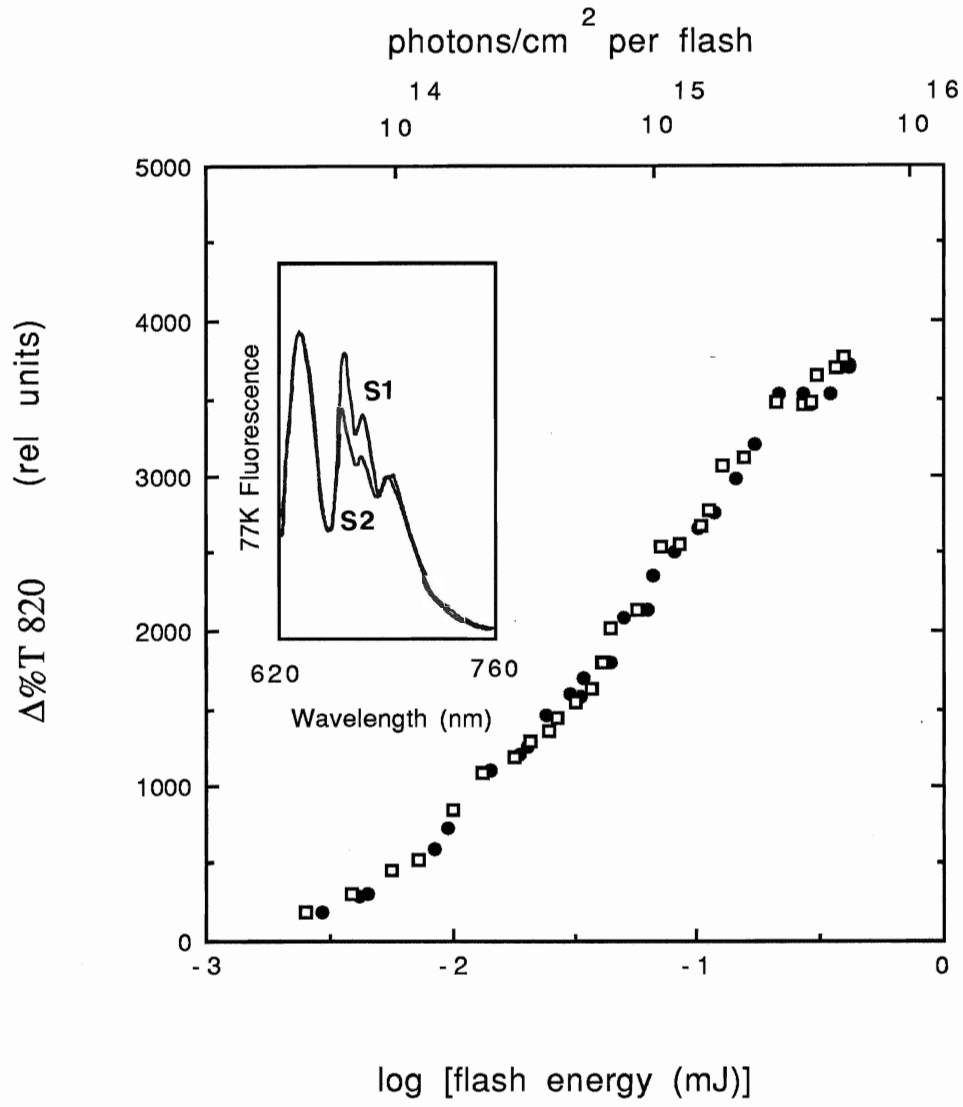
photons/cm 2 per flash
14
10
15
10
16
10
5000
4000
3000
2000
1000
0
-3
-2
-1
0
Δ%T 820 (rel units)
log [flash energy (mJ)]
77K Fluorescence
S1
S2
620
760
Wavelength (nm)

Figure 25. Transmittance changes at 820 nm as a function of log laser flash intensity for 663 nm excitation (Chl a absorption) for intact cells of *Synechococcus sp.* PCC 6301 in state 1 (open squares) and state 2 (filled circles). Inset shows the 77K fluorescence assay for state transition in these cells (see materials and methods). The laser flash energies have also been shown in terms of photons per cm^2.

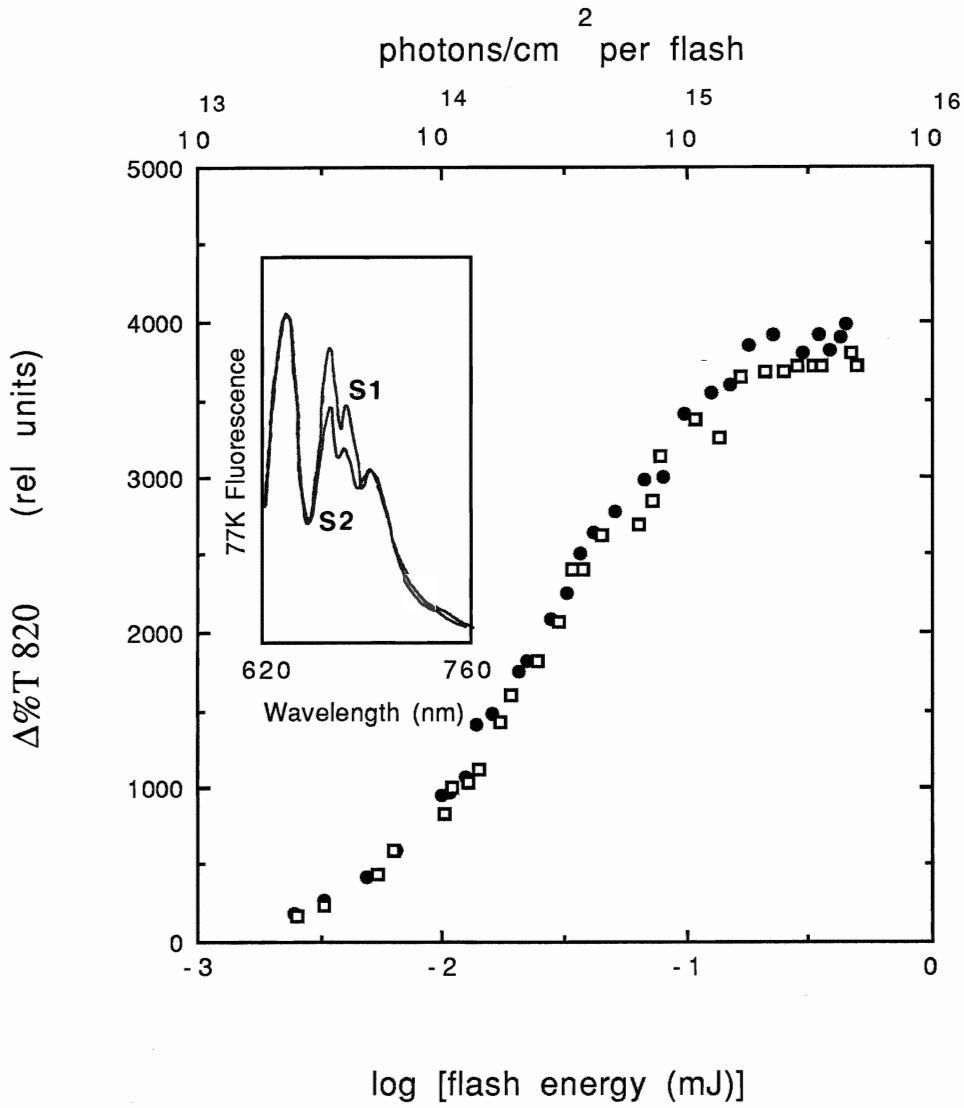
photons/cm 2 per flash
13 14 15 16
10 10 10 10
5000
4000
3000
2000
1000
0
-3 -2 -1 0
ΔT 820 (rel units)
log [flash energy (mJ)]
77K Fluorescence
S1
S2
620 760
Wavelength (nm)

Figure 26. Action spectrum of energy-normalized transmittance changes at 820 nm for an excitation energy of 91 ± 5 μJ for intact cells of *Synechococcus sp.* PCC 6301 in state 1 (open squares) and state 2 (filled circles) between 605 and 690 nm. Inset shows the 77K fluorescence assay for state transition in these cells.

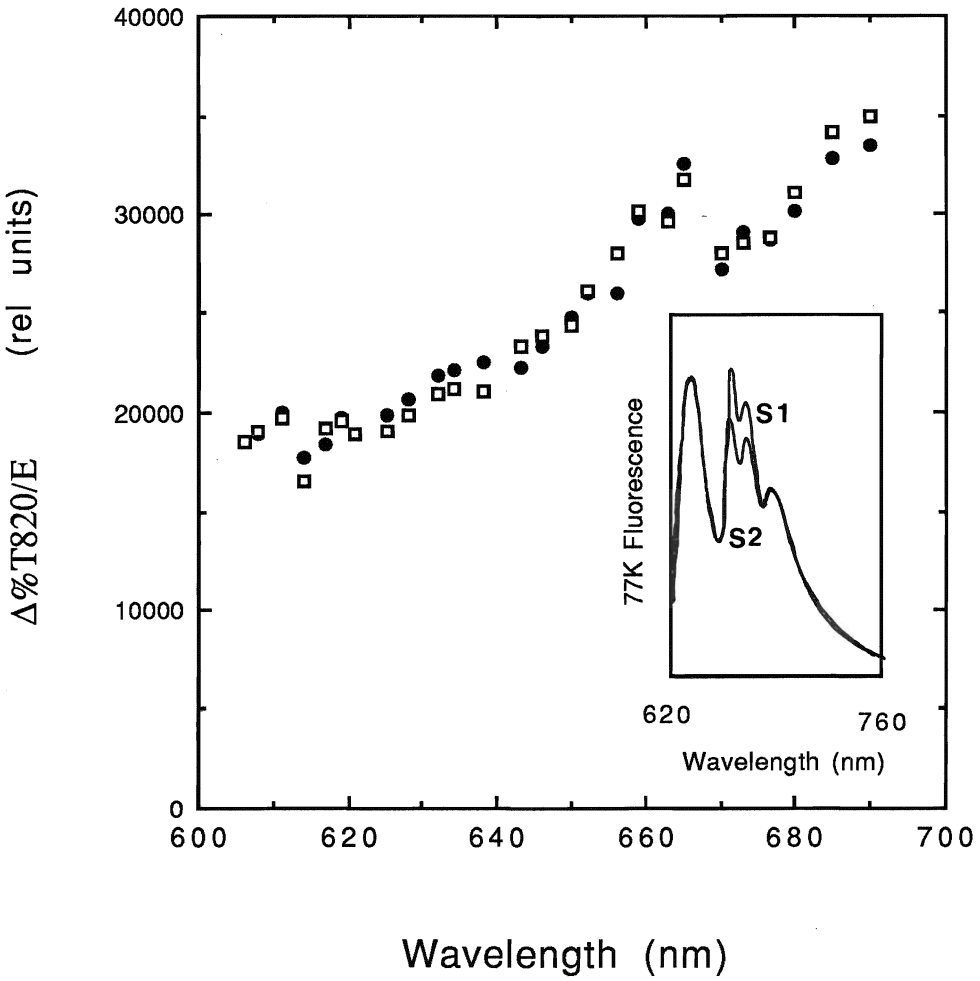
40000
30000
20000
10000
0
600
620
640
660
680
700
Δ%T820/E (rel units)
Wavelength (nm)
77K Fluorescence
S1
S2
620
760
Wavelength (nm)

or the shape of the saturation curve for cells in state 1 and state 2. The inset shows the 77K fluorescence emission spectra of cells in state 1 and state 2 taken during the measurement of the transmittance change at 820 nm. The fluorescence spectra show typical characteristics of state transitions. The excitation wavelength was changed to 663 nm to excite Chl a and measurements of the transmittance changes at 820 nm were made on the same cells as in figure 24 and shown in figure 25. Again no significant difference was observed for the saturation level or the shape of the saturation curve between the cells in state 1 and state 2. The inset shows the 77K fluorescence emission spectra of the cells confirming state transitions in these organisms during the measurements.

Figure 26 shows the action spectrum for the transmittance change at 820 nm for intact cells in state 1 and state 2. The transmittance changes were measured at the same laser flash energy for all the wavelengths studied (91± 5 μJ) and were normalized for this energy. Energy-normalized 820 nm transmittance changes are plotted against wavelength of excitation. A Chl peak is seen at about 665 nm and one at about 690 nm. No significant difference was seen in the signals for cells in state 1 and state 2 at all the wavelengths between 605 nm and 690 nm. Inset shows the 77K fluorescence emission spectra for the cells confirming state transition in these organisms.

DISCUSSION

Fluorescence emission and excitation studies

In this study fluorescence emission spectra were collected for intact cells in state 1 and state 2. These spectra were not normalized to the internal phycobilin emission or to the emission of an added fluorophore as has been the case in the past (Bruce *et al.*, 1985). These spectra did not show any large changes in the phycobilin emission in the two states, but showed typical changes in PS II and PS I fluorescence emission yields characteristic of state transitions. The results will be discussed with respect to the predictions of each of the three models of state transitions in PBS-containing organisms.

Spillover

Both PS II Chl a and PBS are involved in state transition according to this model. Energy absorbed by both PBS and PS II Chl a is competitively distributed between PS I and PS II due to the increase in the excitation energy transfer from PS II Chl a to PS I Chl a in state 2. If we assume that the excitation energy is transferred in the pathway of PBS to PS II Chl a to PS I Chl a (Biggins and Bruce, 1989), where the final step is controlled by the state transition, complementary changes in PS II and PS I activities are predicted for both PBS and Chl a excitations. Our data show an increase in PS I and decrease in PS II fluorescence yields upon transition to state 2, as predicted by the spillover model. However the PS II yield

changes are much larger than PS I yield changes for both Chl a and PBS excitations as seen in table 3. This difference in the yield changes is expected for Chl a excitations since most of the Chl a is associated directly with PS I. If we assume that 15% of the total Chl a is associated with PS II (Myers *et al.*, 1980), then the observed 30% decrease in PS II Chl a contribution to the PS II excitation spectrum (figure 11) would effectively involve only the addition of 30% of 15% or 4.5% of total Chl a to PS I. As mentioned earlier 85% of Chl a is associated with PS I, therefore a 4.5% addition of total Chl a to the 85% Chl a associated with PS I directly, would be observed as a 5.3% increase in the Chl a contribution to PS I excitation spectrum (figure 10) in state 2. A value of 5 ± 1% was observed in this study for contribution of Chl a to PS I in state 2. However only a small increase of 8.4 ± 0.3% in PBS contribution to PS I excitation spectrum accompanied by a 40% decrease in the contribution of PS II excitation spectrum was observed. This is not consistent with the predicted spillover model, unless one assumes that approximately 80-90% of the PBS transfer energy to PS I in state 1, there is no evidence in the literature for this. The data show a large contribution of PBS to PS I excitation spectrum but when it is compared to the PS II excitation spectrum there is clearly a greater differential in the distribution of PBS and Chl a between the two photosystems than predicted by the spillover model to fit the data.

The spillover model predicts that upon transition to state 2, the PS II excitation spectrum should decrease in amplitude

Table 3. Changes in the PS II (695 nm) and PS I (715 nm) components during the state transition for Chl a-absorbed excitations and PBS-absorbed excitations. The changes are shown as increases in PS II component's amplitude and decreases in the PS I component's amplitude, the results shown are the averages of three experiments.

Wavelength (nm)	PS II increase (%)	PS I decrease (%)
Chl a excitation		
430	48.14 ± 7.03	3.86 ± 0.27
435	44.78 ± 5.78	5.04 ± 0.41
440	43.13 ± 6.00	5.99 ± 0.45
445	37.72 ± 6.20	5.01 ± 0.24
PBS excitation		
580	65.33 ± 8.67	8.00 ± 0.54
585	66.86 ± 8.15	8.57 ± 0.63
595	66.38 ± 7.23	8.99 ± 0.68
600	66.98 ± 7.98	8.00 ± 0.71

with no change in the relative contribution of PBS and PS II Chl a while PS I excitation spectrum is expected to be enhanced by both PBS and PS II associated Chl a in the same proportion as lost by PS II. Hence the difference between PS I excitation spectrum in state 2 and state 1 is predicted to be identical to the difference in the PS II excitation spectrum between state 1 and state 2, and also to the PS II excitation spectrum itself. The fluorescence data obtained in this study showed significant differences in the relative contributions of Chl a and PBS to the gains of PS I as compared to the losses of PS II on transition to state 2. This does not support a simple spillover model.

Mobile PBS

In this model only the PBS is involved in the distribution of excitation energy during the state transition. This model predicts complementary changes in PS I and PS II activities for excitations absorbed by PBS only and no changes are predicted for excitations of Chl a. Therefore the PS II excitation spectrum is expected to show a decrease in the contribution of PBS while PS I excitation spectrum is expected to show a complementary increase in the PBS contribution. The data in this study show substantial changes in the contribution of Chl a to both PS II and PS I action spectra and do not support this model.

PBS detachment

This model predicts complementary changes in PS II and PS I activities of PS II Chl a excitation via spillover. As explained above the data for Chl a excitation is consistent with the spillover mechanism.

The detachment of PBS in state 2 in this model predicts a larger decrease in the PBS contribution to the PS II excitation spectrum compared to the Chl a contribution. The PS II excitation spectrum did show a larger decrease in PBS contribution (40% decrease) than Chl a contribution (30% decrease) on transition to state 2. This is consistent with a partial detachment of PBS.

The degree of PBS detachment in this model would predict changes in the relative contribution of Chl a and PBS to both PS II and PS I excitation spectra. This model predicts that after PBS detachment in state 2 the PS I excitation spectrum is enhanced by contributions reflecting the PS II action spectrum. The data from this study showed that increases in the PS I excitation spectrum in state 2 have a lower contribution by PBS relative to Chl a compared to the PS II excitation spectrum in state 2. These results are inconsistent with the PBS detachment model.

The fluorescence emission and excitation results do not support the mobile PBS mechanism. This is in agreement with a number of other studies showing that Chl a is involved in state transition (Biggins and Bruce, 1989; Williams and Allen, 1987) and that the mechanism is functional in the absence of PBS (Bruce *et al.*, 1989a). These data also show that the transition to state 2 resulted in a larger decrease in PBS contribution relative to Chl a, to the PS I excitation spectrum. This supports the idea of a partial PBS detachment. The PBS detachment and spillover models allow for increase in the contribution of the

PBS to PS I in state 2 through excitation energy transfer from PBS to Chl a of PS II and then to PS I Chl a via spillover. Both of these models predict larger increases in the contribution of PBS relative to Chl a to the PS I excitation spectra on transition to state 2 than was observed in this study.

It has been suggested that state transitions serve to regulate the distribution of excitation energy between PS II and PS I to optimize linear electron transport under adverse conditions of light or metabolic demand (Bulte *et al.*, 1990; Turpin and Bruce, 1990; Biggins and Bruce, 1989) or to act as a photoprotective mechanism for PS II by increasing the rate of heat loss (Allen and Melis, 1988; Mullineaux and Allen, 1988). The results from the 77K fluorescence determination study indicate that both roles may be important. Complementary changes in photosystem activity are observed for both PBS and Chl a absorbed excitation, however the changes in PS II are significantly greater.

Heat loss determinations

The results from fluorescence emission spectroscopy studies did not support the mobile PBS mechanism for state transition. The results supported modified versions of spillover and PBS detachment models. A spillover mechanism where all of the energy absorbed by PBS does not make it to PS I and a PBS detachment model where PBS is partially detached from PS II. Direct measurement of heat loss from intact cells in state 1 and state 2 would distinguish between these models; since PBS

detachment model predicts an increase in fluorescence or heat loss in state 2 upon excitation of PBS. No increase in fluorescence yield of PBS have been detected in a number of studies (Salehian and Bruce, 1991; Mullineaux and Holzwarth, 1990). Hence it has been suggested that the excitation energy absorbed by PBS could be dissipated by non-radiative decay processes (Mullineaux and Allen, 1988). Using LIOAS technique direct heat loss measurements were made on intact cells of cyanobacterium *S. sp.* PCC 6301 in state 1 and state 2 within 2 μs of a laser flash.

As mentioned earlier LIOAS of photosynthetic organisms is potentially sensitive to acoustic pulses generated by both heat release and conformational changes induced by charge separation in the reaction centers. When measurements are made at 4 °C, where water reaches a maximum density and a zero thermal expansion coefficient, these two contributions can be separated. This is shown in figure 14. It was found that for cells the zero signal occured at about -4 °C, for the $CuCl_2$ solution in distilled water it was at approximately 3 °C, and upon addition of 0.5 M NaCl this point decreased to -6 °C. The temperature of maximum density was reduced by solutes in a manner analogous to freezing point depression. Hence presence of an acoustic signal below 4 °C in the cyanobacteria could be explained by the high concentration of solutes in the interior of the cyanobacterial cell. The continuing decrease of the acoustic signal for the cells below 4 °C suggest that most of the acoustic signal is thermal.

The values for H_{op}/H_{cl} for excitation at 620 nm calculated from these results are same for cells in state 1 and state 2 (0.43 ± 0.05) and were close to the value reported by Nitsch *et al.*, (1989) for intact cells excited at 628 nm (0.4). At 670 nm excitation the determination of H_{op}/H_{cl} for cells in state 1 or state 2 (0.28 ± 0.05) was similar to their value for isolated PS I particles excited at 677 nm (0.25).

As expected the value for α (the fraction of absorbed energy released as heat) is significantly larger for excitation of PBS at 590 nm and 620 nm than it is for Chl a excitation at 663 nm and 670 nm. Most of this difference is due to the higher internal conversion losses for the shorter wavelength excitation. However, values for ΔE_{rel}, which have been corrected for these losses, show a larger energy-storage for 670 nm and 663 nm than at 590 nm and 620 nm excitations. This is consistent with the relative distribution of PBS and Chl a absorbed excitations to PS II and PS I respectively as energy storage capacity of PS I is higher than PS II on this time scale (Nitsch *et al.*, 1989) due to the difference in the redox potentials of the electron acceptors during 2 μs (Figure 1). The values for ΔE_{rel} calculated here for PBS excitation (approximately 0.65) and Chl a excitation (approximately 0.74) are comparable to the values of relative energy storage reported for isolated PS II particles (0.65) and isolated PS I particles (0.83), respectively by Nitsch *et al.* (1989).

No significant difference in the value of H_{op}/H_{cl} between cells in state 1 and state 2, for excitation of either PBS or Chl a

was observed in any of the experiments. Correction of H_{op}/H_{cl} for different fluorescence losses in state 1 and state 2 did not result in significant difference in the values of α and ΔE_{rel} between the two states.

The results from direct optoacoustic measurements show that the efficiency of excitation energy transfer and primary photochemistry within 2 μs of light absorption in cyanobacteria is the same in state 1 and state 2. These results do not support the PBS detachment model which predicts a decrease in efficiency of energy transfer from PBS to Chl a and an increase in fraction of absorbed energy lost as heat (α) in state 2 (Mullineaux and Holzwarth, 1990; Mullineaux *et al.*, 1990). Recent LIOAS experiments (Mullineaux *et al.*, 1991) have also shown no difference in energy storage upon transition to state 2. However the authors suggest that these results indicate that energy is diverted away from PS II and is transferred to PS I by decoupling of PBS from PS II core complexes and its subsequent coupling to PS I. The authors report a value of 0.81 and 0.88 for fraction of energy stored for 630 nm and 690 nm excitations respectively. These values are larger than values reported in this study and the ones reported for isolated PS I and PS II complexes by Nitsch *et al.* (1988).

PS I activity

In all of the models proposed for the mechanism of state transition in PBS-containing organisms, in state 2, more energy is directed towards PS I by either direct association with PBS or by spillover of excitation energy from Chl a. So the function of

state transition suggested by these models is to balance the photochemical activities of the two photosystems in response to over-excitation of either one. Hence measurement of PS I activity in the two states under PBS and Chl a excitations should determine the nature of the mechanism of state transition in these organisms. Upon transition to state 2 the spillover model predicts an increase in PS I activity for both PBS and Chl a excitations. The mobile PBS model predicts an increase in PS I activity for PBS excitation only and the PBS detachment model predicts an increase in activity of PS I for Chl a excitation and a decrease in the activity for PBS excitation in state 2. The results from P-700 photooxidation measurements at 820 nm did not show any significant difference in the extent of photooxidation in the two states for both PBS excitation (620 nm) or Chl a excitation (663 nm). Measurements of this photooxidation at different wavelengths (605 nm to 690 nm) for a medium intensity laser flash (91 ± 5 μJ) was not significantly different for intact cells in state 1 and state 2. These results are contradictory to all of the existing models of state transition which predict a change in the PS I activity for excitation of Chl and/or PBS during state transition.

Photochemical activity measurements in cyanobacteria and red algae have been done previously. Fork and Satoh (1983) monitored cyt c photooxidation in the two states and Biggins (1983) studied the kinetics of cyt f oxidation in state 1 and state 2. These measurements showed an increase in PS I turnover (determined by measuring rates of cyt c and cyt f

oxidations) in state 2. However these are not direct measurements of PS I activity. In cyanobacteria the photosynthetic and respiratory electron transport pathways share a number of components (figure 2) including cyt f and cyt c, hence measurements of their activities may not reflect PS I photochemistry only. The measurements done in the present study are attributed to PS I only, and also done on a much faster time scale to minimize reduction of P-700 by the respiratory chain during the measurement.

A study of P-700 photooxidation in state 1 and state 2 in cyanobacteria was done by Tsinoremas *et al.* (1989). They used a 337 nm laser flash to excite Chl a and a 532 nm flash for PBS excitation and monitored P-700 change in the two states at 820 nm. They show an absorption increase in state 2 for both 337 nm and 532 nm excitations, and suggest that these results are compatible with the mobile PBS model. However the change seen at 337 nm (Chl a) excitation are not explained by the predictions of the model, and the authors suggest that perhaps the PBS absorbs in this region as well and the increase seen in the absorbance in state 2 is due to the PBS absorption. The authors do not explain how the cells were brought to state 1 and state 2 during the measurement of P-700 photooxidations. If the actinic light 1 (PS I excitation) is on during the measurements (cells are in state 1), P-700 will be photooxidized due to absorption of this light and further excitation by a laser flash would produce a smaller signal for the P-700 oxidation. However the actinic light 2 (PS II

excitation) does not photooxidize P-700 and would thus show a larger absorbance change upon excitation with a laser flash. Hence the results of Tsinoremas *et al.* (1989) could be explained by questionable methods of measurements. If lights used to induce state transition were on during measurements of P-700 photooxidation we would expect to see a higher absorbance for light 2 (state 2) than light 1 (state 1) for any excitation wavelength and this is exactly what the authors got. The present study is an improvement of the above since the actinic lights used to induce state transition were not on during the P-700 oxidation measurements. There was a 3 s dark time before and during the measurement. The cells were ensured to be in state 1 or state 2 by measurements of 77K fluorescence emission spectra prior to the excitation laser flash. Wavelengths of excitation laser flash were selected to preferentially excite Chl a (663 nm) and PBS (620 nm), and the measurements of P-700 photooxidation were done over three orders of magnitude of laser flash intensity.

Several studies on higher plants and green algae (Allen and Melis, 1988; Haworth and Melis, 1983) have shown no difference in the rate of P-700 photooxidation in the two states. The authors have suggested that the so called state transition has no direct effect on PS I photochemistry and primarily serves as a defence against destructive effects of over-excitation of PS II. Several mechanisms of energy dissipation have been suggested. Horton and Lee (1985) suggest an energy dissipating cyclic pathway around PS II. Holzwarth (1986) has

suggested that the major effect of state 2 transition is on PS II heterogeneity. Several other lines of evidence suggest that state transitions may play a role in photoprotection of PS II. Horton and Lee (1983) have shown that in state 2 the efficiency of cyclic electron transport around PS II increases. Later Horton and Lee (1985) showed that phosphorylation of LHC II (state 2) can afford partial protection to thylakoids exposed to photoinhibitory conditions. Therefore in state 2 it is thought that there is a conversion of α-centers to ß-centers (Kyle *et al.*, 1982) or a complementary change in the absorption cross-section of PS II_{α} and PS II_{β} takes place (Holzwarth, 1986).

Huge changes in the cross-section of PS II during state transition are seen. Ley (1984) showed a 50% decrease in PS II cross-section upon transition to state 2 in *P. cruentum* measured by monitoring oxygen evolution. In this study we see a 30% to 40% decrease in fluorescence emission of PS II upon transition to state 2. However no change in the extent of PS I photooxidation is observed during state transitions in this study. This is not supported by any of the existing models of state transition which suggest a transfer of excitation energy to PS I in state 2. These evidences suggest a different function for state transition rather than distribution of excitation energy between the two photosystems.

In higher plants two types of PS II are present (Melis and Homann, 1975) (see section on photosystem II heterogeneity). These PS II centers designated α and β have different antenna size with PS II_{α} having more than twice the

antenna size of the PS II_β centers (Melis *et al.*, 1987; Melis and Anderson, 1983). Due to this difference in the antenna size the PS II_β centers have a lower fluorescence yield (Melis and Duysens, 1979). It has been suggested that the PS II_β centers engage in cyclic electron transport around PS II involving cyt b_{559} (Horton and Croze, 1979). Wendler and Holzwarth (1987) have stated that the major effect of light-induced state transitions on the fluorescence kinetics involves a change in the relative antenna size of α- and β-units brought about by reversible migration of the light-harvesting complexes between α-centers and β-centers. If one of these PS II reaction centers is a more efficient trap than the other one (Melis and Homann, 1976) unidirectional energy transfer can take place between the two. Melis and Duysens (1979) have suggested that the PS II_β center is a more efficient trap. Hence these centers can act like an energy dump with low fluorescence yield.

Based on the above data from higher plants and results from this study a new model for the state transition is proposed and shown in Figure 27. In this model the inactive PS II centers capable of doing cyclic electron transport around PS II via cyt b_{559} (same as PS II_β in higher plants), are farther away from the active PS II centers, capable of oxygen evolution and electron transfer to PS I (same as PS II_α in higher plants), in state 1. A conformational change in the membrane in state 2 brings the inactive PS II centers closer to the active centers. By virtue of a higher efficiency trap the inactive centers act like

Figure 27. This figure shows the model for state transition based on the results of this study. Two types of PS II are present, ones that do cyclic electron transport around PS II (designated with a *) and the other type engages in normal electron transport to PS I producing oxygen in the process. Upon transition from state 1 to state 2 a conformational change in the membrane brings the two types of photosystem II closer to each other increasing energy transfer to the inactive PS II*. This model does not predict any energy transfer to PS I.

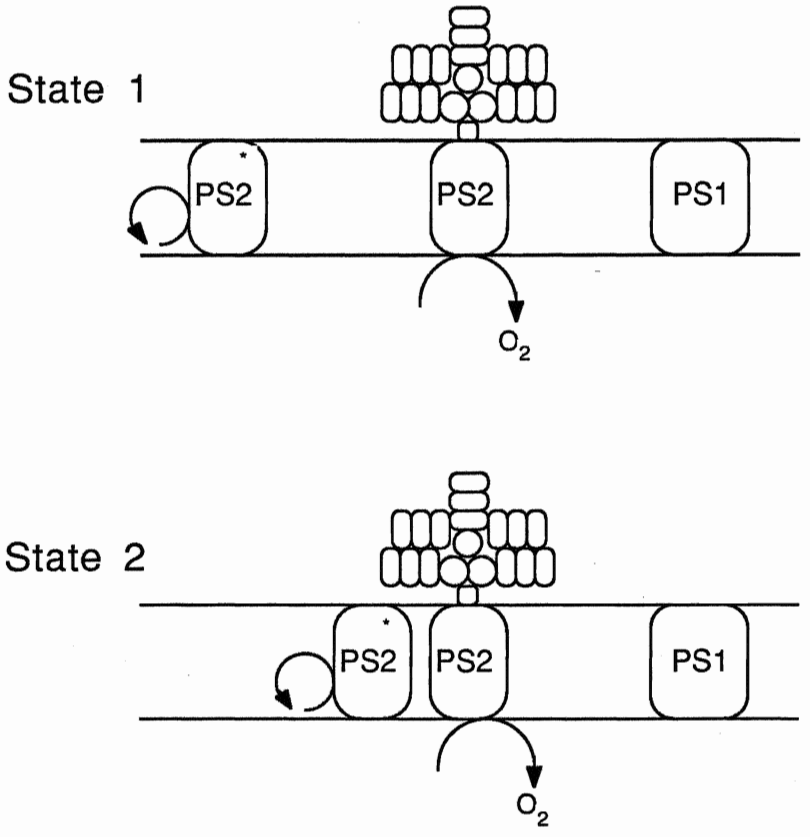
State 1
PS2
PS2
PS1
O_2
State 2
PS2
PS2
PS1
O_2

energy dumps and excitation energy is transferred from active PS II centers' Chl a and PBS to the inactive PS II centers. Since these inactive centers have lower fluorescence yield than the active centers, a lower fluorescence emission is predicted upon transition to state 2. This model also predicts a decrease in oxygen evolution in state 2, however no difference in the activity of PS I is predicted. The main function of this model is protection of PS II by drawing excess excitation energy away from PS II and shunting it into a cyclic electron transport in state 2.

In order to determine that two populations of PS II reaction centers exists in these organisms, single-turnover flash measurements of fluorescence should be done in these organisms as was done in higher plants (Mauzerall, 1978; 1972; Geacintov *et al.*, 1987). If the shape of the saturation curve is the complement of an exponential (ie a simple poissonian) it would indicate that a single population of PS II units is involved, however a sharper than poissonian shaped saturation curve (Falkowski *et al.*, 1987) would suggest that more than one population is involved. Another way to check the validity of the above model is to measure single-turnover flash kinetics of cyt b_{559} oxidation and reduction during state transition, since the above model suggests a differential cyt b_{559} reduction in the two states. This can be done following the method of Herber *et al.* (1979).

Conclusions

Results from fluorescence emission and excitation studies done with *Synechococcus sp.* PCC 6301 showed a large decrease in the fluorescence of PS II components combined with a very small increase in the fluorescence of the PS I component upon transition to state 2 for both PBS and Chl a absorbed wavelengths. These results do not fit the predictions made by the mobile PBS model. However only modified versions of PBS detachment and spillover models would predict these results.

The PBS detachment model predicts an increase in heat loss upon transition to state 2. Measurements of heat loss within 2 μs of a laser flash from intact cells of *S. sp.* PCC 6301 in state 1 and state 2 did not show any differences for excitation wavelengths absorbed by both PBS and Chl a done over three orders of magnitude of intensity.

PS I activity measurements were done by monitoring P-700 photooxidation at 820 nm from intact cells of *S. sp.* PCC 6301 for both Chl a and PBS excitations. All of the existing models for state transition in PBS-containing and Chl a/b-containing organisms state that the main function of state transition is to regulate the distribution of excitation energy between the two photosystems in response to an imbalance. Hence all models predict an increase in PS I activity in state 2. The results in this study showed no difference in the extent of photooxidation of P-700 in the two states for both Chl a and PBS excitations.

Based on these results a new mechanism for the state transition is proposed with photoprotection of PS II as its main function. In this model two populations of PS II centers take part in energy transfer. One population is capable of cyclic electron transfer and has a high efficiency trap with low fluorescence yield. The other type of PS II takes part in normal electron transfer and oxygen evolution. In state 2 excess energy is transferred to the inactive centers, and this excess energy is then dissipated by the cyclic electron transport. In this model there is no increase in the amount of energy transferred to PS I in state 2 by PBS or PS II.

Future experiments to elucidate the role of cyclic electron transport around PS II in the mechanism of state transition are required to find out if the state transition is really a photoprotectory mechanism for photosystem II.

REFERENCES

Allen, J.F. and Horton, P. (1981) Chloroplast protein phosphorylation and chlorophyll fluorescence quenching: activation by tetramethyl-p-hydroquinone, an electron donor to plastoquinone. Biochim. Biophys. Acta 638, 290-295.

Allen, J.F., Bennett, J., Steinback, K.E. and Arntzen, C.J. (1981) Chloroplast protein phosphorylation couples plastoquinone redox state to distribution of excitation energy between photosystems. Nature 291, 25-29.

Allen, J.F., Sanders, C.E. and Holmes, N.G. (1985) Correlation of membrane protein phosphorylation with excitation energy distribution in the cyanobacterium *Synechococcus* 6301. FEBS Lett. 193, 271-275.

Allen, J.F. and Melis, A. (1988) The rate of P-700 photooxidation under continuous illumination is independent of state 1-state 2 transitions in the green alga *Scenedesmus obliquus* . Biochim. Biophys. Acta 933, 95-106.

Aoki, M. and Katoh, S. (1982) Oxidation and reduction of plastoquinone by photosynthetic and respiratory electron transport in cyanobacterium *Synechococcus sp.* Biochim. Biophys. Acta 682, 307-314.

Aoki, M. and Katoh, S. (1983) Size of plastoquinone pool functioning in photosynthetic and respiratory electron transport of *Synechococcus sp.* Plant and Cell Physiol. 24, 1379-1386.

Amesz, J. (1983) The role of mangenese in photosynthetic oxygen evolution. Biochim. Biophys. Acta 726, 1-12.

Arnon, D.I. and Tang, G.M.-S (1988) Cytochrome b-559 and proton conductance in oxygenic photosynthesis. Proc. Natl. Acad. Sci. USA. 85, 9524-9528.

Babcock, G.T. and Sauer, K. (1973) Electron paramagnetic resonance signal II in spinach chloroplasts. II. Alternative spectral forms and inhibitor effects on kinetics of signal II in flashing light. Biochim. Biophys. Acta 325, 504-519.

Babcock, G.T., Widger, W.R., Cramer, W.A., Oertling, W.A. and Metz, J.G. (1985) Axial ligands of chloroplast cytochrome b-559: identification and requirement for a heme-cross-linked polypeptide structure. Biochim. 24, 3638-3645.

Barry, B.A. and Babcock, G.T. (1987) Tyrosyl radicals are involved in the photosynthetic oxygen evolving system. Proc. Natl. Acad. Sci. USA. 84, 7099-7103.

Bassi, R., Giacometti, G.M. and Simpson, D.J. (1988) Changes in the organization of stroma membranes induced by the *in vivo* state 1-state 2 transition. Biochim. Biophys. Acta 935, 152-165.

Batie, C.J. and Kamin, H. (1981) The relation of pH and oxidation-reduction potential to the association state of the ferredoxin-ferredoxin : $NADP^+$ reductase complex. J. Biol. Chem. 256, 7756-7763.

Beddard, G.S., Fleming, G.R., Porter, G., Searle, G.F.W. and Synowiec, J.A. (1979) The fluorescence decay kinetics of *in vivo* chlorophyll measured using low intensity excitation. Biochim. Biophys. Acta 545, 165-174.

Bell, A.G. (1880) On the production and reproduction of sound by light. Am. J. Sci. 20, 305-324.

Bennett, J. (1977) Phosphorylation of chloroplast membrane polypeptides. Nature 269, 344-346.

Bennett, J. (1979) Chloroplast phosphoproteins, the protein kinase of thylakoid membrane is light-dependent. FEBS Lett. 103, 342-344.

Bennett, J., Shaw, E.K. and Michel, H. (1988) Cytochrome b_6f complex is required for phosphorylation of light-harvesting chlorophyll a/b complex II in chloroplast photosynthetic membranes. Eur. J. Biochim. 171, 95-100.

Bennett, J. (1991) Protein phosphorylation in green plant chloroplasts. Ann. Rev. Plant Physiol. Plant Mol. Biol. 42, 281-311.

Berens, S.J., Scheele, J., Butler, W.L. and Magde, D. (1985) Time-resolved fluorescence studies of spinach chloroplasts: evidence for heterogenous chipartite model. Photochem. Photobiol. 42, 51-57.

Biggins, J. (1983) Mechanism of the light state transition in photosynthesis I. Analysis of the kinetics of cyt f oxidation in state 1 and state 2 in red alga *Porphyridium cruentum*. Biochim. Biophys. Acta 724, 111-117.

Biggins, J. and Bruce, D. (1985) Mechanism of the light state transition in photosynthesis. III. Kinetics of the state transition in *Porphyridium cruentum*. Biochim. Biophys. Acta 806, 230-236.

Biggins, J. and Mathis, M. (1988) The functional role of vitamine K1 in photystem I of the cyanobacterium *Synechocystis* 6803. Biochim. 27, 1494-1500.

Biggins, J. and Bruce, D. (1989) Regulation of excitation energy transfer in organisms containing phycobilisomes. Photosynth. Res. 20, 1-34.

Biggins, J., Campbell, C.L., Creswell, L.L. and Wood, E.A. (1984a) Mechanism of the light state transition in *Porphyridium cruentum*. In: Advances in Photosynthesis Research (C. Sybesma ed.) Vol. 2, pp 303-306. Martinus Nijhoff, Dr. W. Junk, The Hague. Boston, Lancaster.

Biggins, J., Campbell, C.L., Bruce, D. (1984b) Mechanism of the light state transition in photosynthesis. II. Analysis of phosphorylated polypeptides in the red alga *Porphyridium cruentum*. Biochim. Biophys. Acta 767, 138-144.

Bonaventura, C. and Myers, J. (1969) Fluorescence and oxygen evolution from *Chlorella pyrenoidosa*. Biochim. Biophys. Acta 189, 366-383.

Bottin, H. and Mathis, P. (1985) Interaction of plastocyanin with the photosystem I reaction center: a kinetic study by flash absorption spectroscopy. Biochim. 24, 6453-6460.

Bottin, H. and Mathis, P. (1987) Studies of the PS I acceptor side by double and triple flash experiments. Biochim. Biophys. Acta 894, 39-48.

Botton, J.R., Hought, A.F. and Ross, R.T. (1981) Photochemical energy storage: an analysis of limits.In: Photochemical Conversion and Storage of Solar energy (Connolly, J.S. ed.) pp 297-300. Academic Press, New York.

Bouchner, F. and Leblanc, R.M. (1981) Photoacoustic spectroscopy of cattle visual pigment at low temperature. Biochim. Biophys. Res. Comm. 100, 385-390.

Braumann, T., Vasmel, H., Grimme, L.H. and Amesz, J. (1986) Pigment composition of the photosynthetic membrane and reaction center of the green bacterium *Prosthecochloris aesturaii*. Biochim. Biophys. Acta 848, 83-91.

Braslavsky, S.E. (1985) Time-resolved photoacoustic and photothermal methods. Applications to substances of biological interest. In: Primary photo-processes in biology and medicine (Bensasson, R.U., Jori, G., Land, E.J., and Truscutt,T.G. eds.) pp 147-158. NATO ASI 85A. Plenum press, New York.

Braslavsky, S.E. (1986) Photoacoustic and photothermal methods applied to study of radiationless deactivation processes in biological systems and in substances of biological interest. Photochem. Photobiol. 43, 667-675.

Braslavsky, S.E. and Heihoff, K. (1989) Photothermal methods. In: Handbook of Organic Photochemistry (Scaiano, J.C. Ed.) CRC Press, Boca Raton, Fl. pp. 327-355.

Braslavsky, S.E., Ellul, R.M., Weiss, R.G., Al-Ekabi, H. and Schaffner, K. (1983) Phytochrome models 7. Photoprocesses in biliverdin dimethyl ester in ethanol studied by laser-induced optoacoustic spectroscopy. Tetrahedron 39, 1909-1913.

Brettel, K., Setif, P. and Mathis, P. (1986) Flash-induced absorption changes in photosystem I at low temperature: evidence that the electron acceptor A is vitamine K. FEBS Lett. 203, 220-224.

Brimble, S. and Bruce, D. (1989) Pigment orientation and excitation energy transfer in *Porphyridium cruentum* and *Synechococcus sp.* PCC 6301, cross-linked in light state 1 and state 2 with glutaraldehyde. Biochim. Biophys. Acta 973, 315-323.

Broadhurst, R.W., Hoff, A.J. and Hore, P.J. (1986) Interpretation of the polarized electron paramagnetic resonance signal of plant photosystem I. Biochim. Biophys. Acta 852, 106-111.

Bruce, B.P. and Malkin, R. (1988) Subunit stoichiometry of the chloroplast photosystem I complex. J. Biol. Chem. 263, 7302-7308.

Bruce, D., Biggins, J., Steiner, T. and Thewalt, M. (1985) Mechanism of the state transition in photosynthesis IV. Picosecond fluorescence spectroscopy of *Anacystis nidulans* and *Porphyridium cruentum* in state 1 and state 2 at 77K. Biochem Biophys. Acta 806, 237-246.

Bruce, D., Brimble, S. and Bryant, D.A. (1989a) State transitions in a phycobilisome-less mutant of the cyanobacterium *Synechococcus sp.* PCC 7002. Biochem Biophys. Acta 974, 66-73.

Bruce, D., Brimble, S. and Salehian, O. (1989b) Regulation of distribution of excitation energy in cyanobacterial photosynthesis. A comparison of mechanisms involving mobile antenna and spillover. In: Photobiology and Biotechnology (Frackowiak, D. ed.) pp 30-35. Wykonano W. Zakladzie. Graficznym Politechniki Poznanskiej, Poland.

Buchanan, B.B. and Evans, M.C.W. (1969) Photoreduction of ferredoxin and its use in $NAD(P)^+$ reduction by a subcellular preparation from the photosynthetic bacterium, *Chlorobium thiosulfatophilum.* Biochim. Biophys. Acta 180, 123-129.

Bulte, L., Gans, P., Rebeille, K. and Wollman, F.A. (1990) ATP control on state transitions *in vivo* in *Chlamydomonas reinhardtii*. Biochim. Biophys. Acta 1020, 72-80.

Bults, G., Horwitz, B.A., Malkin, S. and Cahen, D. (1982) Photoacoustic measurement of photosynthetic activities in whole leaves. Photochemistry and gas exchange. Biochim. Biophys. Acta 679, 452- 465.

Canaani, O. (1986) Photoacoustic detection of oxygen evolution and state 1-state 2 transitions in cyanobacteria. Biochim. Biophys. Acta 852, 74-80.

Canaani, O. (1987) Control of state 1-state 2 transitions in the blue-green alga *Nostoc muscorum* . In: Progress in Photosynthesis Research (Biggins, J. ed.) Vol. 2 pp 769-772., Dordrecht: Martinus Nijhoff.

Canaani, O. (1990) The role of cyclic electron flow around photosystem I and excitation energy distribution between the photosystems upon acclimation to high ionic stress in *Dunaliella salina*. Photochem. Photobiol. 52, 591-599.

Cannani, O. and Malkin, S. (1984) Physiological adaptation to a newly observed low light intensity state in intact leaves reulting in extreme imbalance in excitation energy distribution between the two photosystems. Biohem. Biophys. Acta 766, 525-532.

Carpentier, R., Larue, B. and Leblanc, R.M. (1984) Photoacoustic spectroscopy of *Anacystis nidulans*. III. Detection of photosynthetic activities. Arch. Biochim. Biophys. 228, 534-543.

Carpentier, R.H., Matthijs, C.P., Leblanc, R.M. and Hind, G. (1985a) Monitoring energy conversion in photosystem I of cyanobacterial heterocysts by photoacoustic spectroscopy. Proceedings of Fourth International Topical Meeting on Photoacoustic, Thermal and Related Sciences. Ville D'Esterel, Quebec, Canada. Ecole Polytechnique de Monteral ThA7.

Carpentier, R., Nakatani, H.Y. and Leblanc, R.M. (1985b) Photoacoustic detection of energy conversion in photosystem II submembrane preparation from spinach. Biochim. Biophys. Acta 808, 470-473.

Clark, R.D. and Hind, G. (1983) Spectrally distinct cytochrone b-563 components in a chloroplast cytochrome b-f complex: Interaction with a hydroxyquinoline N-oxide. Proc. Natl. Acad. Sci. USA 77, 7227-7231.

Clark, R.D., Hawkesford, M.J., Coughlan, S.J., Bennett, J. and Hind, G. (1984) Association of ferredoxin-$NADP^+$ oxidoreductase with the chloroplast cytochrome b-f complex. FEBS Lett. 174, 137-142.

Cramer, W.A., Theg, S.M. and Widger, W.R. (1986) On the structure and function of cytochrome b-559. Photosynth. Res. 10, 393-403.

Crofts, A.R. and Wraight, C.A. (1983) The electrochemical domain of photoynthesis. Biochim. Biophys Acta 726, 149-185.

Debus, R.J., Barry, B.A., Babcock, G.T. and McIntosh, L. (1988 a) Site-directed mutagenesis identifies a tyrosine radical in volved in the photosynthetic oxygen evolving system. Proc. Natl. Acad. Sci. USA. 85, 427-430.

Debus, R.J., Barry, B.A., Sithole, I., Babcock, G.T. and McIntosh, L. (1988b) Directed mutagenesis indicates that the donor to $P-680^+$ in photosystem II is tyrosine-161 of the D1 polypeptide. Biochim. 27, 9071-9074.

Dekker, J.P., Van Gorkom, H.J., Brok, M. and Ouwenhand, L. (1984) Optical characterization of photosystem II electron donors. Biochim. Biophys. Acta 746, 301-309.

Delsome, R. (1991) Electron transfer from cytochrome f to photosystem I in green alga. Photosynth. Res. 29, 45-54.

denBlaken, H.J., Hoff, A.J., Jongenelis, A.P.J.M. and Diner, B.A. (1983) High-resolution triplet-minus-singlet absorbance difference spectrum of photosystem II particles. FEBS Lett. 157, 21-27.

deVitry, C., Carles, C. and Diner, B.A. (1986) Quantitation of plastoquinone-9 in photosystem II reaction center particles. FEBS Lett. 196, 203-206.

Diner, B.A. (1986) The reaction center of photosystem II. In: Encyclopedia for Plant Physiology New Series (Staehelin, A. and Arntzen, C.J. eds.) Vol. 19, pp 422-436. Springer-Verlag, Berlin.

Dominy, P.J. and Williams, W.P. (1987) The role of respiratory electron flow in the control of excitation energy distribution in blue-green algae. Biochim. Biophys. Acta 892, 264-274.

Duysens, L.N.M. and Sweers, H.E. (1963) In: Studies on Microalgae and Photosynthetic Bacteria (Japanese Society of Plant Physiology, ed.) pp 353-372. Univ. of Tokyo Press, Tokyo.

Emerson, R. and Lewis, C.M. (1942) The photosynthetic efficiency of phycocyanin in *Chroococcus* and problem of carotenoid participation in photosynthesis. J. Gen. Physiol. 25, 579-595.

Englemann, T.W. (1884) Untersuchungen uber die quantitativen behviehungen zwischen absorption des lichtes und assimilation in pflanzenzelle. Bot. Ztg. 42, 81-87.

Evans, M.C.W. (1974) Determination of the oxidation-reduction potential of the bound iron-sulfur proteins of the primary electron acceptor complex of photosystem I in spinach chloroplasts. FEBS Lett. 49, 111-114.

Evans, M.C.W., Telfer, A. and Lord, A.V. (1972) Evidence for the role of a bound ferredoxin as the primary electron acceptor of photosystem I in spinach chlorpolasts. Biochim. Biophys.Acta 267, 530-537.

Falkowski, P.G., Fujita, Y., Ley, A. and Mauzerall, D. (1986) Evidence for cyclic electron flow around photosystem II in *Chlorella pyrenoidosa*. Plant Physiol. 81, 310-312.

Falkowski, P.G., Zbigniew, K. and Fujita, Y. (1988) Effect of redox state on the dynamics of photosystem II during steady-state photosynthesis in eucaryotic algae. Biochim. Biophys. Acta 933, 432-443.

Fajer, J., Davies, M.S., Forman, A., Klimov, V.V., Dolan, E. and Ke, B. (1980) Primary electron acceptors in plant photosynthesis. J. Am. Chem. Soc. 102, 7143-7145.

Fernyhough, P., Foyer, C.H. and Horton, P. (1984) Increase in the level of thylakoid protein phosphorylation in maize mesophyll chloroplasts by decrease in the transthylakoid pH gradient. FEBS Lett. 176, 133-138.

Fish, L.E., Kuck, U. and Bogorad, L. (1985) Analysis of the two partially homologous P-700 chlorophyll a proteins of maize photosystem I: predictions based on the primary sequences and features shared by other chlorophyll proteins. Mol. Biol. Photosynth. App. 188, 111-119.

Fork, D.C. and Satoh, K. (1983) State 1-state 2 transition in the thermophilic blue-green alga (cyanobacterium) *Synechococcus lividus* . Photochem. Photobiol. 37, 421-427.

Fork, D.C. and Satoh, K. (1986) the control by state transitions of the distribution of excitation energy in photosynthesis. Ann. Rev. Plant Physiol. 37, 335-361.

Foust, G.P., Mayhew, S.G. and Massey, V. (1969) Complex formation between ferredoxin triphosphopyridine nucleotide reductase and electron transfer proteins. J. Biol. Chem. 244, 964-970.

Frackowiak, D., Lorrain, L., Wrobel, D. and Leblanc, R.M. (1985) Polarized photoacoustic, absorption and fluorescence spectra of chloroplasts and thylakoids oriented in polyvinyl alcohol films. Biochim.Biophys. Res. Comm. 126, 254-261.

Fujita, I., Davis, M.S. and Fajer, J. (1978) Anion radicals of pheophytin and chlorophyll a: their role in the primary charge separations of plant photosynthesis. J. Am. Chem. Soc. 100, 6280-6282.

Gal, A., Schuster, G., Frid, D., Canaani, O., Schwieger, H.G. and Ohad, I. (1988) Role of the cytochrome b_6f complex in the redox-controlled activity of *Acetabularia* thylakoid protein kinase. J. Biol. Chem. 263, 7785-7791.

Gantt, E., Lipshultz, C.A. and Zilinskas, B. (1976) Further evidence for a phycobilisome model from selective dissociation, fluorescence emission, immunoprecipitation and electron microscopy. Biochim. Biophys. Acta 430, 375-388.

Geacintov, N.E., Breton, J., France, L., Deprez, J. and Dobek, A. (1987) Laser flash-induced non-sigmoidal fluorescence induction curves in chloroplasts. In: Progress in Photosynthesis Research (Biggins J. ed.) Voll II. pp 107-110. Nijhoff, Dordrecht, The Netherlands.

Gerken, S., Brettel, K., Schlodder, E. and Witt, H.T. (1988) Optical characterization of the immediate donor to chlorophyll a_{II}^+ in O_2-evolving photosystem II complexes. Tyrosine as possible electron carrier between chlorophyll a_{II} and water-oxidizing mangenese complex. FEBS Lett. 237, 69-75.

Ghanotakis, D.F., Topper, J.N., Babcock, G.T. abd Yocum, C.F. (1984) Water-soluble 17 and 23 KDa polypeptides restore oxygen evolution activity by creating high-affinity binding site for Ca^{2+} on the oxidizing side of photosystem II. FEBS Lett. 170, 169-173.

Glazer, A.N. and Bryant, D.A. (1975) Allophycocyanin B (λ_{max} 671, 618 nm). A new cyanobacterial phycobiliprotein. Arch. Microbiol. 104, 15-22.

Glazer, A.N. and Melis, A. (1987) Photochemical reaction centers: structure, organization and function. Ann. Rev. Plant Physiol. 38, 11-45.

Golbeck, J.H. (1987) Structure, function and organization of photosystem I reaction center complex. Biochim. Biophys. Acta 895, 167-204.

Haehnel, W., Propper, A. and Krause, A. (1980) Evidence for complexed plastocyanin as the immediate donor of P-700. Biochim. Biophys. Acta 593, 383-399

Haehnel, W., Holzwarth, A.R. and Wendler, J. (1983) Picosecond fluorescence kinetics and energy transfer in the antenna chlorophylls of green algae. Photochem. Photobiol. 37, 4356-443.

Hansson, O. and Wydrzynski, T. (1990) Current preceptions of photosystem II. Photosynth. Res. 23, 131-162.

Harrison, M.A., Tsinoremas, N.F. and Allen, J.F. (1991) Cyanobacterial thylakoid membrane proteins are reversibly phosphorylated under plastoquinone-reducing conditions in vitro. FEBS Lett. 282, 295-299.

Hauska, G. (1986) Preparation of electrogenic, proton-transposing cytochrome complexes of the b_6f type (chloroplast and cyanobacteria) and bc_1 type (*Rhodopseudomonas sphaeroides*). In: Methods in Enzymology Vol. 126 (Fleischer, S. and Fleischer, B. eds.) pp 271-285. Academic press,Inc. London.

Hauska, G. (1986) Composition and structure of cytochrome bc_1 and b_6f complexes. In, Encyclopedia for Plant Physiology New Series (Staehelin, A. and Arntzen, C.J. eds.) Vol. 19, pp 497-507. Springer-Verlag, Berlin.

Haworth, P. and Melis, A. (1983) Phosphorylation of chloroplast thylakoid membrane proteins does not increase the absorption cross-section of photosystem I. FEBS Lett. 160, 277-280.

Haxo, F.T. and Blinks, L.R. (1950) Photosynthetic action spectra of marine algae. J. Gen. Physiol. 33, 389-422.

Heihoff, K., Braslavsky, S.E. and Schaffner, K. (1987) Study of 124-kilodalton oat phytochrome photoconversion in vitro with laser-induced optoacoustic spectroscopy. Biochim. 26, 1422-1427.

Herber, U., Kirk, M.R. and Boardman, N.K. (1979) Photoreactions of cytochrome b-559 and cyclic electron flow in photosystem II of intact chloroplasts. Biochim. Biophys. Acta 546, 292-306.

Hodges, M. and Barber, J. (1986) Analysis of chlorophyll fluorescence induction kinetics exhibited by DCMU-inhibited thylakoids and the origin of α and ß centers. Biochim. Biophys. Acta 848, 239-246.

Hodges, M., Boussac, A. and Briantis, J.M. (1987) Thylakoid membrane protein phosphorylation modifies the equilibrium between photosystem II quinone electron acceptors. Biochim. Biophys. Acta 894, 138-145.

Hoganson, C.W. and Babcock, G.T. (1988) Electron transfer events near the reaction center in O_2-evolving photosystem II preparations. Biochim. 27, 5848-5855.

Hoganson, C.W. and Babcock, G.T. (1989) Redox cofactor interactions in photosystem II: Electron spin resonance spectrum of P-680$^+$ is broadened in the presence of Y_Z^+. Biochim. 28, 1448-1454.

Hoj, P.B., Svendsen, Ib. Scheller, H.V. and Moller, B.L. (1987) Identification of a chloroplast-encoded 9-KDa polypeptide as a 2(4Fe-4S) protein carrying centers A and B of photosystem I. J. Biol. Chem. 262, 12676-12684.

Holzwarth, A.R. (1986) Fluorescence lifetimes in photosynthetic systems. Photochem. Photobiol. 43, 707-725.

Horton, P. (1981) The effect of redox potentials on the kinetics of fluorescence induction in pea chloroplasts. I. Removal of the slow phase. Biochim. Biophys. Acta 635, 105-110.

Horton, P. and Croze, E. (1979) Characterization of two quenchers of chlorophyll fluorescence with different midpoint oxidation-reduction potentials in chloroplasts. Biochim. Biopohys. Acta 545, 188-201.

Horton, P. and Lee, P. (1983) Stimulation of cyclic electron-transfer pathway around photosystem II by phosphorylation of chloroplast thylakoid proteins. FEBS Lett. 162, 81-84.

Horton, P. and Lee, P. (1985) Phosphorylation of chloroplast membrane proteins partially protects against photoinhibition. Planta 165, 37-42.

Hurt, E.C. and Hauska, G. (1983) Cytochrome b_6 from isolated cytochrome b_6f complexes. Evidence for two spectral forms with different midpoint potentials. FEBS Lett. 153, 413-419.

Ikegami, I. and Itoh, S. (1986) Chlorophyll organization in P-700-enriched particles isolated from spinach chloroplasts. CD and absorption spectroscopy. Biochim. Biophys. Acta 851, 75-85.

Ikegami, I. and Itoh, S. (1988) Absorption spectroscopy of P-700-enriched particles isolated from spinach. Is P-700 a dimer or a monomer? Biochim. Biophys. Acta 934, 39-46.

Jabben, M. and Schaffner, K. (1985) Pulsed laser induced optoacoustic spectroscopy of intact leaves. Biochim. Biophys. Acta 809, 445-451.

Jabben, M., Heihoff, K., Braslavsky, S.E. and Schaffner, K. (1984) Studies on phytochrome photoconversion in vitro with laser-induced optoacoustic spectroscopy. Photchem. Photobiol. 40, 361-367.

Jankowiak, R., Tang, D., Small, G.J. and Seibert, M. (1989) Transient and persistent hole-burning of the reaction center of photosystem II. J. Phys. Chem. 93, 1649-1654.

Jennings, J.V. and Evans, M.C.W. (1977) The irreversible photoreduction of of a low potential component at low temperatures in a preparation of the green photosynthetic bacterium *Chlorobium thiosulphatophilum*. FEBS Lett. 75, 33-40.

Joliot, P., Barbieri, G. and Chabaud, R. (1969) Un nouveau modile des centres photochemique du system II. Photochem. Photobiol. 10, 309-329.

Ke, B., Inoue, H., Babcock, G.T., Fang, Z-X and Dolan, E. (1982) Optical and EPR characterization of oxygen-evolving photosystem II subchloroplast fragments isolated from the thermophilic blue-green alga *Phormidium laminosum*. Biochim. Biophys. 682, 297-306.

Kelley, P.M. and Izawa, S. (1978) The role of chlorine ion in photosystem II. I. Effects of chloride ion on photosystem II electron transport and on hydroxylamine inhibition. Biochim. Biophys. Acta 502, 198-210.

Kirmaler, C. and Hotten, D. (1987) Primary photochemistry of reaction centers from the photosynthetic purple bacteria. Photosynth. Res. 13, 225-260.

Kirschner, J. and Senger, H. (1986) Thylakoid protein phosphorylation in the red algae *Porphyridium cruentum*. In: Regulation of Chloroplast Differentiation, Plant Biology. Vol. 2 (Akoyunoglou, G. and Senger, H. Eds.) pp 339-344. AR Liss Inc. Publishers, New York.

Kischkoweit, C., Leibl, W. and Trissl, H.W. (1988) Theoretical and experimental study of trapping times and antenna organization in pea chloroplasts by means of artificial fluorescence quencher m-dinitrobenzene (DNB). Biochim. Biophys. Acta 933, 276-287.

Klimov, V.V. and Kranovskii, A.A. (1982) Participation of pheophytin in the primary processes of electron transfer at the reaction centers of photosystem II. Biophysics (USSR) 27, 186-198.

Klimov, V.V., Klevanik, A.V., Shuvalov, V.A. and Krasnovsky, A.A. (1977) Reduction of pheophytin in the primary light reaction of photosystem II. FEBS Lett. 82, 183-186.

Klimov, V.V., Dolan, E. and Ke, B. (1980) EPR properties of an intermediary electron acceptor (pheophytin) in photosystem-II reaction centers at cryogenic temperatures. FEBS Lett. 112, 97-100.

Klimov, V.V., Dolan, E., Shaw, E.R. and Ke, B. (1980) Interaction between the intermediary electron accceptor (pheophytin) and a possible plastoquinone-iron complex in photosystem II reaction centers. Proc. Natl. Acad. Sci. USA 68, 77, 7227-7231.

Kok, B., Forbush, B. and McGloin, M. (1970) Cooperation of charges in photosynthetic oxygen evolution: I A linear four step mechanism. Photochem. Photobiol. 11, 457-475.

Knaff, D.B. and Malkin, R. (1976) Iron-sulfur ptoteins of the green photosynthetic bacterium *Chlorobium. Biochim.* Biophys. Acta 430, 244-252.

Knaff, D.B. and Hirasawa, M. (1991) Ferredoxin-dependent chloroplast enzymes. Biochim. Biophys. Acta 1056, 93-125.

Kramer, H.J.K., Westerluis, N.H.J. and Amesz, J. (1985) Physiol. Veg. 23, 535-543.

Krause, G.H. and Behrend, U. (1983) Characterization of chlorophyll fluorescence quenching in chloroplast by fluorescence spectroscopy at 77K. Biochim. Biophys. Acta 723, 176-181.

Kyle, D.J., Haworth, P. and Arntzen, C.J. (1982) Thylakoid membrane protein phosphorylation leads to a decrease in connectivity between photosystem II reaction centers. Biochim. Biophys. Acta 680, 336-342.

Lagoutte, B. and Mathis, P. (1989) The photosystem I reaction center: structure and photochemistry. Photochem. Photobiol. 49, 833-844.

Lavergne, J. (1984) Absorption changes of photosystem II donors and acceptors in algal cells. FEBS Lett. 173, 9-14.

Ley, A.C. and Butler, W.L. (1980) Energy distribution in the photochemical apparatus of *Porphyridium cruentum* in state I and state II. Biochim. Biophys. Acta 595, 349-363.

Ley, A.C. (1984) Effective absorbance cross-section in *Porphyridium cruentum* . Plant Physiol. 74, 451-454.

Malkin, R. (1986) On the function of the two vitamine K1 molecules in the PS-I electron acceptor complex. FEBS Lett. 208, 343-346.

Malkin, R. and Bearden, A.J. (1971) Primary reactions of photosynthesis: photoreduction of a bound chloroplast ferredoxin at low temperature as detected by EPR spectroscopy. Proc. Natl. Acad. Sci. USA 68, 16-19.

Malkin, R. and Bearden, A.J. (1975) Laser-flash-activated electron paramagnetic resonance studies of the primary photochemical reaction in chloroplasts. Biochim. Biophys. Acta 396, 250-259.

Malkin, S., Herbert, S.K. and Fork, D.C. (1990) Light distribution, transfer and utilization in the marine red alga *Porphyra perforata* from photoacoustic energy-storage measurements. Biochim. Biophys. Acta 1016, 177-189.

Manodori, A. and Melis, A. (1986) Cyanobacterial acclimation to photosystem I and photosystem II light. Plant Physiol. 82, 182-189.

Mansfield, R.W. and Evans, M.C.W. (1985) Optical difference spectrum of the electron acceptor A_0 in photosystem I. FEBS Lett. 190, 237-241.

Matthijis, H.C.P., Lunderus, E.M.E., Loffler, H.J.M., Scholts, M.J.C. and Kraayenhof, R. (1984) Energy metabolism in the cyanobacterium *Plectonema boryanum*. Participation of the thylakoid photosynthetic electron transfer chain in the dark respiration of NADPH and NADH. Biochim. Biophys. Acta 766, 29-37.

Mauzerall, D. (1972) Light-induced fluorescence changes in *Chlorella* , and the primary photoreactions for the production of oxygen. Proc. Natl. Acad. Sci. USA 69, 1358-1362.

Mauzerall, D. (1978) Multiple excitations and the yield of chlorophyll a fluorescence in photosynthetic systems. Photochem. Photobiol. 28, 991-998.

Mauzerall, D. and Greenbaum, N.L. (1989) The absolute size of the photosyntehtic unit. Biochim. Biophys. Acta 974, 119-140.

McDermott, A.E., Yachandra, V.K., Guites, R.D., Sauer, K. and Klein, M.P. (1989) EXAFS structural study of F_X, the low-potantial Fe-S center in photosystem I. Biochim. 28, 8056-8059.

McIntosh, A.R. and Bolton, J.R. (1976) Electron spin resonance spectrum of species "X" which may function as the primary electron acceptor in photsystem I of green plant photosynthesis. Biochim. Biophys. Acta 430, 555-559.

Melis, A. (1991) Dynamics of photosynthetic membrane composition and function. Biochim. Biophys. Acta 1058, 87-106.

Melis, A. and Anderson, J.M. (1983) Structural and functional organization of the photosystems in spinach chloroplasts: antenna size, relative electron-transport capacity, and chlorophyll composition. Biochim. Biophys. Acta 724, 473-484.

Melis, A. and Duysens, L.N.M. (1979) Biphasic energy conversion kinetics and absorbance difference spectra of photosystem II of chloroplasts. Evidence for two different photosystem II reaction centers. Photochem. Photobiol. 29, 373-382.

Melis, A. and Homann, P.H. (1976) Heterogeneity of the photochemical system II of chloroplasts. Photochem. Photobiol. 23, 343-350.

Melis, A., Spangfort, M. and Andersson, B. (1987) Light-absorption and electron-transport balance between photosystem II and photosystem I in spinach chloroplasts. Photochem. Photobiol. 45, 129-136.

Michel, H., Shaw, E.K. and Bennett, J. (1987) Protein kinase and phosphatase activities of thylakoid membranes. In: Plant Membranes: Structure, Function, Biogenesis (Leaver, C.J. and Sze, H. eds.) pp 85-102. Alan R. Liss, New York.

Mimuro, M. and Fujita, Y. (1977) Estimation of chlorophyll a distribution in the photosynthetic pigment system I and II of the blue-green alga *Anabaena variablis*. Biochim. Biophys. Acta 459, 376-389.

Mimuro, M. (1990) Studies on excitation energy flow in photosynthetic pigment system; structure and energy transfer mechanisms. Bot. Mag. Tokyo 103, 233-253.

Moenne-Loccoz, P., Robert, B., Ikegami, I. and Lutz, M. (1990) Structure of the primary electron donor in photosystem I: A resonance Raman study. Biochim. 29, 4740-4746.

Moore, T.A. (1983) Photoacoustic spectroscopy and related techniques applied to biological materials. Photochem. Photobiol. Rev. 7, 187-221.

Mullineaux, C.W. and Allen, J.F. (1986) The state 2 transition in the cyanobactrerium *Synechococcus* 6301 can be driven by the respiratory electron flow into the plastoquinone pool. FEBS Lett. 205, 155-160.

Mullineaux, C.W. and Allen, J.F. (1988) Fluorescence induction transients indicate dissociation of photosystem II from the phycobilisome during the state 2 transition in the cyanobacterium *Synechococcus* 6301. Biochim. Biophys. Acta 934, 96-107.

Mullineaux, C.W. and Holzwarth, A.R. (1990) A proportion of photosystem II core complexes are decoupled from the phycobilisome in light-state 2 in cyanobacterium *Synechococcus* 6301. FEBS Lett. 260, 245-248.

Mullineaux, C.W., Griebenow, S. and Braslavsky, S.E. (1991) Photosynthetic energy storage in cyanobacterial cells adapted to light-state 1 and 2. A laser-induced optoacoustic study. Biochim. Biophys. Acta 1060, 315-318.

Murata, N. (1969) Control of excitation energy transfer in photosynthesis I. light-induced change of chlorophyll a fluorescence in *Pophyridium cruentum*. Biochim. Biophys. Acta 172, 242-251.

Murata, N. and Satoh, K. (1986) Absorption and fluorescence emission by intact cells, chloroplasts and chlorophyll-protein complexes. In: Light Emission by Plants and Bacteria (Govindjee, J. Amesz, and D.C. Fork, eds.) pp 138-159. Academic Press, London.

Murty, N.R., Cederstrand, C. and Rabinowitch, E. (1965) Chlorophyll a fluorescence yield in live cells and solutions. Photochem. Photobiol. 4, 917-921.

Nitsch, C., Schatz, G.H. and Braslavsky, S.E. (1989) Laser-induced optoacoustic calorimetry of primary processes in cells of *Rhodospirillum rubrum*. Biochim. Biophys. Acta 975, 88-95.

Nitsch, C., Braslavsky, S.E. and Schatz, G.H. (1988) Laser-induced optoacoustic calorimetry of primary processes in isolated photosystem I and photosystem II particles. Biochim. Biophys. Acta 934, 201-212.

Norris, J.R., Scheer, H., Druyan, M.E. and Katz, J.J. (1974) An electron-nuclear double resonance (ENDOR) study of the special pair model for photo-reactive chlorophyll in photosynthesis. Proc. Natl. Acad. Sci. USA 71, 4897-4900.

Oh-Oka, H., Takahashi, Y., Matsubara, H. and Itoh, S. (1988) EPR studies of a 9 KDa polypeptide with an iron-sulfur cluster(s) isolated from photosystem I complex by n-butanol extraction. FEBS Lett. 234, 291-294.

Olive, J., M'Bina, I., Vernotte, C., Astier, C. and Wollman, F.A. (1986) Randomization of the EF particles in thylakoid membranes of *Synechococystis* 6714 upon transition from state I to state II. FEBS Lett. 208, 308-312.

O'Malley, P.J. and Babcock, G.T. (1984) EPR properties of immobilized quinone cation radicals and the molecular origin of signal II in spinach chloroplasts. Biochim. Biophys. Acta 765, 370-379.

Omata, T., Murata, N. and Satoh, K. (1984) Quinone and pheophytin in the photosynthetic reaction center II from spinach chloroplasts. Biochim. Biophys. Acta 765, 403-405.

Ono, T. and Inoue, Y. (1989) Removal of Ca by pH 3.0 treatment inhibits S_2 to S_3 transition in photosynthetic oxygen evolving system. Biochim. Biophys. Acta 973, 443-449.

Ort, D.R. (1986) Energy transduction in oxygenic photosynthesis: an overview of structure and mechanism. In: Encyclopedia of Plant Physiology Vol. 19 (Staehelin, L.A. and Arntzen, C.J. eds.) pp 143-196. Springer-Verlag, Berlin.

Owens, G.C. and Ohad, T. (1983) Changes in thylakoid phosphorylation during membrane biogenesis in *Chlamydomonas reinhardtii* y-1. Biochim. Biophys. Acta 722, 234-241.

Papageorgiou, G. (1975) Chlorophyll fluorescence: an intrinsic probe of photosynthesis. In: Bioenergetics of Photosynthesis (Govindjee, ed.) pp 319-371. Academic Press, New York.

Patel, C.K.N. and Tam, A.C. (1981) Pulsed optoacoustic spectroscopy of condensed matter. Rev. Mod. Phys. 53, 517-550.

Peschek, G.A. (1987) Respiratory electron transport. In: The Cyanobacteria (P. Fay and C. Van Baalen eds.). pp 119-161, Elsevier, Amsterdam.

Peschek, G.A. and Schmetterer, G. (1982) Evidence for plastoquinol-cytochrome f/b-563 reductase as a common electron donor to P-700 and cytochrome oxidase in cyanobacteria. Biochim. Biophys. Res. Comm. 108, 1188-1195.

Pierson, B.K. and Olson, J.M. (1987) Photosynthetic bacteria. In: Photosynthesis (Amesz, J. ed.). pp 21- 42, Elsevier, Amsterdam.

Porter, G., Tredwell, C.J., Searle, G.F.W. and Barber, J. (1978) Picosecond time-resolved energy transfer in *Porphyridium cruentum*. Part 1. In intact alga. Biochim. Biophys. Acta 501, 232-245.

Pullin, C.A., Brown, R.G. and Evans, E.H. (1979) Detection of allophycocyanin in photosystem I preparations from the blue-green alga, *Chlorogloea fritschii*. FEBS Lett. 101, 110-112.

Rehm, A.M., Gulzow, M. and Ried, A. (1989) Changes in the photosynthetic apparatus of red algae induced by spectral alteration of the light field. I. A decrease in the apparent quantum yield of PS I caused by preillumination with light 1. Biochim. Biophys. Acta 973, 131-137.

Rehm, A.M., Gulzow, M., Marquardt, J. and Ried, A. (1990) Changes in the photosynthetic apparatus of red algae induced by spectral alteration of the light field. II. Further characterization of the light-dependent regulation of the apparent quantum yield of PS I. Biochim. Biophys. Acta 1016, 127-135.

Ried, A. and Reinhardt, B. (1980) Distribution of excitation energy between photosystem I and photosystem II in red algae. II. Kinetics of the state transition between state 1 and state 2. Biochim. Biophys. Acta 460, 25-35.

Ried, A. and Reinhardt, B. (1980) Distribution of excitation energy between photosystem I and photosystem II in red algae. III. Quantum requirements of a state 2-state 1 transition. Biochim. Biophys. Acta 592, 76-86.

Ried, A., Hessenberg, B., Metzner, H. and Zeigler, R. (1977) Distribution of excitation energy between photosystem I and photosystem II in red algae. 1. Action spectra of light reactions I and II. Biochim. Biophys. Acta 459, 175-186.

Rijgersberg, C.P. and Amesz, J. (1980) Fluorescence and energy transfer in phycobiliprotein-containing algae at low temperature. Biochim. Biophys. Acta 593, 261-271.

Robinson, H.H. and Crofts, A.R. (1983) Kinetics of the oxidation-reduction reactions of the photosystem II quinone acceptor complex, and the pathway for deactivation. FEBS Lett. 153, 221-226.

Rothberg, L.J., Bernstein, M. and Peters, K.S. (1983) Time-resolved photoacoustic spectroscopy applied to properties of picosecond transients. J. Chem. Phys. 79, 2569-2576.

Rutherford, A.W. (1981) EPR evidence for an acceptor functioning in photosystem II when the pheophytin acceptor is reduced. Biochim. Biophys. Res. Comm. 102, 1065-1070.

Rutherford, A.W. (1985 a) Orientation of EPR signals arising from components in Photosystem II membranes. Biochim. Biophys. Acta 807, 189-201.

Rutherford, A.W. (1985 b) How close is the analogy between the reaction center of Photosystem II and that of purple bacteria? Biochim. Soc. Trans. 14, 15-17.

Rutherford, A.W. and Mullet, J.E. (1981) Reaction center triplet states in Photosystem I and Photosystem II. Biochim. Biophys. Acta 635, 225-269.

Rutherford, A.W., Paterson, D.R. and Mullet, J.E. (1981) A light-induced spin-polarized triplet detected by EPR in photosystem II reaction centers. Biochim. Biophys. Acta 635, 205-214.

Saito, K., Williams, W.P., Allen, J.F. and Bennett, J. (1983) Comparison of ATP-induced and state 1/state 2-related changes in excitation. Biochim. Biophys. Acta 724, 94-103.

Salehian, O., and Bruce, D. (1991) Distribution of excitation energy in photosynthesis: quantification of florescence yields from intact cyanobacteria. J. Luminescence 50, (In press).

Sanders, C.E., Holmes, N.G. and Allen, J.F. (1986) Membrane protein phosphorylation in the cyanobacterium *Synechococcus* 6301. Biochim. Soc. Trans. 14, 66-67.

Sanders, C.E. and Allen, J.F. (1988) The 18.5 kDa phosphoprotein of the cyanobacterium *Synechococcus* 6301: A component of the phycobilisome. In: Progress in Photosynthesis Research (Biggins J. ed.) Voll II. pp 761-764. Nijhoff, Dordrecht, The Netherlands.

Sandusky, P.O. and Yocum, C.F. (1984) The chloride requirement for photosynthetic oxygen evolution. Analysis of the effects of chloride and other anions on amine inhibition of the oxygen-evolving complex. Biochim. Biophys. Acta 766, 603-611.

Satoh, K. (1979a) Properties of light-harvesting chlorophyll a/b protein, and photosystem I chlorophyll a protein, purified from digitonin extracts of spinach chloroplasts by isoelectric focusing. Plant Cell Physiol. 20, 499-512.

Satoh, K. (1979b) Polypeptide composition of the purified photosystem II pigment-protein complex from spinach. Biochim. Biophys. Acta 546, 84

Satoh, K. (1982) Fractionation of thylakoid-bound chlorophyll-protein complexes by isoelectric focussing. In: Methods in Chloroplast Molecular Biology (Edelman, M., Hallick, R.B. and Chua, N.H. eds.) pp 845-856. Elsevier/North Holland Biomedical Press, Amsterdam.

Satoh, K. and Fork, D.C. (1983) A new mechanism for adaptation to changes in light intensity and quality in the red alga, *Porphyra perforata*. I. Relation to state 1-state 2 transitions. Biochim. Biophys. Acta 722,190-196.

Sauer, K., Mathis, P., Acker, S. and Van Best, J.A. (1978) Electron acceptors associated with P-700 in triton solubilized photosystem I particles from spinach chloroplasts. Biochim. Biophys. Acta 503, 120-134.

Sauer, K., Mathis, P., Acker, S. and Van Best, J.A. (1979) Absorption changes of P-700 reversible in milliseconds at low tempearture in triton-solubilized photosystem I particles. Biochim. Biophys. Acta 545, 466-472.

Schatz, G.H. and Van Gorkom, H.J. (1985) Absorbance difference spectra upon charge transfer to secondary donors and acceptors in photosystem II. Biochim. Biophys. Acta 810, 283-294.

Scahtz, G.H., Brock, A. and Holzwarth, A.R. (1988) Kinetic and energetic model for the primary processes in photosystem II. Biophys. J. 54, 397-405.

Scheller, H.V., Svendsen, Ib. and Moller, B.L. (1989) Subunit composition of photosystem I and identification of center X as a [4Fe-4S] iron-sulfur cluster. J. Biol. Chem. 264, 6929-6934.

Scherer, S. (1990) Do photosynthetic and respiratory electron transport chains share redox proteins? Trends In Biochim. Sci. 15, 458-462.

Staehelin, L.A. and Arntzen, C.J. (1983) Regulation of chloroplast membrane function: protein phosphorylation changes in the spatial organization of membrane components. J. Cell Biol. 97, 1327-1337.

Svensson, B., Vass, L., Cedergren, E. and Styring, S. (1990) Structure of donor side components in photosystem II predicted by computer modelling. EMBO J. 9, 2051-2059.

Takabe, T., Ishikawa, H., Niwa, S. and Itoh, S. (1983) Electron transfer between plastocyanin and P-700 in highly-purified photosystem I reaction center complex. Effects of pH, cations and subunit peptide composition. J. Biochim. 94, 1901-1911.

Tam, A.C. (1986) Applications of photoacoustic sensing techniques. Rev. Mod. Phys. 58, 381-431.

Tam, A.C. (1985) Pulsed photothermal radiometry for noncontact spectroscopy, material testing and inspection measurements. Infrared Phys. 1/2, 305-313.

Tam, A.C. (1984) Pulsed-laser generation of ultrashort acoustic pulses: application for thin-film ultrasonic measurements. Appl. Phys. Lett. 45, 510-512.

Tam, A.C. and Patel, C.K.N. (1980) Ultimate corrosion-resistant cell for spectroscopy in liquids. Opt. Lett. 5, 27-29.

Tamura, N., Yamamoto, Y. and Nishimura, M. (1980) Effect of surface potential on P-700 reduction in chloroplasts. Biochim. Biophys. Acta 592, 383-399.

Telfer, A., Bottin, H., Barber, J. and Mathis, P. (1984) The effect of magnesium and phosphorylation of the light-harvesting chlorophyll a/b protein on the yield of P-700 photooxidation in pea chloroplasts. Biochim. Biophys. Acta 764, 324-330.

Tel-Or, E. and Malkin, S. (1977) The photochemical and fluorescence properties of whole cells, spheroplasts and spheroplast particles from the blue-green alga *Phormidium luridum*. Biochim. Biophys. Acta 459, 157-174.

Theg, S.M. and Homana, P.H. (1982) Light-, pH- and uncoupler-dependent association of chloride with chloroplast thylakoids. Biochim. Biophys. Acta 679, 221-234.

Thielen, A.P.G.M. and Van Gorkom, H.J. (1981) Redox potentials of electron acceptors in photosystem IIα and IIß. FEBS Lett. 129, 205-209.

Thompson, L.K. and Brudvig, G.W. (1988) Cytochrome b-559 may function to protect photosystem II from photoinhibition. Biochim. 27, 6653-6658.

Thurnauer, M.C. and Gast, P. (1985) Q-band (35 GHz) EPR results on the nature of A1 and the electron spin polarization in photosystem I particles. Photobiochem. Photobiophys. 9, 29-38.

Tiede, D.M. and Dutton, P.L. (1981) Orientation of the primary quinone of the bacterial photosynthetic reaction centers contained in chromatophore and reconstituted membranes. Biochim. Biophys. Acta 637, 278-290.

Turpin, D.H. and Bruce, D. (1990) Regulation of photosynthetic light harvesting by nitrogen assimilation in the green alga *Selenastrum minutum* . FEBS Lett. 263, 99-103.

Upadhyaya, V., Tiwari, L.B. and Mishra, S.P. (1985) A study of the fluorescence quenching of chlorophyll by photoacoustic spectrometry. Spectrochim. Acta 41A, 833-836.

Vallejos, R.H., Ceccarelli, E. and Chan, R. (1984) Evidence for the existence of a thylakoid intrinsic protein that binds ferredoxin-$NADP^+$ oxidoreductase. J. Biol. Chem. 259, 8048-8051.

Van Gorkom, H.J. (1974) Identification of the reduced primary electron acceptor of photosystem II as a bound semiquinone anion. Biochim. Biophys. Acta 347, 439-442.

Vermaas, W.F.J., Rutherford, A.W. and Hansson, O. (1988) Site-directed mutagenesis in photosystem II of the cyanobacterium *Synechocystis sp.* PCC 6803: Donor D is a tyrosine residue in D2 protein. Proc. Natl. Acad. Sci. USA. 85, 8477-8581.

Vermaas, W.F.J., Renger, G. and Dohnt, G. (1984) The reduction of the oxygen-evolving system in the chloroplast by thylakoid components. Biochim. Biophys. Acta 704, 194-202.

Vernotte, C., Astier, C. and Olive, J. (1990) State 1-state 2 adaptation in the cyanobacterium *Synechocystis* PCC 6714 wild type and *Synechocystis* PCC 6803 wildtype and phycocyanin-less mutant. Photosynth. Res. 26, 203-121.

Voigtman, E., Jurgensen, A. and Winefordner, J. (1981) Condensed phase photoacoustic spectroscopy: detection of porphyrines and dyes. Anal. Chem. 53, 1442-1446.

Wang, R.T., Stevens, C.L.R. and Myers, J. (1977) Action spectra for photoreactions I and II of photosynthesis in the blue-green alga *Anacystis nidulans.* Photochem. Photobiol. 25, 103-108.

Wasielewski, M.R., Johnson, D.J., Seibert, M. and Govindjee (1989) Determination of the primary charge seperation rate in isolated photosystem II reaction centers with 500 fs time resolution. Proc. Natl. Acad. Sci. USA. 86, 524-528.

Wasielewski, M.R., Smith, V.H. and Norris J.R. (1982) ESR study of the primary electron donor in highly ^{13}C-enriched *Chlorobium limicola f. thiosulfatophilum.* FEBS Lett. 149, 138-140.

Weaver, E.C. (1984) State I-state II transitions in *Porphyridium cruentum* : observations on photosystem I by electron paramagnetic resonance spectroscopy. Photobiochem. Photobiophys. 7, 195-203.

Wendler, J. and Holzwarth, A.R. (1987) State transitions in green alga *Scenedesmus obliquus* probed by time-resolved fluorescence spectroscopy and global data analysis. Biophys. J. 52, 717-728.

Williams, W.P. and Allen, J.F. (1987) State 1/state 2 changes in higher plants and algae. Photosynth. Res. 13, 19-45.

Williams, W.P., Glazer, A.N. and Lundell, D.J. (1983) Cyanobacterial photosystem I: morphology and aggregation behavior. Proc. Natl. Acad. Sci. USA 80, 5923-5926.

Wynn, R.M., Omaha, J. and Malkin, R. (1989) Structural and functional properties of the cyanobacterial photosystem I complex. Biochim. 28, 5554-5560.

Yamazaki, I., Mimuro, M., Murao, T., Yamazaki, T., Yoshihara, K. and Fujita, Y. (1984) Excitation energy transfer in light harvesting antenna system of the red alga *Porphyridium cruentum* and the blue-green alga *Anacystis nidulans* : analysis of time-resolved fluorescence spectra. Photochem. Photobiol. 39, 233-240.

Yocum, C.F. (1986) Electron transfer on the oxidizing side of photosystem II. In: Encyclopedia for Plant Physiology New Series (Staehelin, A. and Arntzen, C.J. eds.) Vol. 19, pp 437-446. Springer-Verlag, Berlin.

Zanetti, G. and Merati, G. (1987) Interaction between photosystem I and ferredoxin. Identification by chemical cross-linking of the polypeptide which binds ferredoxin. Eur. J. Biochim. 169, 143-146.

Zhao, J., Warren, P.V., Li, N., Bryant, D.A. and Golbeck, J.H. (1990) Reconstitution of electron transport in photosystem I with Psa C and Psa D proteins expressed in *Escherichia coli*. FEBS Lett. 276, 175-180.

Zilinskas, B.A. (1982) Isolation and characterization of the central component of the phycobilisome core of *Nostoc sp.* Plant Physiol. 70, 1060-1065.

Appendix A

Calculation of error in fluorescence excitation spectra

The ratio of PS II peak at 695 nm and the PS I peak at 715 nm was measured for three sets of fluorescence emission spectra at all the different excitation wavelengths. The standard deviation calculated for each wavelength was used as the error of the fluorescence measurements.

Calculation of error of P-700 photooxidation measurements at 820 nm

Below is a hypothetical oxidation curve for P-700.

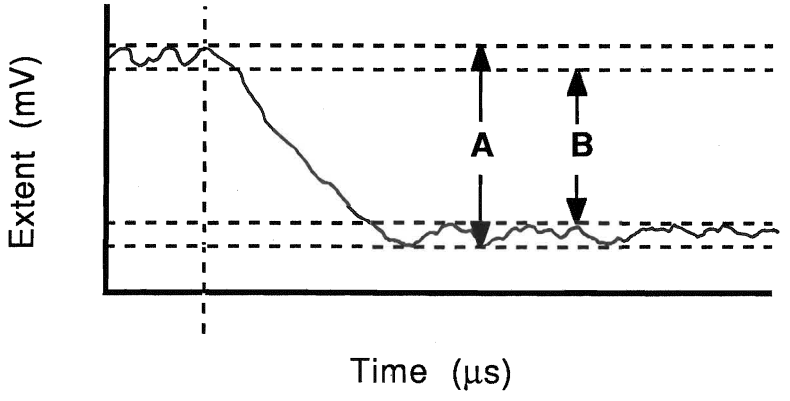

The distance A is measured as the maximum extent and the distance B is the minimum extent. From these measurements the extent is determined to be:

$$(A+B)/2 \pm (A-B)/2$$

Calculation of error in LIOAS measurements

The same method for determination of error was followed for LIOAS measurements as was for extent of P-700 photooxidation. Maximum and minimum extents were measured and the above formula was used to calculate the errors.

Appendix B

Composition of BG-11 Medium

Chemical (g/L)	Final Concentration
100X BG-FPC	10 ml stock*
Ferric ammonium citrate	0.006
Na_2CO_3	0.020
K_2HPO_4	0.031
*100X BG-FPC	
$NaNO_3$	149.58
$MgSO_4.7H_2O$	7.49
$CaCl_2.2H_2O$	3.60
Citric Acid	0.60
Na.EDTA, pH 8.0, 0.25 M	1.12 ml/L
Trace Minerals	100 ml/L stock**
**Trace Minerals	
H_3BO_3	2.86
$MnCl_2.4H_2O$	1.81
$ZnSO_4.7H_2O$	0.222
$Na_2MoO_4.7H_2O$	0.39
$CuSO_4.5H_2O$	0.079
$Co(NO_3)_2.6H_2O$	0.0494